

THESIS SUMMARY

EVALUATION OF STOPE SUPPORT USING A SYSTEMATIC BUSINESS APPROACH

EVALUATION OF STOPE SUPPORT USING A

M.J. PRETORIUS

ROCKMASS STIFFNESS APPROACH

Supervisor:

MARTIN JOHANNES PRETORIUS

Department:

Mining Engineering

University:

University of Pretoria

Degree:

**A thesis submitted in fulfilment of
the requirements for the degree of**

The study that is described in this thesis deals with stope support design using a rockmass stiffness approach. Three models were developed and combined into a single one in the third model. The first model describes stope support design using a rockmass stiffness approach. The second model describes rockmass behavior and is referred to as the rockmass demand. The two models are represented on a stress-strain load-deformation graph during the third model of the study. Here the design of the stope support is determined according to the position of the rockmass demand curve on the graph. The third model is a design configuration of rock type and support type results in a unique load-deformation curve that is allowed according to position.

PHILOSOPHIAE DOCTOR (ENGINEERING)

The first model describes stope support with all the factors having an influence on its performance, where this is referred to as the rockmass demand. The second model describes rockmass behavior and is referred to as the rockmass demand. The two models are represented on a stress-strain load-deformation graph during the third model of the study. Here the design of the stope support is determined according to the position of the rockmass demand curve on the graph. The third model is a design configuration of rock type and support type results in a unique load-deformation curve that is allowed according to position.

in the

support as a whole. In this model the design of the stope support is determined according to the position of the rockmass demand curve on the graph. The third model is a design configuration of rock type and support type results in a unique load-deformation curve that is allowed according to position.

SCHOOL OF ENGINEERING,

THE BUILT ENVIRONMENT AND INFORMATION TECHNOLOGY

according to the position of the rockmass demand curve on the graph. The third model is a design configuration of rock type and support type results in a unique load-deformation curve that is allowed according to position.

FACULTY OF ENGINEERING

UNIVERSITY OF PRETORIA

March 2004



THESIS SUMMARY

EVALUATION OF STOPE SUPPORT USING A ROCKMASS STIFFNESS APPROACH

M.J. PRETORIUS

Supervisor: Professor J.N. van der Merwe
Department: Mining Engineering
University: University of Pretoria
Degree: Philosophiae Doctor (Engineering)

The study that is described in this thesis deals with stope support design from a rockmass stiffness approach. Three models were developed and combined into a single one in the third part of the study in an attempt to describe and quantify the stope support and rockmass interaction.

The first model describes stope support with all the factors having an influence on its performance, where this is referred to as the capacity of the stope support. The second model describes rockmass behaviour and is referred to as the rockmass demand. These two models are represented on a common load-deformation graph during the third part of the study. Here the demand of the rockmass is compared to the capacity of the stope support as a whole. In contrast to previous design attempts, both the demand and the capacity for any given situation are considered as variables. The demand varies according to the position relative to the abutments and the capacity varies according to the state of deformation of the support. Each combination of mining configuration, rock type and support type results in a unique base set within which variation is allowed according to position.

This is achieved by:

- (a) comparing the energy released by the rockmass to the energy absorbed by the support system for a given deformation interval; and
- (b) comparing the rockmass stiffness to that of the support system at any given point of deformation.

The methodology is tested by two case studies on Beatrix Gold Mine. In the first study the condition of unstable failure of the support was evaluated where the support failed and the stope collapsed in a relatively short span of time. This is referred to as unstable failure of the stope. The underground observations were confirmed by the outcome of this study. The energy released by the rockmass, that is rockmass demand, exceeded the capacity of the stope support after a given stage of mining. The absolute value of the rockmass stiffness was also less than the absolute value of the load-deformation curve of the stope support for the same mining interval.

During the second case study some elements of the stope support failed while the excavation remained open and stable. Underground observations again confirmed the model during this study. Here the Pencil Props failed some distance from the stope face. In this case the absolute value of the rockmass stiffness was less than the magnitude of the negative load-deformation curve of the Pencil Props, while the Matpacks have a positive load-deformation behaviour throughout the deformation process. In the latter case the total energy generated by the rockmass never exceeded the capacity of the permanent stope support. This is referred to as stable failure of the stope support.

The study proves that it is possible to evaluate stope support even when a combination of different supports is used as permanent support. The latter is achieved by adding the capacities of the stope support as deformation takes place and comparing that to the rockmass demand for the same mining steps.

KEY WORDS:

1. Stope support
2. Tabular orebody
3. Rockmass demand
4. Support capacity
5. Influencing variables
6. Stability analysis
7. Energy
8. Stiffness
9. Unstable failure
10. Stable failure

ACKNOWLEDGEMENTS

I wish to express my appreciation to the following organisations and persons who made this thesis possible:

| | PAGE |
|---|------|
| 1.1 INTRODUCTION | 1 |
| <ul style="list-style-type: none"> • This thesis is based on a research project on Beatrix Gold Mine where the performance of stope support was evaluated. Permission to use the material is gratefully acknowledged. The opinions expressed are those of the author and do not necessarily represent the policy or opinions of Gold Fields Limited. | 11 |
| 1.2 | 12 |
| <ul style="list-style-type: none"> • Professor J.N. van der Merwe, my supervisor, for his guidance, motivation and support. | 14 |
| 1.3 | 14 |
| <ul style="list-style-type: none"> • For SMT Mining Timber and Grinaker-LTA for the provision of data during the course of the study. | 15 |
| 1.4 | 15 |
| <ul style="list-style-type: none"> • A very special word of thanks to my very special family, my wife Christa, and children Christine, Stefan and Martin for their love, encouragement and support. | 17 |
| 1.5 | 18 |
| <ul style="list-style-type: none"> • A word of thanks to my friends and colleagues for their support and encouragement. | 19 |
| 1.6 | 19 |
| <ul style="list-style-type: none"> • A special word of thanks to my parents for their interest and encouragement. | 21 |
| References - Chapter 1 | 21 |
| | |
| CHAPTER 2 - REVIEW OF PUBLISHED DESIGN METHODOLOGIES | 22 |
| 2.1 INTRODUCTION | 22 |
| 2.2 STOPE SUPPORT AND POLYGENESIS INTERACTION | 22 |
| 2.2.1 Stope and stope support | 22 |
| a. SIMRAC Project GAP32: Stope and stope support | 22 |
| b. Key block analysis using 4-block | 22 |
| c. Review and application of stope support design models | 22 |
| 2.2.2 SIMRAC Project GAP33: Stope face support systems | 22 |
| 2.3 STATUTORY REQUIREMENTS | 22 |
| 2.4 CONCLUSION | 22 |
| References - Chapter 2 | 22 |

| INDEX | | PAGE |
|--|---|------|
| CHAPTER 1 – EVALUATION OF STOPE SUPPORT USING A ROCKMASS STIFFNESS APPROACH | | 1 |
| 1.1 | INTRODUCTION | 1 |
| 1.2 | CONTRIBUTION OF THIS RESEARCH | 7 |
| 1.3 | ROCKMASS BEHAVIOUR | 9 |
| 1.3.1 | The concept of rockmass stiffness | 10 |
| 1.4 | EXCAVATION STABILITY | 11 |
| 1.5 | SUPPORT CHARACTERISTICS – SUPPORT CAPACITY | 13 |
| 1.5.1 | Review of database | 13 |
| 1.5.2 | Mathematical representation of support performance | 14 |
| 1.6 | SUPPORT PERFORMANCE FEATURES | 14 |
| 1.7 | DESIGN METHODOLOGY | 15 |
| 1.7.1 | Established usage | 15 |
| 1.7.2 | Trial and error | 15 |
| 1.7.3 | Empirical observation | 15 |
| 1.7.4 | Comparative empirical simulation | 16 |
| 1.8 | OBJECTIVE OF THESIS | 17 |
| 1.9 | SCOPE OF STUDY | 18 |
| 1.9.1 | Support model | 18 |
| 1.9.2 | Rockmass model | 19 |
| 1.9.3 | Combined model | 19 |
| 1.10 | LAYOUT OF THE THESIS | 20 |
| References – Chapter 1 | | 22 |
| CHAPTER 2 – REVIEW OF PUBLISHED DESIGN METHODOLOGIES | | 25 |
| 2.1 | INTRODUCTION | 25 |
| 2.2 | STOPE SUPPORT AND ROCKMASS INTERACTION | 26 |
| 2.2.1 | Stope and gully support | 27 |
| a. | SIMRAC Project GAP032: Stope and gully support | 27 |
| b. | Key block analysis using J-block | 31 |
| c. | Review and application of stope support design criteria | 32 |
| 2.2.2 | SIMRAC Project GAP330: Stope face support systems | 35 |
| 2.3 | STATUTORY REQUIREMENTS | 36 |
| 2.4 | CONCLUSION | 37 |
| References – Chapter 2 | | 39 |

| | |
|--|----|
| CHAPTER 3 – BASIS FOR THE DESIGN METHODOLOGY | 42 |
| 3.1 OBJECTIVES OF THE DESIGN METHODOLOGY | 42 |
| 3.2 DESIGN METHODOLOGY | 43 |
| 3.2.1 Development of the models | 48 |
| a. Stope support model - Capacity | 48 |
| b. Rockmass model – Demand | 50 |
| c. Combined model | 56 |
| i. Stiffness comparison analysis | 57 |
| ii. Energy comparison analysis | 58 |
| References – Chapter 3 | 60 |
| CHAPTER 4 – STOPE SUPPORT MODEL | 61 |
| 4.1 INTRODUCTION TO THE STOPE SUPPORT MODEL | 61 |
| 4.2 METHODOLOGY ADOPTED FOR DEVELOPMENT OF THE MODEL | 62 |
| 4.2.1 Mathematical representation of laboratory test results | 63 |
| 4.3 FACTORS THAT INFLUENCE SUPPORT PERFORMANCE | 65 |
| 4.3.1 Creep | 65 |
| 4.3.2 Height of pack | 66 |
| 4.3.3 Buckling failure of elongate support | 66 |
| 4.3.4 Pre-stress of support | 67 |
| 4.4 QUANTIFICATION OF INFLUENCE PARAMETERS | 67 |
| 4.4.1 Loading rate effect | 67 |
| a. Lightweight cementitious packs | 67 |
| b. Timber packs | 69 |
| c. Timber elongate support | 72 |
| 4.4.2 Support height factor | 74 |
| a. Lightweight cementitious packs | 74 |
| b. Timber packs | 76 |
| 4.4.3 Buckling failure of timber elongate support | 77 |
| 4.5 ADJUSTED MODEL | 79 |
| 4.5.1 Pack support performance function | 79 |
| 4.5.2 Timber support elongate performance function | 79 |
| 4.6 OUTPUT FROM THE ADJUSTED SUPPORT MODELS | 80 |
| 4.6.1 In-situ load | 80 |
| 4.6.2 Support resistance | 82 |
| 4.6.3 Stiffness of support unit | 82 |
| 4.6.4 Energy absorption capacity | 84 |

| | | |
|-----------------------------|---|-----|
| 4.6.5 | Stress exerted onto hangingwall during quasi-static and dynamic loading | 86 |
| 4.7 | OTHER APPLICATIONS | 87 |
| 4.8 | CONCLUSIONS | 91 |
| | References – Chapter 4 | 93 |
| CHAPTER 5 – ROCKMASS MODEL | | 98 |
| 5.1 | BACKGROUND TO THE STUDY – ROCKMASS STIFFNESS CONCEPT | 98 |
| 5.2 | BACKGROUND TO THE FIRST APPROACHES | 99 |
| 5.2.1 | Instrumentation | 99 |
| 5.2.2 | M-factor approach | 99 |
| 5.2.3 | a. Shortcomings of the M-factor approach | 102 |
| 5.2.3 | b. Elliptical approach | 103 |
| 5.3 | APPLYING THE YIELD LINE THEORY AND CONCEPTS | 105 |
| 5.4 | DEVELOPMENT OF ATTRIBUTED AREA ANALYSIS | 106 |
| 5.4.1 | Introduction | 106 |
| 5.4.2 | Attributed area | 107 |
| 5.4.3 | Magnitude of force component for rockmass stiffness | 111 |
| 5.4.4 | Deformation component of rockmass stiffness | 111 |
| 5.4.5 | Rockmass stiffness representation | 112 |
| 5.5 | FACTORS INFLUENCING ROCKMASS STIFFNESS MODEL | 113 |
| 5.6 | CONCLUSIONS | 113 |
| | References – Chapter 5 | 115 |
| CHAPTER 6 – COMBINED MODELS | | 116 |
| 6.1 | PRINCIPLE OF SUPERIMPOSED DATA | 116 |
| 6.2 | STABILITY TEST | 117 |
| 6.2.1 | Stiffness comparison | 118 |
| 6.2.2 | Energy comparison | 118 |
| 6.3 | INPUTS AND ITS INFLUENCE ON THE COMBINED MODEL | 119 |
| 6.3.1 | Demand - Rockmass model | 120 |
| | a. Layout and configuration of underground mining environment | 120 |
| | b. Stope face position for successive mining intervals | 121 |
| | c. Position and presence of regional support | 121 |
| | d. Physical position of point of interest in stope | 122 |
| | e. Closure at the point of interest for different mining | |

| | | |
|---------------------------------------|--|-----|
| 9.1.3 | Back intervals | 122 |
| 9.1.4 | f. Hangingwall beam thickness | 123 |
| 6.3.2 | Capacity - Stope support model | 125 |
| 9.2.1 | a. Rate of deformation | 126 |
| 9.2.2 | b. Height of pack tested versus installed | 126 |
| 9.2.3 | c. Buckling failure of timber elongate support | 126 |
| 9.2.4 | d. Installation spacing of support | 126 |
| 9.2.5 | e. Support pre-stressing | 127 |
| 6.4 | CONCLUSION | 128 |
| | References – Chapter 6 | 129 |
| CHAPTER 7 – CASE STUDIES | | 130 |
| 7.1 | INTRODUCTION | 130 |
| 7.2 | CASE STUDY 1: 15A47 STOPE – UNSTABLE SUPPORT FAILURE | 131 |
| 7.2.1 | Support capacity | 131 |
| 7.2.2 | Rockmass demand | 132 |
| a. | Stability analysis | 132 |
| 7.3 | CASE STUDY 2: 23A79 STOPE – STABLE SUPPORT FAILURE | 139 |
| 7.3.1 | Support capacity | 139 |
| 7.3.2 | Rockmass demand | 140 |
| a. | Stability analysis | 143 |
| 7.4 | CONCLUSION | 146 |
| | References – Chapter 7 | 147 |
| | APPENDIX 1 | 148 |
| CHAPTER 8 – CONCLUSION FROM THE STUDY | | 150 |
| 8.1 | INTRODUCTION | 150 |
| 8.2 | STOPE SUPPORT CAPACITY | 150 |
| 8.3 | ROCKMASS DEMAND | 152 |
| 8.4 | COMBINED MODELS | 153 |
| 8.5 | FUTURE WORK | 154 |
| | References – Chapter 8 | 156 |
| CHAPTER 9 – GLOSSARY OF TERMS | | 157 |
| 9.1 | DESIGN AREAS FOR SUPPORT | 157 |
| 9.1.1 | Face area | 157 |
| 9.1.2 | Working area | 158 |

| | | |
|------------------------|---|-----|
| 9.1.3 | Back area | 158 |
| 9.1.4 | Remote back area | 158 |
| 9.2 | SUPPORT TYPES AND AREAS IN WHICH USED | 158 |
| 9.2.1 | General | 158 |
| 9.2.2 | Elongates | 160 |
| 9.2.3 | Timber packs | 161 |
| 9.2.4 | Cementitious packs | 162 |
| 9.2.5 | Reef pillars | 162 |
| References – Chapter 9 | | 164 |
| Figure 1.4 | Principles of rock support; interaction for a tunnel | 11 |
| Figure 3.1 | Fracturing around a stope (after Roberts and Breckenridge) | 41 |
| Figure 3.2 | Unstable and stable failure of rock specimens in soft and stiff testing machines | 49 |
| Figure 3.3 | Illustration of the elliptical fit to a rock specimen geometry | 52 |
| Figure 3.4 | Yield lines shown for square and rectangular packs | 55 |
| Figure 3.5 | Yield lines for a cone underground geometry (vs Figure 3.3) | 57 |
| Figure 3.6 | Mining geometry showing attributes of area | 58 |
| Figure 3.7 | Graphical representation of load line deviation; rockmass behaviour | 56 |
| Figure 3.8 | Graphical representation of ridge use in a box and stope support models on compressive force-deformation axes | 57 |
| Figure 3.9 | Combined models illustrating failure of supports | 58 |
| Figure 3.10 | Graphical representation of unstable failure of a support system | 58 |
| Figure 4.1 | Mathematical fit to laboratory data of a solid Hailgun Matpack | 64 |
| Figure 4.2 | Mathematical fit to laboratory data of a Wedge Prop | 63 |
| Figure 4.3(a) | Y-Factor for timber, lightweight concrete packs and elongates for quasi-static loading conditions | 71 |
| Figure 4.3(b) | Y-Factor for timber, lightweight concrete packs and elongates under rapid loading conditions | 71 |
| Figure 4.4 | Force correction factor for timber elongates as developed by | 72 |
| Figure 4.5 | Correlation between quadratic Y-factor and LDM correction | 74 |
| Figure 4.6 | Sustained load and mathematical representation of the peak data for different heights of cementitious packs | 75 |
| Figure 4.7 | Prediction of a 1.1 m high solid matpack from different heights of packs | 75 |

LIST OF FIGURES

| | PAGE |
|---------------|------|
| Figure 1.1 | 4 |
| Figure 1.2 | 4 |
| Figure 1.3(a) | 5 |
| Figure 1.3(b) | 6 |
| Figure 1.4 | 11 |
| Figure 3.1 | 41 |
| Figure 3.2 | 44 |
| Figure 3.3 | 52 |
| Figure 3.4 | 53 |
| Figure 3.5 | 54 |
| Figure 3.6 | 55 |
| Figure 3.7 | 56 |
| Figure 3.8 | 57 |
| Figure 3.9 | 58 |
| Figure 3.10 | 58 |
| Figure 4.1 | 64 |
| Figure 4.2 | 65 |
| Figure 4.3(a) | 71 |
| Figure 4.3(b) | 71 |
| Figure 4.4 | 72 |
| Figure 4.5 | 73 |
| Figure 4.6 | 74 |
| Figure 4.7 | 77 |

| | | |
|---------------|---|-----|
| Figure 4.8 | Effect of buckling on the performance of a Profile Prop | 78 |
| Figure 4.9 | Laboratory and in-situ performance of a Brick Composite Pack | 80 |
| Figure 4.10 | Effect of loading rate and buckling on load generated by a | 81 |
| Figure 4.11 | Profile Prop of strain hardening and strain softening of supports | 81 |
| Figure 4.11 | Difference in stiffness of laboratory and in-situ performance of a Brick Composite pack | 83 |
| Figure 4.12 | Effect of rate of deformation and buckling on the performance of a Profile Prop | 84 |
| Figure 4.13 | Effect of load rate and support height on energy absorption capacity of a Brick Composite pack | 85 |
| Figure 4.14 | Damage to stope hangingwall during a rockburst with a stiff type of stope support | 86 |
| Figure 4.15 | Schematic layout of area modelled for determining modified Young's Modulus | 88 |
| Figure 4.16 | Support resistance contours for Hercules type of timber pack | 90 |
| Figure 5.1 | Illustration of elliptical fit to a mining geometry | 104 |
| Figure 5.2 | Yield lines for Figure 5.1 layout | 105 |
| Figure 5.3(a) | Regional support represented by a single point | 107 |
| Figure 5.3(b) | Line demarcating attributed area between point of interest and solid abutment | 108 |
| Figure 5.3(c) | Attributed line for two parts of a slab | 108 |
| Figure 5.3(d) | Attributed line for a slab supported on the edge of an abutment with regional support in the area | 109 |
| Figure 5.3(e) | Attributed lines for a solid abutment, regional pillar and measuring station | 109 |
| Figure 5.3(f) | Attributed line dividing the corner at an abutment | 110 |
| Figure 5.4 | Mining geometry showing load attributed area | 110 |
| Figure 5.5 | Load line representing rockmass behaviour | 112 |
| Figure 6.1 | Graphical representation of rockmass and stope support models | 117 |
| Figure 6.2 | Combined models demonstrating unstable failure of support | 118 |
| Figure 6.3 | Excessive energy released by rockmass | 119 |
| Figure 6.4 | Attributed area at point of interest | 120 |
| Figure 6.5 | Decrease in rockmass stiffness for consecutive mining steps | 121 |
| Figure 6.6 | Two-dimensional mining slot showing closure at different positions | 122 |
| Figure 6.7 | Rockmass stiffness history for a measuring station | 123 |
| Figure 6.8(a) | Effect of increased beam thickness on rockmass stiffness with | |

| | | |
|---------------|---|-----|
| | Same deflection | 124 |
| Figure 6.8(b) | Effect of increased beam thickness on rockmass stiffness with same attributed area force | 124 |
| Figure 6.9 | Illustration of strain hardening and strain softening of supports | 125 |
| Figure 6.10 | Graphical representation of rockmass and support models for the 5 th stage of mining | 127 |
| Figure 6.11 | Effect of timber creep on performance of a Profile Prop | 128 |
| Figure 7.1 | Load-deformation curve for the Beatrix end-grain pack | 131 |
| Figure 7.2 | Layout and mining steps of the 15A47 Stope | 132 |
| Figure 7.3 | Stope closure at the measuring stations – 15A47 Stope | 134 |
| Figure 7.4(a) | Voussoir beam model for a roof bed after Kotzé | 135 |
| Figure 7.4(b) | Forces operating voussoir beam system | 135 |
| Figure 7.5 | Voussoir beam analysis for Beatrix Mine after Kotzé | 136 |
| Figure 7.6 | Rockmass-support interaction for the 15A47 Stope | 136 |
| Figure 7.7 | Load-deformation curve for a Pencil Prop for 23A79 Stope | 139 |
| Figure 7.8 | Load-deformation curve for a Matpack for 23A79 Stope | 140 |
| Figure 7.9 | Layout and mining steps of the 23A79 Stope | 140 |
| Figure 7.10 | Stope closure at the measuring stations – 23A79 Stope | 141 |
| Figure 7.11 | Rockmass and stope support interaction at Station 1B (23A79) | 143 |
| Figure 7.12 | Comparison of rockmass stiffness for 15A47 and 23A79 Stopes | 145 |
| Figure 9.1 | Mechanism of the Q-block after Jeppe (1946) | 159 |

LIST OF TABLES

CHAPTER 1

| EVALUATION OF STOPE SUPPORT USING A BUSINESS STRESS APPROACH | | PAGE |
|--|---|------|
| Table 4.1 | Modified Young's Modulus for different closure rates | 89 |
| Table 4.2 | Constants of polynomials for pack and elongate types of support | 95 |
| Table 5.1 | M-factor for the 15A47 Stope | 101 |
| Table 7.1 | Summary of closure and closure rates for 15A47 Stope | 133 |
| Table 7.2 | Summary of attributed areas for measuring stations – 15A47 | 134 |
| Table 7.3 | Stability analysis summary for Station 1 – 15A47 Stope | 138 |
| Table 7.4 | Summary of closure and closure rates for 23A79 Stope | 141 |
| Table 7.5 | Summary of attributed areas for measuring stations – 23A79 | 142 |
| Table 7.6 | Stability analysis summary for Station 1B – 23A79 Stope | 144 |

CHAPTER 1

EVALUATION OF STOPE SUPPORT USING A ROCKMASS STIFFNESS APPROACH

1.1 INTRODUCTION

As early as in 1556 Georgius Agricola described in his book *De Re Metallica* the total mining process from the exploration phase to the extractive metallurgical processes for different minerals, as it is known today. He describes in much detail each step and process from the exploration, the functions of each of the Officers from the Mining Prefect that is appointed by the King, the Bergmeister that oversees the mining practices and who reported to the Mining Prefect, the Mine Manager, the Foreman (Shiftboss as we know it today) as well as that of the Miner, including all the services that are related to the above including that of the Surveyor and the Clerk of the Bergmeister.

Agricola identified certain geotechnical environments but did not have the means or the technical knowledge that we have today to address the problems he encountered. He refers to the geotechnical properties of the rockmass as being “crumbling”, “hard”, “harder” and “hardest.” He also stated: “Since the whole mountain, or more especially the whole hill, is undermined, it is necessary to leave the natural pillars and arches, or the place is timbered”. This will be described as pillars i.e. regional support in today’s terminology.

He further went on to say: “But sometimes when a vein is very hard it is broken by the fire, whereby it happens that the soft pillars break up, or the timbers are burnt away, and the mountain by its great weight sinks into itself, and then the shaft buildings are swallowed up in the great subsidence. Therefore it is advisable to sink some shafts which are not subject to this kind of ruin, through which the materials that are excavated may be carried out, not only while the pillars and underpinning still remain whole and solid, but also after the supports have been destroyed by fire and have fallen”. We would refer to this as mining layout and having a second outlet.

In the latter part of the book he simplistically states that the rockmass in a shaft or tunnel that is “crumbling” to “hard” requires “more timbering” than the other and that in some instances the “harder” and “hardest” rocks do not require any support at all. It is evident that timber played a major part in the mining process since it was advisable that a mine be situated where trees and water were readily available. The timber was

required for support of the shafts and tunnels while the water was essential for the washing process during the extraction of the minerals from the ore.

Interesting to note is the fact that there were even then the critics that claimed: "..... mining is a perilous occupation to pursue, because the miners are sometimes killed by pestilential air which they breathe; sometimes their lungs rot away; sometimes the men perish by crushed in masses of rock; sometimes, falling from the ladders into the shafts, they break their arms, legs, or necks; and it is added that there is no compensation which should be thought great enough to equalise the extreme dangers to safety and life". He went on to say that: "These occurrences, I confess, are of exceeding gravity, and moreover, fraught with terror and peril, so that I should consider that the metals should not be dug up at all, if such things were to happen very frequently to the miners, or if they could not safely guard against such risks by any means. Who would not prefer to live rather than to possess all things even metals?"

Throughout the history of the mining industry the support of the underground excavations has remained one of the primary activities not only for the stability of the workings, but also ensure the safety of the workforce. The material used for the support of these excavations has to be available in sufficient quantity and in close proximity to the mine while at the same time cost effective. Timber was used as support from the days of Agricola and even today still forms the major component of stope support in the South African gold and platinum mines.

Timber has also been used for the support of stopes and auxiliary excavations since the discovery of gold on the Witwatersrand. At present a variety of timber and concrete packs and props are still in use in both shallow and deep mines.

Stope support design is one of the more complex design issues in the field of mining engineering. The objective of stope support has never changed from the early days of shallow gold mining on the Witwatersrand until now. The aim has always been to ensure the stability of the underground excavation and in so doing create a stable, safe and production friendly working environment for the underground workforce.

Stope support is to be designed in a way that it meets the requirements of different conditions underground. The selection of stope support type in the early days was based on mining experience as well as knowledge and interpretation of local underground rock conditions. The support materials used were those that were readily

available in volume in relatively close proximity to the mining operation at reasonable cost.

In those early days the miners practised some of the important concepts that are generally accepted in stope support design methodology today. Miners were for instance aware of the need for pre-stressing of stope support during installation, and one development that satisfied this need was the development of the so-called "Q-block." Limitations of ordinary timber props or sticks were also realised early on. According to Jeppe (1946) attempts to overcome the lack of yieldability in a stick was achieved by sharpening one end of the stick to induce yield at a lower load. Jeppe also reported favourably on a compressible pipe support filled with sand.

No evidence could be found in literature that a rigorous engineering approach was adopted in the design of stope support during the early days of gold mining in the Witwatersrand.

Stope support is designed for the following areas of interest:

- Face area;
- Working area;
- Back area; and
- Remote back area.

The definitions of those areas are described in the Glossary of Terms, Chapter 9.

According to the information obtained from the Department of Minerals and Energy (2002) the current rock production from the gold and platinum mining industries in South Africa is some 180 million tons per annum. It is predominantly produced from stopes that require support of some type. This production relates to an annual expenditure of just over R1 Billion per annum (Kruger, 2002) for the support of these on-reef excavations.

It is believed that the work described in this thesis will contribute towards a safe and production friendly production environment. Much progress has been made over the past number of years in reducing the rockfall accidents for all mining sectors, as illustrated in Figure 1.1. The fatalities that are related to seismicity show an increasing trend for the same period. The 2002 data is a projection from January to May for the

same year. It is for this reason that the mining industry will continuously strive to improve safety and it is believed that this thesis may contribute towards a better understanding of the rockmass-support interaction.

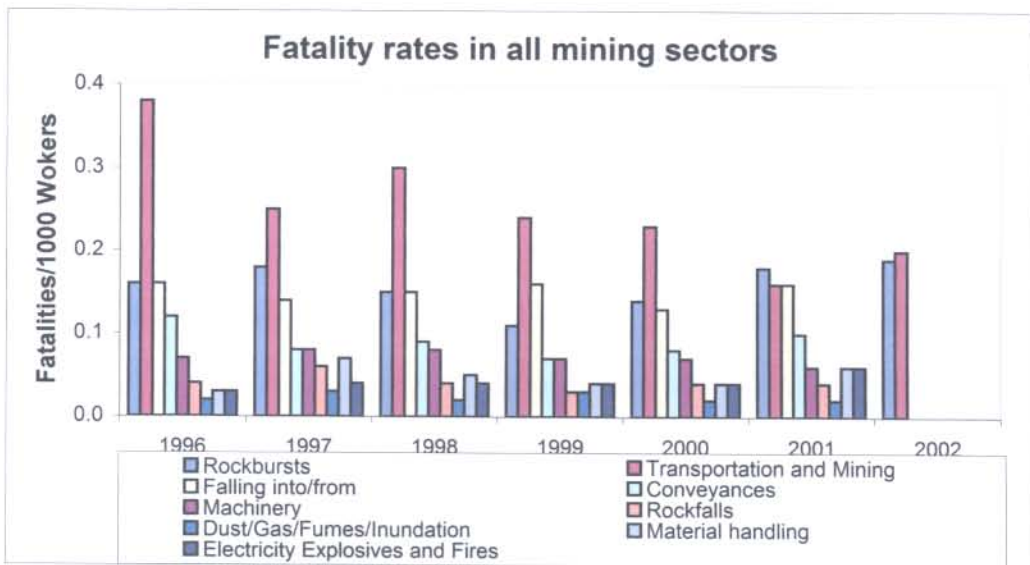


Figure 1.1: Fatality rates for different categories for all mining sectors from 1996 to 2002

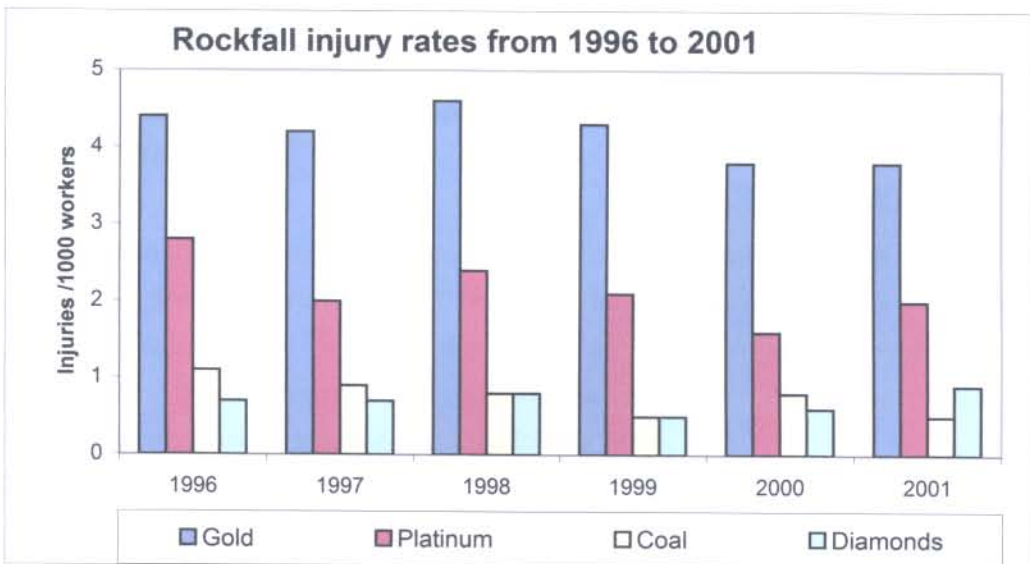


Figure 1.2: Rockfall injury rates for the four largest mining commodity sectors for 1996 to 2001

The majority of the rockfall accidents occur in the gold and platinum mining sectors, as shown in Figure 1.2.

The stope face is the focus for the design of support that is described in this thesis. Figures 1.3(a) and 1.3(b) confirms that the majority of the accidents occur on the stope face. This research may contribute to improve on the safety through a proper understanding of the ability of the support to react to the support demand required from the rockmass.

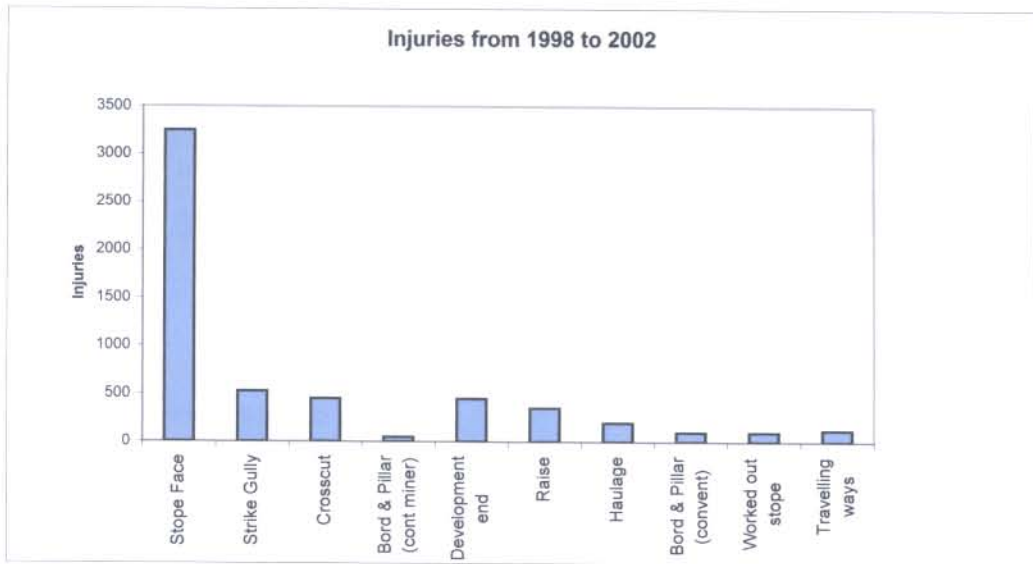


Figure 1.3(a): Rock related (including rockfall and rockburst) injuries by working place from 1998 to 2002

The primary function of support installed in a stope is to maintain the continuity and integrity of the fractured hangingwall beam in the stoping area. This is achieved by applying a sufficient force to the immediate hangingwall so as to generate frictional forces between individual segments of the hangingwall beam. The support must be able to perform this while experiencing varying closure rates.

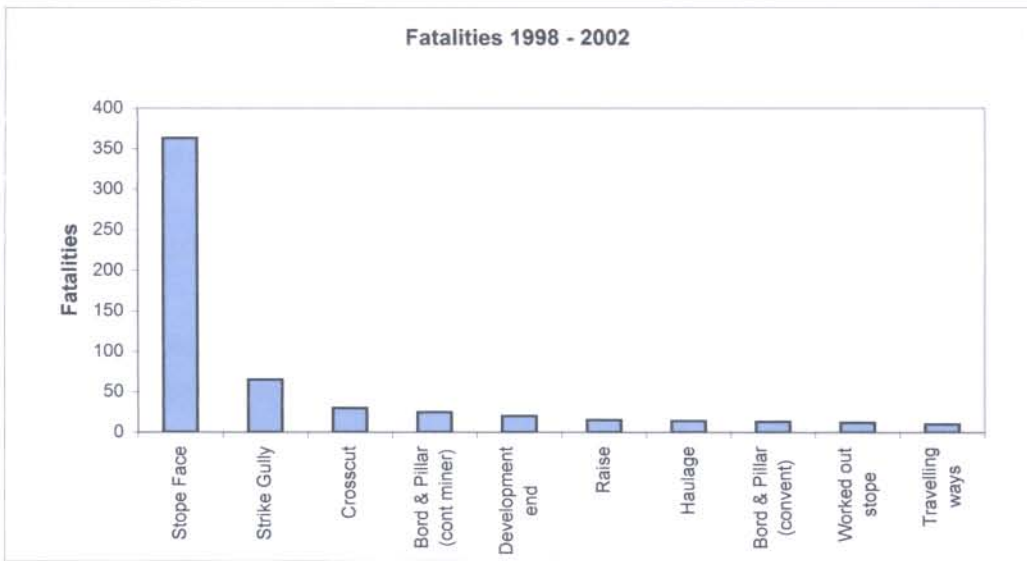


Figure 1.3(b): Rock related (including rockfall and rockburst) fatalities by the working place from 1998 to 2002

Support in the mining industry is divided into a number of categories. The support types used in the mining industry can be categorised according to:

Function of support

- Temporary support;
- Permanent support;

Characteristics of support

- Stiff support;
- Soft support;
- Active support;
- Passive support;

Position of support

- Face support;
- Regional support;

Description of support

- Tendon support;
- Elongate type of support;
- Props;
- Sticks;
- Timber packs;

- Cementitious packs; and
- Reef pillars.

These are listed and defined in the Glossary of Terms, Chapter 9.

1.2 CONTRIBUTION OF THIS RESEARCH

The stability analysis described in the thesis investigates the stability of the stope as this impacts on both the safety of the workforce and the stability of the stope as the single most important excavation.

The research includes most of the support types used in the South African mining industry today and investigates and evaluates stope support for the stope as a district. It includes the face area, working area, back area and remote back area.

The support that is investigated for the purpose of stability analysis at any one time depends on the loading, which is determined by the so-called attributed area that is considered by this design process.

The attributed area as described in Chapter 5 is determined in a manner that the influence of stope abutments and regional support is taken into account. All support types that are installed in these areas are taken into consideration as well as the factors influencing their performance. The in-situ performance or capacity of stope support is used in the analysis process. This is compared to the demand placed on the support from the model describing rockmass behaviour.

The following is a summary of issues described by the research to address some of the current shortcomings of stope support design in the field of rock engineering:

- The methodologies described in the thesis take into consideration the support demand from the rockmass, considering rockmass behaviour, as well as the performance or capacity that the stope support units can offer. Both are considered as variables according to the position relative to the stope face and other abutments and the state of deformation of the support. Factors influencing both of these are described mathematically and incorporated into the final model where the impact of these on excavation stability is evaluated. The outcome of the analysis are expressed and compared on a common x-y axis.

- The approach is a novel one describing rockmass behaviour in terms of the stiffness of the surrounding rockmass in comparison to the stiffness of the support element at different stages of deformation.
- Strain softening of a support unit forms an integral component of the design. This characteristic of slope support has been neglected in the past during the design process. No evidence could be found in literature where strain softening is determined and its effect on excavation stability analysed. The important role of this phenomenon in the design and analysis of support is illustrated in the thesis.
- The model that is developed takes into account the varying performance characteristics of a support unit(s) during the process of its deformation. It includes aspects such as load generated by the support unit, varying stiffness and energy absorption capacity. Esterhuizen (1996) developed a three-dimensional design methodology that is available to the rock engineer as a design tool is one of the models. This model only takes into account the presence and position of support units in relation to the slope face.
- As far as could be established in literature, this is a first where the performance characteristics of support elements are described and presented in a mathematical format. This provides a tool in the hand of the rock engineer that could be viewed as similar to a seismic waveform that is described through a Fourier transformation. By manipulation of the mathematical equation it is possible to generate the source parameters and characteristics of that particular event. The approach described in the thesis makes it possible that the support performance function is manipulated mathematically to compensate for factors that influence its performance and present the real or in-situ performance of the unit.
- The methodology takes face shape and presence and position of regional support into consideration. The support design methodology that is proposed is simple to use and does not require time-consuming numerical computer modelling. It would be attractive as a design tool to rock engineering practitioners in general.
- The mathematical equations that have been developed can be used with current pseudo three-dimensional numerical design programs such as Minsim W in order to compare various support types. In-situ support resistance generated by a

support system that is installed at any given spacing can be calculated and contoured in this way. This is achieved by dividing the support performance function by the tributary area supported by each support unit. It takes face shape and presence and position of regional support into consideration.

1.3 ROCKMASS BEHAVIOUR

A substantial amount of research has been done in the mining industry with the objective to describe and predict rockmass behaviour. It seems unfortunate that this work has never been incorporated into a three dimensional design procedure that could be used by rock engineering practitioners for stope support design. Brummer (1985) described the behaviour of the immediate hangingwall of a stope by dividing the hangingwall into triangular blocks or wedges. Even though this work generated valuable insight into the behaviour and failure of the stope hangingwall, the analysis is restricted to two dimensions.

Backfill is probably one of the fields most thoroughly researched in terms of support and its interaction with the stope hangingwall. Although the majority of these papers do not explicitly describe hangingwall behaviour, Goldbach (1991) has done valuable research in quantifying ground motion by analysing the effect of backfill on the rockmass in comparison to conventional (unfilled) supported stopes. The results from this study together with work on ground motion analysis in backfilled stopes, show how backfill can reduce the overall ground motion during seismic events. The in-situ modulus of the rockmass has also been determined by Gurtunca and Adams (1991) through the use of backfill instrumentation.

The research described in the thesis is an attempt to describe rockmass behaviour by quantifying the rockmass stiffness at a given point in space and in time for a given mining geometry and layout. The strata stiffness can be calculated for different mining stages and geometry with varying rates of closure and different support types at any point of interest. The analysis can include both areas with and without regional support. The interaction of the stope support and the rockmass for a number of case studies is evaluated and the outcome of the stability analysis compared to underground observations.

1.3.1 The concept of rockmass stiffness

This research is aimed at developing a better understanding and description of the interaction that exists between the rockmass and stope support. This is investigated from an original and novel approach utilising the concept of rockmass stiffness and is an innovative approach applied in the scope of stope support evaluation.

The concept of rockmass stiffness forms the basis for the design methodology described in the thesis. In literature only some reference is made to the concept of strata stiffness with regard to rockmass behaviour. Ozbay and Roberts (1988) discussed pillar failure and referred to “possible load lines” during an analysis of yield pillars in stopes. No definite or fixed values for the stiffness of the load lines is quoted, but the comment made that the more pillars there are, the stiffer the strata. This statement is confirmed in this research, where values for the stiffness of strata are quoted.

Ryder and Ozbay (1990) focus on a methodology for the analysis and design of a pillar-mining layout. It was stated that the strata stiffness is nominally a property of the strata alone, and is in fact directly proportional to the Young's modulus of the strata. They confirm and also suggested that strata stiffness is a very complex concept. This research shows that the strata stiffness underground is strongly influenced by the geometry of mining and in particular by the number and position of regional support pillars. Ryder and Ozbay (1990) accepted the latter but no further comments were made, or values for the stiffness of the strata quoted in their work. They accepted that as the number of pillars subject to collapse increases, so the governing critical strata stiffness tends to decrease; generating conditions less and less favourable for stability. In the limit, for a very large mined out area featuring no regional support, the strata stiffness approaches zero; thus implying regional collapse if the pillars are overloaded and exhibit any post-failure negative slope. This statement that was made by these two authors is confirmed by this research.

The stope hangingwall is not taken as an elastic homogeneous rockmass with a linear rate of deformation from the stope face towards the back area as is the case with the stope and gully support design. In this research the actual closure is taken at a point of interest during different intervals of mining and the strata stiffness calculated for each mining step. The geometry of the underground layout is also taken into account during the analysis as well as the position and presence of regional support. This is seen as a very important aspect in the design of stope support and believed to be a

limitation of the other design methodologies. It is believed to be unique to the work described in the thesis and this methodology may therefore be classed as fully three-dimensional.

1.4 EXCAVATION STABILITY

The stability of the underground excavation is of utmost importance not only for the safety of the workforce and protection of equipment, but also to ensure a continuous and uninterrupted production cycle. The interaction of the support and the rockmass is not unique to this study and has been studied by a number of authors.

One of the more prominent of these previous studies is the rock-support interaction for tunnels that is described by Hoek and Brown (1980) and Brady and Brown (1985). The interaction between the support and the rockmass for a *tunnel* is represented by means of the *required support lines* for the excavation walls and the support reaction or *available support lines* and presented on a common support pressure-tunnel deformation axes as illustrated in Figure 1.4.

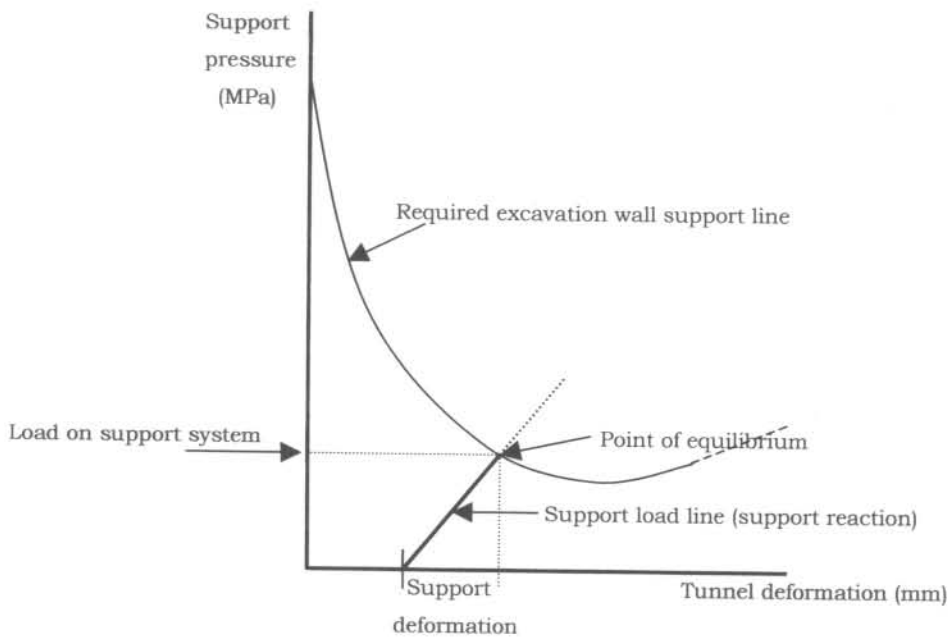


Figure 1.4: Principles of rock-support interaction for a tunnel, after Hoek and Brown (1980)

University of Pretoria etd – Pretorius, M J (2006)

The support for a tunnel typically loads along a path such as shown in Figure 1.4 and is known as the support reaction or available support line. The curve representing the behaviour of the rockwalls is known as the ground characteristic or required support line. Equilibrium between the rock and the support is reached at the point of equilibrium as illustrated. The major role of the support and reinforcement is thus to control the rock displacements. The stiffness of the support element, its strength and the time of installation of the support have an important influence on this displacement control, and hence the stability of the tunnel.

The concept of evaluating support based on the interaction of support units and the rockmass, is not new. However, the concepts have not yet been applied to tabular stope excavations and the various parameters have not been quantified in real situations.

In the study described in this thesis, the rockmass is not approached as a homogeneous, isotropic and elastic medium as assumed in elastic numerical modelling, but fails in a number of different ways. The prediction and description of rockmass failure is complex and difficult to describe and quantify. To ensure the stability of the underground excavation and improve the safety of the workforce it is essential that the in-situ performance of different support elements in different localities relative to the stope face be predicted for the accurate design of a support system. It is of paramount importance that the mode of failure of each of these elements be properly understood and addressed.

Stope support units have a finite strength depending on its dimensions and the type of material from which the unit is constructed. Support will yield and fail in different ways during the process of deformation. The support-rockmass interaction that is presented in the thesis focuses on the rockmass load line that describes the way in which the support is loaded by the rockmass during successive stages of mining. The reaction of the support is described and the mode of failure is determined. This failure can take place in either a controlled- or uncontrolled fashion.

1.5 SUPPORT CHARACTERISTICS – SUPPORT CAPACITY

1.5.1 Review of database

The Support Catalogue that was published as part of the SIMRAC GAP032 research project by CSIR Mining Technology (1995) was used as database from which the base support curves of the different elements were extracted. These were then adjusted to reflect in situ behaviour. The laboratory load-deformation test curves were used showing the load generated by the support element in kilonewton versus deformation in millimetres. The support type, height of support unit tested and the test rate of deformation (mm/minute) are also published in the database.

This Support Catalogue is widely used as database for support test curves in the mining industry. Curves of the more popular support types used in mining industry and in particular the ones for the areas of interest for the research were utilised. Some of the packs that are described were however developed subsequent to the publication of the Support Catalogue. Laboratory test results in such cases were obtained from the manufacturer.

The characteristics of the various support elements are described by studying their load-deformation curves. From these curves the initial stiffness, load bearing capacity whilst deformation takes place, post failure stiffness and energy absorption ability of the support can be determined and compared to other support units. These characteristics are summarised and defined as the support *capacity* of a support unit.

The database used in the thesis includes a variety of timber- and timber composite packs, lightweight cementitious packs, timber elongates and sticks with varying base dimensions, diameters and heights.

This information becomes of particular interest when adjustments are made to the laboratory performance of the support elements to quantify the in-situ behaviour of such an element. This process is described in detail in Chapter 4.

1.5.2 Mathematical representation of support performance

The curves in the Support Catalogue produced by the CSIR Division of Mining Technology as part of the GAP032 SIMRAC research project are used to describe the behaviour of stope support mathematically. Polynomials of the n^{th} order are fitted to the curves of the most popular support elements used in the mining industry at the time. Pretorius (1995) showed that the force generated by a support element could be expressed as a function of its deformation by a mathematical equation. This approach makes it possible that the equation be manipulated mathematically to compensate and quantify the influence that different parameters have on support performance.

A load at deformation intervals of 5 millimetres or less was taken so that an accurate representation of the laboratory result could be produced mathematically. This was repeated for all the support elements of interest and the data tabled in load-deformation (x-y) co-ordinates. The support curve is reproduced mathematically by fitting an n^{th} order polynomial to the x-y co-ordinates. In most cases a sixth order polynomial produced the most accurate representation of the laboratory curve. These functions are described in Chapter 4.

The factors that influence the performance of a support element were also described in a mathematical format. These factors are the pre-stress force during installation, rate of deformation, creep, influence of the height of pack installed as opposed to the one tested and buckling potential in the case of a timber elongate type of support. This mathematical function is combined with the original support function into what is referred to as the combined or adjusted mathematical function for support. The adjusted functions are all described in Chapter 4.

1.6 SUPPORT PERFORMANCE FEATURES

The performance characteristics that are calculated for a support element represents the in-situ performance of each unit taking into consideration the factors that influence its performance. The function is manipulated mathematically so that the following performance features can be determined through the analysis:

1.6.1 In-situ load generated by the support element; (kN)

1.6.2 Support resistance generated by the support element; (kN/m²)

1.6.3 Stiffness of support (both strain hardening and softening); (kN/mm)

1.6.4 Energy absorbed by the support element for a given deformation interval; (kJ) and

1.6.5 Stress exerted onto rockwalls during quasi-static or dynamic loading. (MPa)

1.7 DESIGN METHODOLOGY

Design methodologies that are commonly practised in the mining industry are the following:

1.7.1 Established usage

This is done by establishing what type(s) of support is successfully used elsewhere in the industry under conditions similar to the one being investigated. For this method to be successful is it important that the underground conditions be comparable and that ground conditions be of similar geotechnical classification. This method is commonly practised in the South African mining industry.

1.7.2 Trial and error

This is one of the more popular methodologies used in the South African mining industry for many years. The fact that stope support is such a complex design issue makes this a very attractive option. With this methodology different support elements are put on trial and their performance monitored carefully. Alterations and modifications are made to the support system on a continuous basis when and if required. This could in a way be compared to the New Austrian Tunnel Method (NATM) where support is adjusted after certain underground conditions are observed.

1.7.3 Empirical observation

In this case the rock engineer relies on what he can observe and measure from experiments and underground trials rather than design strictly according to a stope support design theory or prescribed methodology. This methodology is practised quite often especially with the design and development of new types of support. The underground support spacing is altered on an ongoing basis until such time that the rock engineering practitioner is confident that the support satisfies set criteria that are often not quantified but based on underground observation and experience. The spacing of the support elements is often determined and influenced by practical

considerations such as the lower limit for strike support spacing in breast mining that is often dictated by the width of the face scraper.

1.7.4 Comparative experimental simulation

Testing of support elements is nothing new, and not unique to the mining industry of today but was done by Bowden in the early 1900's. Extensive load-compression tests have been done on all types of packs including concrete reinforced packs. He highlighted for instance the effect of timber density on pack performance. This led to the conclusion then that timber support elements could be constructed in a way that it is as effective as any other of the support combinations tested.

The fact was even then identified that the support characteristics determined from laboratory tests are different to the underground performance of that same unit. Research at the time by Riemann (1986) indicated that the load bearing ability of timber supports from conventional laboratory tests does not provide reliable information for predicting underground performance.

Roberts, Jager and Riemann (1987) and Taggart (1996) have done valuable work since then to quantify the effect that loading rate has on the performance of both timber packs and timber elongates. The relevant adjustment factors were determined and described. These factors have been included in the thesis while the remainder were developed and mathematical models drawn up to describe the effect that it has on the performance of support elements such as cementitious and composite types of support.

Probabilistic keyblock analyses by Daehnke et al (1998) have shown that, for a typical discontinuity spacing and attitude as encountered in intermediate- and deep-level gold mines, the support spacing in the dip direction can be increased by a factor of approximately 1.5 of the strike spacing, while maintaining an equal probability of keyblock failure in the dip versus the strike direction. It is therefore recommended in general that the support spacing in the dip direction should not exceed 1.5 times the spacing in the strike direction.

1.8 OBJECTIVE OF THESIS

In spite of the many advances that have been made in the fields of numerical modelling and rock mechanics the behaviour of the hangingwall of a stope is still not fully understood. Several anomalies exist between the observed behaviour of the rock in the immediate hangingwall of a stope, and the predictions of the various modelling techniques currently available to the industry.

It is essential that the behaviour of the hangingwall, and in particular the interaction between the hangingwall rockmass and the support system be better understood to effectively design stope support.

A study of the behaviour of a rockmass and expressing that in terms of exact scientific values is almost impossible. No firm scientific figures can be quoted for any rockmass and exact rockmass behaviour predicted from that. A rockmass will not repeatedly react in exactly the same manner under similar conditions.

The different approaches taken by researchers and engineers to produce an "all-inclusive" model for stope support design reflect the complexity of this topic. The current study on stope support design was initiated during years of careful observation of different stope support types and its reaction during various stages of mining at varying depths for both quasi-static and dynamic loading conditions.

The thesis is an attempt at developing an engineering design approach for stope support that will address at least some of the limitations of other methods. It is done with the aim to describe both the capacity of a support system and compare that to the demand placed on a support system by the underground excavation it is intended to support.

Much emphasis is placed on the interaction that exists between stope support and its immediate hangingwall, introducing concepts of support- and rockmass stiffness and energy absorption capacity. Both the behaviour of stope support and that of the surrounding rockmass are analysed for different mining geometries at varying stages of mining.

The author believes that the research done and presented in the thesis can quantify and reproduce to some extent aspects of the behaviour of stope support observed

underground. Limitations perceived to exist in the mining industry and particularly with regard to the design of stope support are addressed. It is believed that this work will contribute towards a better understanding, analysis and design of stope support in the discipline of rock engineering.

The last phase of the thesis contains descriptions that will enable the design engineer to perform his/her own evaluations by varying some or all of the parameters like:

- The geometry of the underground excavation;
- Point of interest within the underground excavation;
- Presence and position of regional support;
- Stope width;
- Rate of closure;
- Support spacing; and
- Hangingwall beam thickness.

The influence that the above have on the stability of the excavation is determined qualitatively.

One of the major contributions of this research towards the discipline of rock engineering design is the ability to represent both rockmass demand and support capacity on common axes and test for stability by varying parameters that are common and influence both.

1.9 SCOPE OF STUDY

1.9.1 Support model

The main objective of the thesis can be summarised as developing a stope support design and analysis methodology. The study comprises three phases of models to compare the demand imposed on stope support by the rockmass to the capacity of the support.

A stope support model is developed to describe the behaviour or performance of stope support mathematically. A number of factors influence the performance of stope

support elements. These factors are also described in a mathematical format to compensate for it.

This process makes it possible that adjustments can be made to the original mathematical model describing the support element to compensate for any of the influences. The final combined mathematical equation gives a representation of the in-situ performance of the support element under discussion.

1.9.2 Rockmass model

The aim of the second model, that is the rockmass demand model, is to describe rockmass behaviour in a way that it can be linked directly to the stope support model.

The manner in which this is achieved is by the utilisation of the concept of strata stiffness. The local strata stiffness for any point in the underground environment is calculated using the force component from the attributed area and the closure component from underground measurements at that point.

The slope of the force-deformation line represents the strata stiffness. This is determined for the different stages of mining represented by a change in the excavation geometry.

Magnitudes for deformation (that is the x-axis) are obtained from underground instrumentation where stope closure is measured at certain intervals for the point(s) of interest. These values are therefore model independent.

The value for force (on the y-axis) is determined originally through the application of yield lines as described by Johansen (1962). This principle was developed further during the study to what is referred to as the attributed area concept. Through this analysis an area gets attributed to a point of interest at an underground measuring station for a given stope geometry and closure. A representative force is calculated from the attributed area at any point for a given mining stage.

1.9.3 Combined model

The two models, these are for stope support and rockmass behaviour, are combined into a single model during the third stage of the study. During this stage the capacity

of the support is compared to the demand imposed on it by the rockmass. The data is represented on a common x-y axis.

Factors influencing any one or both models can be varied and the effect that it may potentially have on the stability of the excavation is quantified.

1.10 LAYOUT OF THE THESIS

The study described in the thesis is done in three phases. A mathematical model describes each of these phases. The first phase consists of a model that represents the capacity of stope support where laboratory test results of different support elements are described mathematically.

The factors that influence the performance characteristics or capacity of the support elements are also described mathematically and combined with laboratory tests into a single function that represents the in-situ performance of a particular support element.

This procedure is described in detail in Chapter 4.

The behaviour of the rockmass is described during the second phase of the research introducing the concept of strata stiffness. The concept of yield lines as described by Johansen (1962) were introduced and developed further to what is referred to as the attributed area concept. From the analysis the strata stiffness is determined during different stages of mining taking cognisance of the mining geometry and presence of regional support. **This is described in Chapter 5.**

These two stages are combined into a single mathematical representation of the rockmass demand versus support capacity. This constitutes the third phase of the study. The combined representation takes into account all aspects influencing demand of the rockmass as well as those influencing support performance.

In **Chapter 6** the rockmass demand is compared to the support capacity through manipulation of the models by varying the influences that are related to both. These are typically aspects such as rate of closure (quasi static to dynamic), underground geometry, face shape, presence and position of regional support, type and spacing of stope support, thickness of immediate hangingwall beam, stoping width, height of test pack and rate of deformation during laboratory test.

The outcomes of these analyses are used to establish and quantify the effect that this variable would have on the stability of the underground excavation. In **Chapter 7** the stability is evaluated and assessed in case studies by comparing the stiffness of the stope support to that of the rockmass. The energy absorption capacity of the support in relation to that generated by the rockmass is also evaluated. The capacity of the support system as a whole is compared to the demand placed on it by the rockmass this way.

In isolated cases some of the diagrams are repeated. This is done with the objective to make easier reading of the document.

i 17 359144
b16348333

REFERENCES:

- Agricola G. (1556). *De Re Metallica*, Translated from the first Latin edition of 1556 by Herbert Clark and Lou Henry Hoover, New York: Dover Publications, 1950.
- Brady B.G.H. & Brown E.T. (1993). *Rock mechanics for underground mining*, Second Edition, Chapman and Hall, London, 1993.
- Brummer R.K.A. (1985). *Simplified modelling strategy for describing rockmass behaviour around stope faces in deep hard rock gold mines* – Research Report, Rock Mechanics Laboratory, Chamber of Mines of S.A.
- Daehnke A., Anderson L.M., De Beer D., Esterhuizen G.S., Glisson F.J., Grodner M.W., Hagan T.O., Jaku E.P., Kuijpers J.S., Peake A.V., Piper P.S. Quaye G.B., Reddy N., Roberts M.K.C., Schweitzer J.K., Stewart R.D. & Wallmack T. (1998). *Stope face support systems*, Final Report for SIMRAC Project GAP 330, CSIR division of Mining Technology, 1998.
- Esterhuizen G.S. (1996). *J-Block user's manual and technical reference*. Pretoria.
- Goldbach O.D. (1991). *Ground motion studies in a backfilled stope at West Driefontein mine*. Reference Report 24/91 Project No. GRIC, October 1991.
- Gürtunca R.G. & Adams D.J. (1991). *Determination of the in-situ modulus of the rockmass by the use of backfill measurements* – Journal South African Institute for Mining and Metallurgy, March 1991.
- Herrmann D.A. (1987). *Fracture control in the hangingwall and the interaction between the support system and the overlying strata*. MSc Dissertation. University of the Witwatersrand, Johannesburg.
- Hoek E.T. & Brown E.T. (1980). *Underground excavations in rock*, The Institution of Mining and Metallurgy, London, 1980.

Jager A.J. & Ryder J.A. (Editors)(1999). *A handbook on rock engineering practice for tabular hard rock mines – The Safety in Mines Research Advisory Committee (SIMRAC)*, Johannesburg.

Jeppe C.B. (1946). *Gold mining on the Witwatersrand* pp. 815-829, Transvaal Chamber of Mines.

Johansen K.W. (1962). *Yield-line theory*, London: Cement and Concrete Association.

Kruger F.J.A. (2002). *Personal communication*.

Ozbay M.U. & Roberts M.K.C. (1988). *Yield pillars in stope support – Proceedings of 1st Regional Conference for Africa, South African National group on Rock Mechanics, Swaziland*.

Pretorius M.J. (1995). *Seismic evaluation and the design of permanent stope support for both quasi-static and dynamic conditions*. – MSc Research Report, University of the Witwatersrand, 1995.

Riemann K. (1986). *Support characteristics determined from laboratory and underground tests – Proceedings of the South African National Group of Rock Mechanics Stope Support Seminar 25 August 1986*.

Roberts M.K.C. et al (1995): *SIMRAC Project GAP032, Stope and gully support*. The Safety in Mines Research Advisory Committee (SIMRAC), Johannesburg, Web site www.simrac.co.za.

Roberts M.K.C. et al (1998): *SIMRAC Project GAP330, Stope face support systems*. The Safety in Mines Research Advisory Committee (SIMRAC), Johannesburg, www.simrac.co.za.

Roberts M.K.C., Jager A.J. & Riemann K.P. (1987). *The performance characteristics of timber props*. Chamber of Mines Research Report No. 35/1987, Johannesburg.

Ryder J.A. & Ozbay M.U. (1990). *A methodology for designing pillar layouts for shallow workings*, Chamber of Mines of South Africa.

Taggart P.N. (1996). *Dynamic laboratory testing of pack based support elements. Part 1: The laboratory evaluation of timber and composite packs, single rise pack elements and pack and grout pre-stressing units*. Internal note: CSIR Mining Technology August 1994. Journal of the South African Institute for Mining and Metallurgy, Volume 92 No. 2, 1996.

CHAPTER 2**REVIEW OF PUBLISHED DESIGN METHODOLOGIES AND CURRENT PRACTICES IN THE MINING INDUSTRY****2.1 INTRODUCTION**

Single stope support element performance is described by a number of authors where the support practices are described and often referred to as stope support design. A number of papers simply reflect the current state, type and spacing of stope support (titled as a stope support design), while no engineering design methodology is given or described in these papers.

Jager (1986) gives in his paper a review of stope support developments of the previous decade. Waldeck (1986) describes the different types of permanent stope support used but does not give any indication of stope support design methodology or design considerations during the selection of permanent stope support.

In his summary of stope support practices Coggan (1986) states that the main philosophy behind stope support design is to maintain the integrity of the immediate hangingwall and prevent key stone fall-out by maintaining the horizontal clamping forces. This is achieved by utilising the frictional forces in the fractured rock. Requirements of support elements have also been identified and described by him as: "Ideally support should have sufficient initial stiffness to prevent bed separation in the immediate hangingwall and yields in a controlled manner as a result of the irresistible elastic closure. Timely and efficient installation is pre-requisites for effective local support in the face area." No indication as to how this is to be achieved is described in this paper.

During the discussion of the stope support practices at E.R.P.M. by Spengler (1986), Free State by Davies (1986), Evander by Steyn (1986), Springs by Steyn (1986) and of Randfontein Estates Gold Mine by Spearing (1986), the selection for stope support types of the different mining districts are given. No mention is made of engineering design approaches that were adopted for the design of the specific stope supports that are listed.

Research has been done and these are all well documented where the performance of a support element type has been researched. For instance, Roberts (1991) discusses the ability of yielding timber props to absorb energy during a rockburst and investigates the capability to withstand a range of dynamic loading. It was found that the stope closure prior to a rockburst strongly influences the behaviour of the support system during a rockburst. Roberts also suggested that a strain hardening support system such as packs or backfill be considered for rockburst conditions. This recommendation is confirmed by the research described in this thesis.

Roberts and Brummer (1988) first documented the support requirements for stope support in rockburst conditions. A value of 200 kN/m² was published as the support resistance required under rockburst conditions. They made the assumption that 3.0 m of hangingwall will be separated from the hangingwall during a rockburst. The need for integration of hydraulic props with stope support is emphasised. This became one of the stope support criteria widely used in the gold mining industry for rockburst conditions.

The methodology that is described in the thesis has an approach towards seismicity where both the energy criteria as well as the strata- versus support stiffness during dynamic loading are evaluated.

2.2 STOPE SUPPORT AND ROCKMASS INTERACTION

Roberts (1986) identified the need in the late 1980's to address the interaction between the support element and the rockmass. He pointed out that the interaction of support and the rockmass may be described by two aspects, namely the interaction of the individual support units with the immediate fractured hangingwall, and secondly the interaction of the support system with the large volume of inelastic rock around the stope. From this work it became increasingly apparent that the function of support in the working area is to maintain the integrity of the first few metres of hangingwall strata and not to prevent bedding plane separation, as opposed to comments made earlier by Coggan (1986). Roberts (1986) also showed that stope support need not to support the full thickness of the hangingwall up to the limit at which bedding separation occurs. Conclusions at the time revealed that support systems with only moderate support resistance are adequate and that more attention should be given to the areal support ability of support units.

The methods to be adopted when designing and evaluating stope support are described in: "A handbook on rock engineering practice for tabular hard rock mines" edited by Ryder and Jager (1999). Factors governing the design of support systems are described. The publication does not prescribe a design methodology in terms of the design parameters such as quality of the rockmass to be supported, rockmass deformation, support reaction or rockmass-support interaction, but refers to the design rationale as published by Roberts et al (1995) the GAP032 SIMRAC report in principle. It refers to support design methodologies for both rockfall and rockburst conditions, taking the relevant parameters such as closure rate, beam thickness and energy absorption capacity into consideration.

Izakson (1981) is one of the few authors who listed the importance of support stiffness in the design of underground workings, and realised that deformation of support results in the generation of force(s) in a support element. Displacement and forces from structures (a square plate) were analysed for different loading conditions, but the research stopped short by not investigating typical support elements and its yieldability for various mining configurations. No evidence that this research was developed any further, could be found.

A number of design methodologies have been developed recently to address the issue of stope support design. The main objective is to develop a user-friendly support design model that can be used by rock engineering practitioners as a tool for the design of stope support as summarised in Chapter 1.

The following is a summary of the more important recent work done in South Africa with regard to stope support design. An unbiased and balanced critique of the work is attempted with the objective to evaluate the methodology taking into consideration fundamental laws of physics and good engineering practice.

2.2.1 Stope and gully support

(a) SIMRAC Project GAP032: Stope and gully support

A stope support design program commonly used in the gold and platinum mining industry today is the one developed by the CSIR Division of Mining Technology as a SIMRAC Project GAP032 by Roberts et al (1995) that addresses stope and gully support design. The initial project had two objectives namely to develop a rationale for the

design of stope support systems and to develop a support resistance criteria for the support of stope gullies under both static and dynamic loading conditions. The criteria listed in the research refer to a study of the Vaal Reef, Ventersdorp Contact Reef and Carbon Leader reef.

The support resistance of a support system is defined as the force applied by the support unit per tributary square metre of hangingwall, and is presented in kN/m^2 . It therefore depends on the force-deformation characteristic of the support element, the rate of closure and spacing of support elements. The program is developed in a way that deformation of a support element is determined from a given rate of closure at a specific distance back from the stope face, given an installed distance from the stope face. The load generated (kN) by the support element is determined and the support resistance (kN/m^2) calculated from the spacing of the support elements. This value is compared to the criteria required for that area.

Design criteria

The criterion from which the required support resistance is calculated, is based on the thickness of the immediate hangingwall that collapsed with stope support that might or might not have been in place. The required support resistance criterion is determined from fall out heights derived from a reef specific rockfall fatal database containing a large number of cases. The required support resistance criterion is then determined from the fallout height representing 95% cumulative fallout thickness based on all these cases in the database. Databases from which this information is extracted are based on statistics where in some cases supports were installed and failed, and in other cases no support was installed at all.

The determination of the ability of a support system to absorb energy with the objective of reducing rockburst damage is realised in the research as not a simple one since it depends on a number of variables. One of these variables is identified as the ability of the support system to yield during rapid deformation and so absorb energy.

As in the case with the support resistance calculation, is it necessary to have a good estimate of the stope closure rate that would occur prior to and during dynamic closure. Other variables that also influence the ability of a stope support system to absorb energy are the spacing of the support elements, the velocity of dynamic stope closure and the distance in which the hangingwall must be brought to rest.

The area underneath the load-deformation curve represents the energy absorption *ability* of the support element and is expressed in kilojoules (kJ). As deformation takes place, the amount of energy that the support system can absorb will decrease. The amount of normal stope closure that occurs prior to any potential dynamic closure increases from the stope face towards the back area. This means that the ability of the support system to absorb energy during dynamic closure reduces from the face towards the back area.

The required energy absorption criterion in kilojoules per square metre (kJ/m²) is determined from the ejection thicknesses derived from a rockburst fatal database containing a large number of cases. The required energy absorption criterion is then determined from the ejection thickness representing 95% cumulative fallout thickness based on all the cases in the database.

Support spacing

During the design process the spacing of the support elements can be changed and the support types varied. The program addresses both temporary- and permanent stope support types. The effect of those changes can be viewed and the performance of the various options compared to the criteria set for both falls of ground and rockburst conditions.

Criticism

- Even though the final project report shows that several numerical rockmass models were used during the research process, this does not form part of the final design process published. It is stated in the final project report that results of the studies are purely qualitative and values used should not be applied in practice without first collecting sufficient data from underground to calibrate the model.
- The support design analysis is modelled in two dimensions only and the mining geometry in the third dimension is not taken into account. Systematic regional support such as pillars cannot be taken into consideration with this methodology. The hangingwall is assumed to be a solid beam with linear stope closure towards the back area. This approach can be used to determine the support reaction of a given support element in comparison to another. It can

therefore be viewed as a support evaluation rather than a design approach, when considering the main two parameters used in the analysis namely support resistance (kN/m^2) and energy absorption criteria (kJ/m^2).

- Support resistance generated by a support element changes as deformation of the support takes place. It is the opinion of the author of the thesis that this may not reflect the true *capacity* of a support element. It may therefore correct to suggest that the design analysis only shows a snapshot in time for the parameters quoted. A support element well capable in having the potential to meet the support requirements as deformation takes place might not meet the support requirements shortly after installation according to this analysis. A typical example of such a unit would be a solid matpack.
- Another criticism of this approach is the fact that the support resistance generated by the stope face is ignored. The design methodology does not take into account the stope resistance offered by the stope face. It is suggested that the support offered by the stope face, as is the case with regional pillars, be taken into consideration when analysing stope support.
- A gully ledge is damaged by the stress exerted onto the ledge by the gully support. The stress exerted onto the ledges by a support element is a function of both the force generated by the support unit and its footwall/hangingwall contact area. It is suggested that the criterion for gully support is expressed in stress rather than force or load, as is possible with the methodology published in this thesis.
- For the analysis of a support system during dynamic loading, the energy absorption capacity of the support element is analysed. The support stiffness and stress exerted onto the hangingwall during dynamic loading of the hangingwall is neither calculated nor taken into consideration. In practice this means that even a very stiff and strong support that is well capable to absorb energy and meet the design requirements, may cause damage to the hangingwall during dynamic loading according to Pretorius (1995). This is as a consequence of the magnitude of the stress exerted onto the hangingwall. The opposite is also true; that is that a softer support element with less energy absorption capacity but with a positive load-deformation curve may not meet the design

criteria. The pack will not exert an excessively high stress onto the hangingwall during dynamic loading that causes punching failure to the hangingwall.

(b) Key block analysis using J-Block

This support analysis approach is based on the block theory as described by Goodman and Shi (1983). Esterhuizen (1996) has applied this theory into a software design programme. The program is designed to analyse the generation of three-dimensional blocks by the intersection of joint sets, bedding planes and other geological discontinuities. Although discontinuities have to be planar, dip and dip direction can be simulated as having a normal distribution around an average. The spacing of the joints can be defined as varying between a specified minimum and maximum value, while the user specifies the average joint spacing. Joint lengths are specified in a similar manner. This allows for a more natural and accurate representation of the input data.

The analysis assumes a planar hangingwall and determines blocks by combining joints with varying dip and dip directions according to specified input parameters. The blocks that are generated this way vary as the joint orientations are also assumed to be subject to variation. A typical analysis therefore requires the generation of multiple blocks in order to be of statistical relevance. Removable blocks* are determined from the blocks that are generated this way. (*Removable blocks can be defined as those that can be dislodged from the hangingwall.)

The way that removable blocks can be prevented from being removed is by providing support that is presented by point forces at specified points. In the analysis it is assumed that these forces are sufficient to prevent fall-out of blocks. Support failure is thus ignored and only blocks that could fall out between support elements are recorded.

No face stresses are assumed to be present, and no frictional resistance taken into consideration, with only gravity acting on the blocks. The three-dimensional geometry will control the ultimate behaviour of the hangingwall relative to the type and spacing of support.

This approach allows for a realistic comparative analysis between different support elements for varying mining layouts. Results are generated relatively quickly as there is no need for time-consuming stress/deformation calculations, and output is well

presented and easy to understand. Input parameters are crucial, but are limited to joint and fracture orientations and spacing.

Even with its shortcomings, this programme provides the rock engineer with a practical tool to analyse local conditions, which is a major step in the engineering design of stope support. The program does not take cognisance of the support reaction and magnitude of forces generated during the deformation of support.

(c) Review and application of stope support design criteria: Daehnke A., van Zyl M. and Roberts M.K.C. (2001).

Stope support has over the years evolved into a comparatively complex discipline involving the quantification of various rockmass and support parameters. This paper reviews some of the fundamental rockmass and support design criteria that form the basis of an improved support design methodology. The proposed support design methodology that needs to be followed is summarised in the form of a flowchart indicating the principal design steps that need to be implemented when designing stope support for any given geotechnical area.

The design process is systematically done for both quasi-static and dynamic conditions in 9 sections and illustrated at the end of the paper with a support design example in order to illustrate the procedure.

The stope design methodology that is reviewed in the paper consists of the following sections:

Section 1: This section addresses the *critical rockmass parameters* and describes the height of the potential rock falls and stope closure rates for both quasi-static and dynamic conditions. It also addresses the compressive hangingwall stresses, discontinuity spacing, and orientation and interface properties. Each of these is well illustrated and properly defined.

Section 2: This section addresses the *critical support performance parameters* such as the effect of the support length and its effect on the potential for buckling failure of support. It gives a detailed summary of all previous work done on the buckling of a Profile Prop type of elongate, timber packs, hydraulic props and mechanical props. The effect that the closure rate has on the performance of timber elongates, timber packs and cementitious packs is also shown. The support performance variability of support

and the areal coverage of support systems are all described in this section. Examples of recent developments by the CSIR Division of Mining Technology are shown in the paper.

Section 3: This section deals with the *testing programme to evaluate support performance* and proposes a test procedure to provide a systematic approach to the performance of elongates. The test procedure entails various laboratory and underground compression tests of the support units with emphasis on repeated tests using units of the same type. This is done to investigate the performance variability and to obtain a statistical distribution of the load-deformation performance curves.

Section 4: *Stope support design based on the tributary area theory* is described in this section of the paper. It describes the tributary area requirements for both rockfall and rockburst conditions as well as tributary area requirements that are related to stope closure. This section of the paper contributes much to the general understanding of the tributary area concept that is very often simply accepted as the product of the centre-to-centre dip- and strike spacing of underground support elements.

Section 5: This section reviews the a formulation by Daehnke et al (1999) *quantifying stable hangingwall spans between support units* and assessing the influence of rock discontinuities on stable hangingwall spans. Hangingwall span stability is assessed by considering two failure mechanisms namely (i) beam buckling, and (ii) shear/rotational failure due to slip at the abutments. A very useful buckling stability envelope of a discontinuous hangingwall beam showing the relationship between beam thickness and maximum stable spans between supports is part of this section. This section of the paper concludes with the remark that the stability of a keyblock delineated by extension and shear fractures is dependent on buckling, shear and/or rotational failure mechanisms. When investigating the stability of the keyblocks the possibility of each of the three failure mechanisms need to be considered. If the keyblock is unstable in any of the three failure modes, the unsupported span between adjacent support units needs to be decreased until neither buckling, shear nor rotational failure can occur.

Section 6: The *zone of support influence* is quantified in this section and forms a substantial part of the paper. The zone of support influence for a homogeneous hangingwall beam i.e. a continuous beam not discretized by any discontinuities is given and the model expanded to an unclamped hangingwall beam fragmented by discontinuities, and further expanded to a clamped hangingwall beam fragmented by discontinuities. The effect that shear fractures have on the zone of support influence is

University of Pretoria etd – Pretorius, M J (2006)

also shown in this section of the report. The zone of *support* influence for intermediate- and deep-level mines and the zone of influence of the *stope face* in intermediate-, deep-level- and shallow mines are quantified. This section is concluded with the quantification of the zone of influence of backfill.

Section 7: A *unified engineering approach to quantify stable hangingwall spans with face parallel fractures* is proposed in this section of the paper. It is intended as a design tool of practical value that will enable the rock engineer to make initial designs of appropriate support spacing by using a few comparatively simple graphs. In this section the zones of influence is combined with keyblock stability while the support spacing requirements for both rockfall- and rockburst conditions of hangingwalls with face-parallel fractures is determined.

Section 8: The *support spacing requirements for blocky conditions* is described in this section of the paper and addresses both rockfall- and rockburst conditions. This section summarises a second approach to support spacing requirements which is particularly applicable for blocky hangingwall conditions, whereas the previous section of the paper is only applicable if the hangingwall stability is controlled by sliding and rotating of keyblocks, or by beam buckling.

Section 9: The last section of this paper describes the *choice of the appropriate support spacing based on the tributary area and the maximum stable spans*. It gives the support spacing for both a face-parallel fractured- and blocky hangingwall.

Criticism

- This paper is gives a very detailed summary of the most up-to-date design methodology for stope support design in the South African Mining industry to date, where most of the critical issues that are related to stope support design are included.
- Section 2 describes the influence of the length of a support element on its load bearing capacity, and gives general rules for the slenderness ratio of elongates, timber packs, hydraulic props and mechanical props. No general rule is published for cementitious packs like a Durapak that forms quite a substantial part of current stope support, particularly in some of the higher risk areas of the South African gold mining industry.

University of Pretoria etd – Pretorius, M J (2006)

- Even though the paper gives a detailed design methodology it does not show the mode of failure that can be expected of the support element(s). The report stated if the prop is compressed for a distance exceeding its yielding range, rapid and unpredictable failure due to buckling or punching can occur. The work described in this thesis is an attempt to determine whether the support unit will fail in a stable- or unstable fashion once a certain amount of deformation is reached.

2.2.2 SIMRAC Project GAP 330: *Stope face support systems*

Research done by the CSIR Division of Mining Technology as part of SIMRAC research report on Stope face support systems, Project GAP330 (1998), evaluates stope face support systems. The study focuses on relating the geotechnical area properties to existing support types used and the occurrence of fatalities. During the research, support performance and implementation as well as rockmass behaviour were addressed.

During the study geotechnical areas are delineated on the basis of different rockmass behaviour. The use and performance of existing support systems were also evaluated, and a detailed analysis done on rock-related accidents. A study on the interaction between the rockmass and support concludes that local support did not affect the (inelastic) closure in a longwall stope according to Herrmann (1987). It was not possible to investigate the support interaction as unrealistically thick layers had to be represented due to numerical constraints. The slenderness of the beams had to be limited in order to obtain reliable results. This is a universal problem and affects all traditional numerical models. This problem needs to be addressed by mining industry.

The study also indicated that many local rockmass instabilities are the result of the inability of the rockmass to bridge the span between the individual support units. The report also suggests that the main support units should not have to be designed to provide local stability. Such stability needs to be ensured either by the rockmass itself or by a combination of that rockmass and some form of appropriate and effective reinforcement. The study suggests that additional work be conducted to quantify the effect of arbitrary oriented discontinuities of geological origin on support spacing. Particularly in the case of steep dipping fractures stresses transmitted across discontinuities could stabilise the hangingwall, leading to wider permissible spans. Further work could re-address the influence of the modified hangingwall stress

distribution due to loading by the stope face, support units and backfill. The work described in the thesis takes into consideration the presence of the stope face as well as regional support such as pillars and backfill.

The research into the application of keyblock methods in the design of a support system for deep gold mines has shown that:

- Most keyblocks will be held in position by horizontal clamping stresses in the hangingwall under quasi-static conditions. It is only when shallow dipping discontinuities exist or when clamping stresses are lost through falls of ground, that keyblock stability becomes a concern. Under dynamic loading conditions the additional load may dislodge keyblocks that were previously stable.
- Slab shaped keyblocks are very stable even if clamping stresses are low. Wedge shaped keyblocks are most likely to fail and their occurrence and stability may be evaluated using keyblock techniques. The ratio of slabs to wedges in a stope hangingwall may be an indication of its stability.
- While the dominant stress fracture in a stope hangingwall is steeply dipping, shallow dipping fractures occur and are likely to result in keyblock type failures. Geological structures are often flat dipping and may define unstable keyblocks.
- Keyblock analysis techniques are suitable for the analysis of the effect of stress fractures and geological structures on the stability of a stope hangingwall. The analysis provides a realistic block size distribution, and can therefore assist in optimising support design for local geotechnical conditions.

The investigation into the keyblock method has shown that keyblock analysis techniques are able to provide insight into the interaction between support units and the fractured hangingwall. The method may therefore be used to account for site specific geological and stress fracturing conditions in support design.

2.3 STATUTORY REQUIREMENTS

The importance of stope support design in the mining industry is reflected in the Guidelines for the Codes of Practice to Combat Rock Fall and Rock Burst Accidents in Tabular Metalliferous Mines (2002) as well as the Mine Health and Safety Act published in 1996. The Guideline for the Compilation of a Mandatory Code of Practice to Combat Rock Fall and Rock Burst Accidents in Tabular Metalliferous Mines is issued in terms of the Mine Health and Safety Act, 1996 (Act No. 29 of 1996). Section 9(3) requires that a

Code of Practice shall be drawn up in accordance with guidelines issued by the Chief Inspector. Failure by the employer to prepare and implement a Code of Practice in compliance with the Guideline is a breach of the Mines Health and Safety Act.

The objective of the Guideline is to enable the employer at every mine to compile a Code of Practice, which, if properly implemented and complied with, would reduce the number of rock fall and rock burst accidents at the mine since the majority of the accidents occurring at the mines are as a result of rock falls, are either seismically or gravitationally induced. The Guideline is a generic document and is not intended to address the rock related accident problems encountered on a particular mine. The guidelines pertaining to the design, geometry and support requirements are not rigid and prescriptive due to the complexity and variability of conditions at the mines. An approach was adopted which allows for the local expertise, experience and knowledge of the mines to be effectively utilised.

Section 11 of the Mine Health and Safety Act stipulates that the manager must assess and respond to risks. Stope support design can be classed as one of the elements that have an influence in managing some of these risks. The work described in this thesis is an attempt to contribute towards achieving this objective.

2.4 CONCLUSION

During the years of mining in the South African gold and platinum industries, valuable work has been done with regard to stope support and numbers of papers have been published in this respect. A study of literature has shown that very little work has been done with regard to the rockmass-support interaction for stope support. Papers describe either the reaction of the support medium or the behaviour of the rockmass and not much about the interaction of the two. The research should be viewed as complementary to the existing stope support design methodologies developed by researchers and engineers in the South African mining industry over many years. It describes the interaction of the hangingwall beam and stope support in order to determine whether the stope support will fail in a stable- or unstable manner. This is done by comparisons of (a) the rockmass and support stiffness at a given deformation, and (b) the energy for a given deformation interval. It differs from the conventional methodologies in that it does not take into consideration the fallout thickness of the immediate hangingwall.

A rigorous engineering approach is defined as one where the interaction between the support medium and that of the excavation it is intended to support is evaluated and described systematically in terms of the laws of physics. The research published in the thesis conforms to a rigorous but simple engineering approach and is described in terms of and conforms to the laws of physics.

REFERENCES:

- Brummer R.K.A. (1985). *Simplified modelling strategy for describing rockmass behaviour around stope faces in deep hard rock gold mines* – Research Report, Rock Mechanics Laboratory, Chamber of Mines of S.A.
- Coggan J.S. (1986). *Support practices in the Klerksdorp mining district* – Proceedings of the South African National Group of Rock Mechanics Stope Support Seminar 25 August 1986.
- Davies D. (1986). *Support practices in the Orange Free State mining district* – Proceedings of the South African National Group of Rock Mechanics Stope Support Seminar 25 August 1986.
- Department of Mineral and Energy. (2002). *Guidelines for the compilation of a mandatory code of practice to combat rockfall and rockburst accidents in tabular metalliferous mines*.
- Daehnke A. & Roberts M.K.C. (2001). *Review and application of stope support design criteria*, The Journal of the South African Institute of Mining and Metallurgy pp 135-164, Johannesburg, May/June 2001.
- Daehnke A., Salamon M.D.G. & Roberts M.K.C. (1999). *Investigating zones of stope support influence and quantifying stable hangingwall spans between support units*, To be published: The Journal of the South African Institute of Mining and Metallurgy, Johannesburg, 1999.
- Esterhuizen G.S. (1996). *J-Block user's manual and technical reference*. Pretoria.
- Goldbach O.D. (1991). *Ground motion studies in a backfilled stope at West Driefontein mine*. Reference Report 24/91 Project No. GRIC, October 1991.
- Goodman R.E. & Shi G. (1983). *Block theory and its application to rock engineering*, Prentice Hall.

Herrmann D.A. (1987) *Fracture control in the hangingwall and the interaction between the support system and the overlying strata*. MSc Dissertation. University of the Witwatersrand, Johannesburg.

Izakson V. Yu. (1981). *Underground working support design according to measured movements of the periphery* - Civil Engineering Institute, Makeevka. (Translated from Fiziko-Tekhnicheskie Problemy Razabotki Poleznykh Iskopaemykh, No 4, pp. 23-28, July-August 1981. Original article submitted March 19, 1979.)

Jager A.J. (1986). *Review of stope support developments in the past ten years* - Proceedings of the South African National Group of Rock Mechanics Stope Support Seminar 25 August 1986.

Jager A.J. & Ryder J.A. (Editors)(1999). *A handbook on rock engineering practice for tabular hard rock mines* - The Safety in Mines Research Advisory Committee (SIMRAC), Johannesburg.

Pretorius M.J. (1995). *Seismic evaluation and the design of permanent stope support for both quasi-static and dynamic conditions*. - MSc Research Report, University of the Witwatersrand, 1995.

Riemann K. (1986). *Support characteristics determined from laboratory and underground tests* - Proceedings of the South African National Group of Rock Mechanics Stope Support Seminar 25 August 1986.

Roberts M.K.C. (1991). *An evaluation of yielding timber props as a support system in rockburst conditions*. - The Safety in Mines Research Advisory Committee (SIMRAC), Johannesburg.

Roberts M.K.C. (1986). *The interaction between hangingwall and support - a review of in-situ experiments in deep mines* - Proceedings of the South African National Group of Rock Mechanics Stope Support Seminar 25 August 1986.

University of Pretoria etd – Pretorius, M J (2006)

Roberts M.K.C. et al (1995). Project Manager: *SIMRAC Project GAP032, Stope and gully support*. The Safety in Mines Research Advisory Committee (SIMRAC), Johannesburg, www.simrac.co.za.

Roberts M.K.C. et al (1998): *SIMRAC Project GAP330, Stope face support systems*. The Safety in Mines Research Advisory Committee (SIMRAC), Johannesburg, www.simrac.co.za.

Roberts M.K.C & Brummer R.K. (1988). *Support requirements in rockburst conditions* - Journal of the South African Institute for Mining and Metallurgy, March 1988.

Roberts M.K.C., Jager A.J. & Riemann K.P. (1987). *The performance characteristics of timber props*. Chamber of Mines Research Report No. 35/1987.

Spearing A.J S. (1986). *Stope support practices at Randfontein Estates Gold Mine* – Proceedings of the South African National Group of Rock Mechanics Stope Support Seminar 25 August 1986.

Spengler M.G. (1986). *Support practices at E.R.P.M. Ltd.* - Proceedings of the South African National Group of Rock Mechanics Stope support seminar 25 August 1986.

Steyn S.M. van H. (1986). *Support practices in the Evander and Springs mining districts* – Proceedings of the South African National Group of Rock Mechanics Stope Support Seminar 25 August 1986.

Waldeck H.G. (1986). *Support practices in the Far West Rand Mining District* – Proceedings of the South African National Group of Rock Mechanics Stope Support Seminar 25 August 1986.

Mines Health and Safety Act 1996.

CHAPTER 3 BASIS FOR DESIGN METHODOLOGY

3.1 OBJECTIVES OF THE DESIGN METHODOLOGY

Stope support design is one of the more complex design issues in the mining of tabular orebodies. The objective of the research described in the thesis is to quantify stope support and rockmass interaction and through this, develop a methodology that can be used by the rock engineering fraternity for the evaluation of a stope support system.

Figure 3.1 shows the fracturing around a stope in a deep level mining environment according to Roberts and Brummer (1998). It indicates the shear- and extension fractures as well as bed separation that develop around the excavation in a rockmass as a result of the mining process. As mining progresses the stress around the excavation will continue to change in both magnitude and direction, causing a progressive deformation and possible fracturing of the rockmass. Deformation of the rockmass results in the elastic and inelastic closure of the stope excavation.

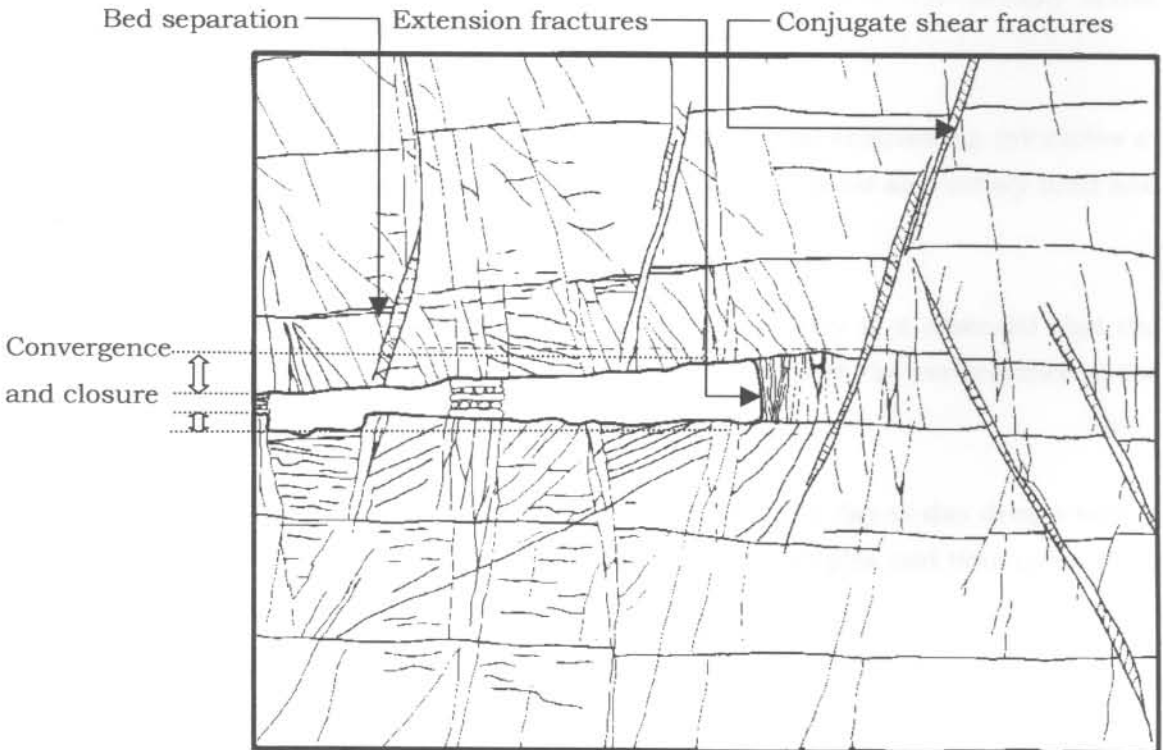


Figure 3.1: Fracturing around a stope (after Roberts and Brummer (1998))

The rockmass surrounding the stope places a certain demand on the support elements to ensure the stability of the excavation. The support elements in turn have a certain capacity to react to that. The inter-relationship between the capacity of the stope support elements on the one hand, and demand from the surrounding rockmass on the other, forms the basis of this study.

A stope support design methodology should relate realistically to the underground environment to be of practical use for the rock engineer. To accomplish that the mining geometry must be taken into consideration and provision must be made for aspects like face shape, panel leads and lags as well as presence and position of regional support.

The support design methodology should preferably be based on observations and measurements that were taken from underground instrumentation and observations. A model that is developed from this will be more reliable in reflecting the physical underground environment. Underground measurements for the purpose of developing a model, must be taken at regular intervals to fully capture the in-situ rockmass deformation at any particular site for that given mining geometry. The design procedure that is developed from this must be consistent and mathematically stable throughout the total mining process.

The design procedure must further comply with fundamental engineering principles at all times and be described in terms of the laws of physics. It must also satisfy fixed and defined design criteria.

To be of practical use and of relevance to the mining industry is it essential that the methodology takes into consideration factors that influence both the performance of the support element(s) as well as the demand of the rockmass.

For any design procedure to be used in a meaningful way as a day-to day design tool, it must be simple to use and the process should not involve complex and time-consuming computer modelling.

3.2 DESIGN METHODOLOGY

The stope support and rockmass interaction that are described in the thesis can be compared, and is based on the interaction that exists between a rock testing machine and a rock specimen when performing a uniaxial compressive test. The behaviour of

the rockmass relates to that of the testing machine, while the reaction of the stope support can be compared to that of the rock specimen.

The testing apparatus could either be stiff or soft depending on the design and properties of the equipment. In a similar way the rockmass surrounding the stope will react as either a stiff- or a soft environment. The behaviour of the rockmass depends on the factors governing its behaviour such as mining depth, mining span, presence and position of regional support and rockmass properties.

The area underneath the force-deformation curve for the test machine represents the energy released by the equipment for the specific interval of deformation. Similarly the area underneath its load-deformation curve will represent the energy that is absorbed by the rock specimen for that deformation interval.

When the stiffness of the machine is less than the post failure stiffness of the rock specimen, in other words the energy contained in the testing machine due to deformation of the testing machine itself, for a given interval of deformation, is more than required by the specimen, the specimen will fail in an uncontrolled way. This is referred to as unstable failure and is illustrated diagrammatically in Figure 3.2(a). The opposite is also true where the stiffness of the testing machine is stiffer than that of the rock specimen, the specimen will fail in a controlled fashion or there will be stable failure as illustrated in Figure 3.2(b). The reason for this is that further deformation of the specimen can only occur by the external provision of more energy.

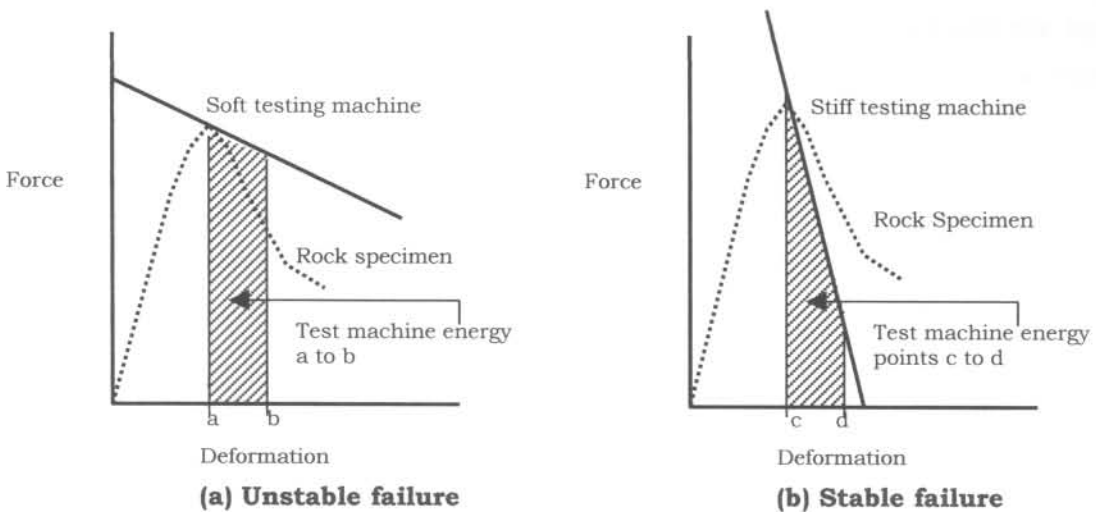


Figure 3.2: Unstable- and stable failure of a rock specimen for soft- and stiff testing machines

The use of this analogy makes it possible to compare and represent both the demand of the rockmass and the capacity of a support element in a similar fashion. The fact that both of these can be compared and presented on a common force-deformation axis makes this a very attractive approach.

Similar to that of the testing machine the stiffness of the rockmass can be presented on a force-deformation diagram. The rockmass behaviour is represented by the mathematical function:

$$g(x) = mx + F_0 \quad (3.1)$$

where:

$g(x)$ = Force (kN) exerted by the rockmass at any deformation x (mm);

m = Rockmass stiffness (kN/mm); and

F_0 = Rockmass force at zero deformation, i.e. where $x = 0$.

The rockmass stiffness at any point for that particular mining stage and excavation geometry is represented by the slope (m) of the function $g(x)$.

It is assumed that the rockmass stiffness is linear. This approach may be criticised, but further work is required to determine it more accurately. The assumption is based on the following:

- Salamon and Oravecz (1976) use the loading machine and rock specimen interaction to describe controlled- and uncontrolled failure of pillars and also illustrate this principle by means of linear load lines. This can be interpreted in mining terms where the rock specimen corresponds to the pillars and the loading machine is analogous to the rockmass surrounding the workings. They stated that the slope of the loading line is determined by the properties of the strata and the mining geometry, and shows that the relative stiffness of the strata decreases with an increase in the number of pillars. The practical implication of this is that as the number of pillars in a panel and, consequently the width of the panel, are increased, the surrounding strata behave as a progressively softer loading machine, so that the likelihood of an uncontrolled collapse becomes higher. The strata stiffness is represented as a single figure by them namely the slope of the loading line as illustrated on pp39 of this reference. The illustration by Salamon and Oravecz (1976) showing a decrease in the strata stiffness with an increasing panel width is confirmed in this study.

- Mauracher (1998) in his Master Thesis studied the behaviour of the hangingwall strata on Beatrix Mine. He concluded that local strata stiffness is a way to describe the hangingwall behaviour and describes the local strata stiffness as being linear.
- No literature could be found that describes the load line of the hangingwall rockmass as being non-linear for a given condition. Research is still required in this field of rockmass behaviour to confirm the assumption made in the thesis.
- This approach may also apply to the UE1a Reef at Randfontein in the Witwatersrand Basin and perhaps the UG2 Reef of the Bushveld Complex. (Personal communication, Roberts (2004)). Applicability to the Carbon Leader and Vaal Reef is less certain and needs to be researched.

The stope support load-deformation curve can be related to that of the rock specimen, and presented on the same force-deformation diagram than that of the rockmass. The mathematical function describing the behaviour (or capacity) of a support element is given by the following n^{th} order polynomial:

$$y = f(x) = c_1x^6 + c_2x^5 + c_3x^4 + c_4x^3 + c_5x^2 + c_6x + c_7 \quad (3.2)$$

where:

- y = $f(x)$ = Load generated by support element (kN);
 x = Deformation (mm);
 c_n = Constants with $n = 1, 2, \dots, 6$; and
 c_7 = Pre-stressing during installation. (kN)

The behaviour and hence failure of a support unit is in a way analogous to the pillar stress-strain behaviour shown by Ryder and Jager (2002) where different pillar behaviour, and hence different pillar mode of failure, may be expected with different ratios of pillar width to pillar height. The behaviour of the pillar changes from crush- to elastic- to yield- to squat pillar with an increased width to height ratio. Here the slope of the post peak portion of the curve becomes flatter with an increased pillar width to pillar height ratio. The failure of a timber mine pole can be compared to that of a crush pillar while the behaviour of a mat pack with a low height to width ratio can be related to that of a squat pillar.

According to Daehnke et al. (2001) that if a prop is compressed for a distance exceeding its yielding range, rapid and unpredictable failure can occur. The research described in this thesis attempts to describe this failure as either stable- or unstable failure.

The support element will start to *shed load* where the tangent to the performance function is negative, i.e. where:

$$\partial/\partial x[f_a(x)] < 0 \quad (3.3)$$

with:

$$f_a(x) = f(x).Y.H_f \text{ - for timber- and cementitious packs} \quad (3.4)$$

$f_a(x)$ = Adjusted support function;

$f(x)$ = Function describing the performance of a specific pack;

Y = Loading rate factor; and

H_f = Support height factor.

The adjusted support performance function for a timber elongate is given as:

$$f_a(x) = f(x).Y.B_f \quad (3.5)$$

where:

$f(x)$ = Mathematical function describing the performance of an elongate; and

B_f = Buckling failure factor for elongates.

Failure of support, that can either be stable- or unstable failure, will depend on the magnitude of the tangent to the support function in relation to that of the slope of the line representing rockmass behaviour at that stage of mining and for the given mining geometry. This is where $|\partial/\partial x.[f_a(x)]| > |\partial/\partial x.[g(x)]|$ for both pack - and elongate support at a given deformation.

The stable and unstable failure of support is demonstrated in the two case studies in Chapter 7.

The capacity to absorb energy is another way of comparing the demand placed on the support by the rockmass to its capacity. The energy for both the rockmass and the stope support element(s) is determined by the integration of the mathematical functions that describe its behaviour. This is done for the given deformation interval that is examined.

Load shedding of the support will take place where the rockmass energy demand exceeds the capacity of the support system. This is true where $\int g(x)\partial x > \int f_a(x)\partial x$ for a given deformation interval x .

The behaviour and performance of stope support are described in detail in Chapter 4.

3.2.1 Development of the models

The research that is described in the thesis consists of two models that were developed and described in a mathematical format. The first model represents the performance or capacity of the support, while the second represents the support demand from the rockmass.

The objective of combining these into a single model is to represent a combined and comprehensive technique that can be used as a design tool. The model can either be used as a retrospective tool by means of which the past performance of stope support can be studied and quantified where in-situ closure measurements were taken. More importantly it can also be used as a pro-active tool to quantify and compare the behaviour of different supports for a planned mining geometry. The design engineer must have a reliable estimate of stope closure for different stages of mining for the latter purpose. This estimate can either be from underground measurements and or accurate non-elastic numerical modelling of the closure at any point for a given mining geometry.

(a) Stope support model - Capacity

The first model describes the behaviour of the stope support elements with the objective to quantify its capacity. For this purpose load-deformation curves were used from the series of laboratory tests conducted and published by the CSIR Division of Mining Technology (1995) as part of a SIMRAC GAP032 Research project. Laboratory test results were also obtained from manufacturers of stope support products namely Scholtz (1997) and Smit, Erasmus and Grobler (1998).

The laboratory load-deformation curves of the support elements were reproduced mathematically by fitting an n^{th} order polynomial function to the laboratory test data.

Factors that influence support performance must be taken into consideration in order to reproduce and represent the in-situ performance of a support element. Factors such as the effect of the rate of deformation, height of pack installed as opposed to the one tested, buckling potential (in the case of timber elongates) and pre-stressing during installation are taken into consideration. All these factors are described mathematically

as separate variables and combined with the support performance function into a final function ($f_a(x)$) to represent the in-situ performance of a support element.

The final sets of equations are written into spreadsheets that were developed to graphically display the performance of a support unit. Factors influencing the support performance can be varied and the effect(s) that it has on the performance of the support element displayed. The spreadsheets were compiled in a way that the in-situ support performance can be compared directly to the laboratory results. The effect(s) and impact of these factors in comparison to the laboratory results can be observed visually when changed or varied. The major advantage of the visual representation of the support performance this way is that it quantifies these influences in a way that the end-user develops an appreciation for the influence that these factors have on the performance of support in direct comparison to laboratory results.

The spreadsheet representation has the advantage that the factors influencing support performance can be changed quite easily and the following calculated for any given in-situ condition:

1. Load (kN) generated by the support unit for a specified deformation;
 2. Support resistance (kN/m²) generated by the support element for a given dip- and strike support spacing;
 3. Stiffness (kN/mm) of a support element for any specified deformation;
 4. Energy (kJ) generated by the support element for a given deformation interval;
- and
5. Stress (MPa) exerted onto the stope hanging- and footwall during quasi-static and dynamic loading of the support.

An offshoot of the theory and mathematical models representing support is the application of this approach into a three-dimensional numerical computer model.

It is possible that an estimate of the support resistance generated by a support type can be calculated and contoured. This way the support resistance for a given mining geometry with a given type and support density can be quantified. A program like Minsim W could be utilised for this. The Modulus of Elasticity (E) is modified to a value where the elastic convergence calculated by the numerical analysis approximates underground measurements. It is important to note that the stresses shown by this model will not be reliable in such cases and may be incorrect.

To determine values for the Modulus of Elasticity, an area was modelled and the convergence at the centre of the panel calculated and compared to various closure rates (expressed in mm/m face advance) that were measured underground.

The following mathematical function is introduced in the so-called OWN variable where the engineer defines and describes his own variable to be calculated as part of the numerical output. Support resistance can be calculated and contoured for an on-reef sheet of benchmarks. The variable function that is imported into the program as follows:

$$\text{OWN} = f_a(s_z - s_n) / (D_s \cdot S_s) \quad (3.6)$$

where:

- $f_a(x)$ = Adjusted support function for a specific type of support;
- s_z = Elastic convergence (mm) calculated by Minsim W at the point of interest;
- s_n = Convergence that has taken place prior to the installation of the support at a distance n-meters from the stope face;
- D_s = Dip spacing (m) of support elements; and
- S_s = Strike spacing (m) of support elements.

This application will not be explored any further in this thesis.

(b) Rockmass model - Demand

The second model describes and represents the behaviour of the rockmass. The concept of rockmass stiffness was introduced to describe and quantify rockmass behaviour.

The objective of this part of the research is to develop a methodology that will describe and quantify the behaviour of the rockmass surrounding a stope. The rockmass stiffness is experimentally determined and a wide range of elements that influence its behaviour such as the horizontal stress and the inherent rockmass properties are inclusive of the underground measurements. The behaviour of the rockmass and its response to mining is determined here by means of underground closure profiles.

This model describes the support demand of the rockmass on the stope support. The rockmass behaviour must preferably be described in a way that it can be linked directly

to the performance or capacity of slope support while giving a true reflection of underground environment.

The rockmass model is developed in such a way that it quantifies the rockmass stiffness at any specific point of interest in the slope for the given mining geometry. This is described by the function $g(x) = mx + F_0$, where the rockmass stiffness is represented by the slope (m) of the line at that particular point for the given geometry.

The methodology to develop this technique has undergone different stages of development. For the very first attempt a correlation between the cumulative square metres mined in a specific area of interest and the force calculated numerically by means of an elastic numerical model, was established. This method yielded a constant ratio between the cumulative square meters mined and the force calculated. The major shortcoming of this approach was establishing the initial area that was mined to be used as the so-called "starting area" that is described in Chapter 5.

The second attempt in quantifying the rockmass stiffness was to evaluate the combined deflection of two orthogonal beams with its centre positioned at the underground point of interest in the slope. This was accomplished by fitting two orthogonal beams at the point of interest to the closest solid abutments (or regional pillars) for the given mining geometry.

The forces that were calculated using numerical modelling at that point were compared to different variables of the ellipse described by the short- and long axis of the two orthogonal beams. This approach initially seemed to give a reasonable correlation between the force calculated numerically and the "effective side" of the ellipse. (The effective side is defined as the square root of the area of the ellipse.) The major shortcoming of this approach is that mining could take place outside the area covered by the ellipse but still in close enough proximity to the measuring station to have an influence on the force calculated by the numerical analysis. This methodology is not able to detect this and calculations or force predictions done under such circumstances can be grossly inaccurate. Figure 3.3 illustrates the elliptical fit to a specific mining geometry at the point of interest as shown.

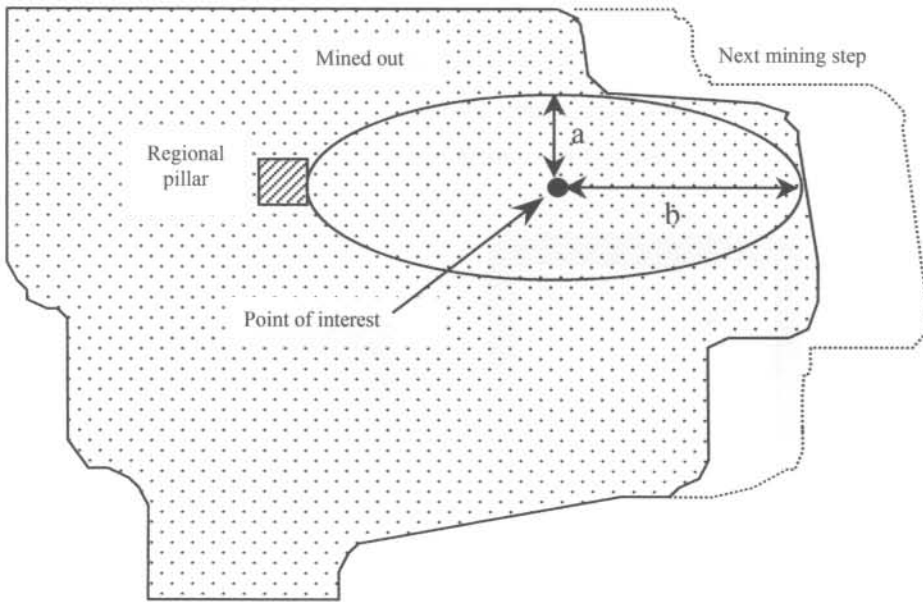


Figure 3.3: Illustration of the elliptical fit to a specific mining geometry

The third attempt that was adopted was the evaluation and study of the applicability of the yield line concept. The reason for reverting to this concept was to arrive at some methodology to determine the rockmass stiffness where it would be possible to take into consideration the face shape, mining geometry and presence of regional support.

The magnitude for the force component on the y -axis of the force-deformation representation is determined through the application of yield lines as described by Johansen (1962). Yield lines apply to plastic plates, such as reinforced concrete slabs and steel plates that are so lightly reinforced that failure begins when the reinforcement yields. The assumption was made that the hangingwall of the stope will react in the same manner when considering its closure profile and the fact that the hangingwall beam remains intact during stope closure similar to a reinforced concrete slab.

The positive ultimate moment corresponds to yielding of the bottom reinforcement and the negative ultimate moment to yielding of the top reinforcement. At failure, plastic deformations occur along yield lines where the reinforcement has yielded and the parts into which the slab is divided by the yield lines are only deformed elastically. Since the elastic deformations can be ignored in comparison with the plastic ones, the individual parts of the slab can be regarded as a plane, and their intersections, that is the yield lines, regarded as straight lines with a good degree of approximation.

It is thus assumed that deformation occurs only in the yield lines, consisting of relative rotation of the two adjoining parts of the slab about axes whose location depends upon the supports. Each part may be regarded as plane, and will be evaluated as that. Yield lines for square and rectangular slabs are shown in Figure 3.4.

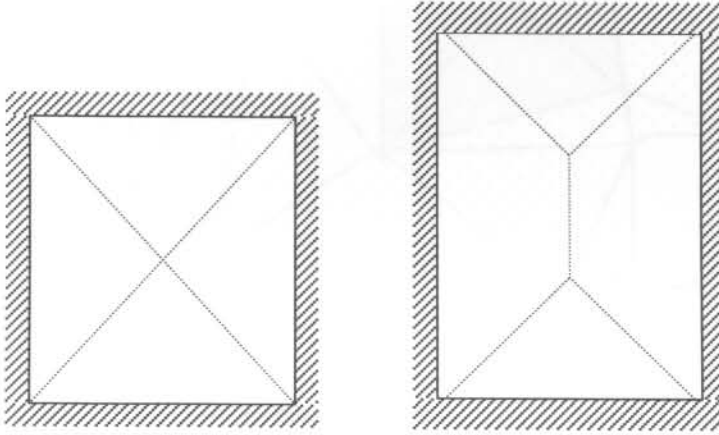


Figure 3.4: Yield lines shown as dotted lines for square and rectangular plates supported at the edges

The following basic rules are applied in establishing the yield lines. These rules are applied to the underground workings as illustrated and described in Chapter 5.

1. The yield lines between two parts of a slab must pass through the point of intersection of their axes of rotation.
2. For a part of a slab supported along its edge, the axis of rotation must lie along the edge, and for a part supported on a column the axis will pass over the column.

Yield lines for the same underground geometry as shown in Figure 3.3 are illustrated in Figure 3.5. The process applied during the construction of the yield lines is discussed in more detail in Chapter 5.

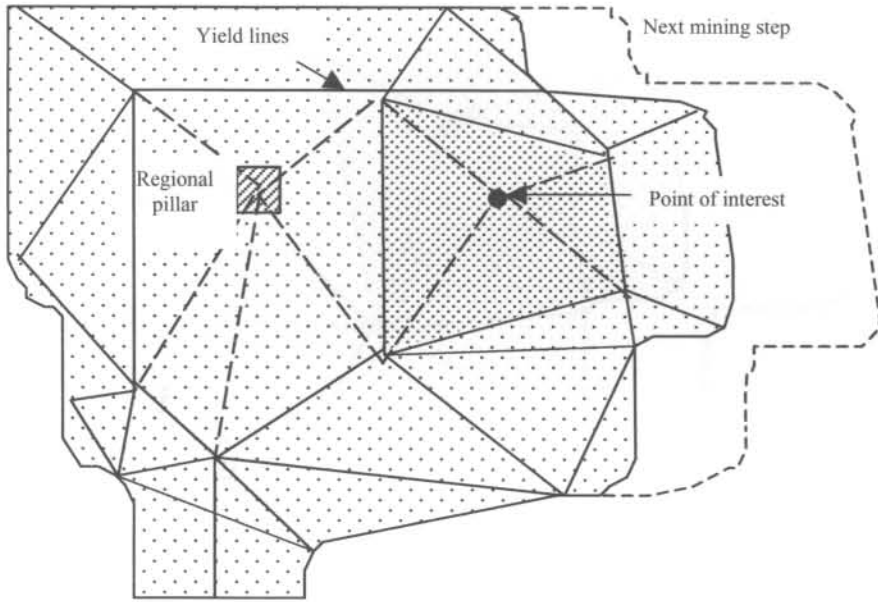


Figure 3.5: Yield lines for the same underground geometry as shown in Figure 3.3

The area represented by the yield lines around the point of interest was compared to the numerical value of the force determined numerically at that point for the given mining geometry. A good correlation was found to exist between the shaded area shown in Figure 3.5 and the force calculated at the point of interest for a given mining geometry.

This yield line principle was developed further to what is referred to as the attributed area concept. An area denoted as A_a is attributed to a point of interest for a given mining geometry. A representative force is calculated for this point of interest at a given mining stage and stope face shape from the attributed area A_a .

The local rockmass stiffness for that specific point underground is calculated using the force component from the attributed area. A certain thickness of hangingwall that is to be supported is taken into account while the closure component is taken as that measured underground. This process is described in detail in Chapter 5.

Figure 3.6 shows the mining layout previously used with the area attributed to the point of interest for the same mining geometry.

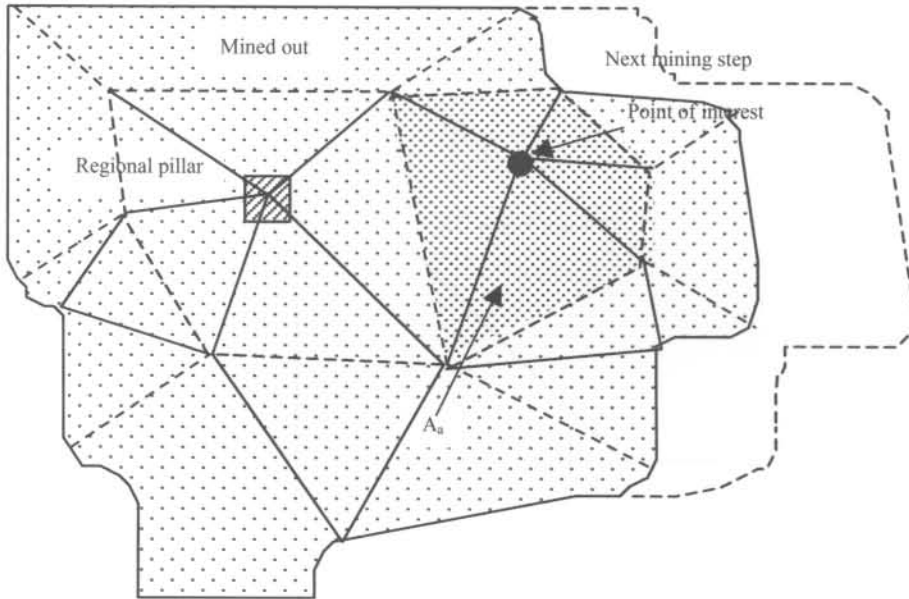


Figure 3.6: Mining geometry showing the attributed area A_a for the given point of interest

An area A_a is attributed to the point of interest and the force component for the rockmass stiffness diagram calculated. The force is a function of attributed area A_a and the thickness of the immediate hangingwall to be supported. The attributed area force is given by:

$$F_o = \rho \cdot h \cdot A_a \cdot g \quad (\text{N}) \quad (3.7)$$

where:

- F_o = Attributed area force (N);
- ρ = Rockmass density (kg/m^3);
- h = Thickness of hangingwall beam (m);
- A_a = Attributed area (m^2); and
- g = Gravitational acceleration. (m/s^2)

The rockmass load line is described by the following equation for varying deformation x :

$$g(x) = mx + F_o \quad (3.8)$$

where:

- m = Rockmass stiffness (N/m);
- x = Deformation of the stope (m); and
- F_o = Attributed area force (N) where $x = 0$.

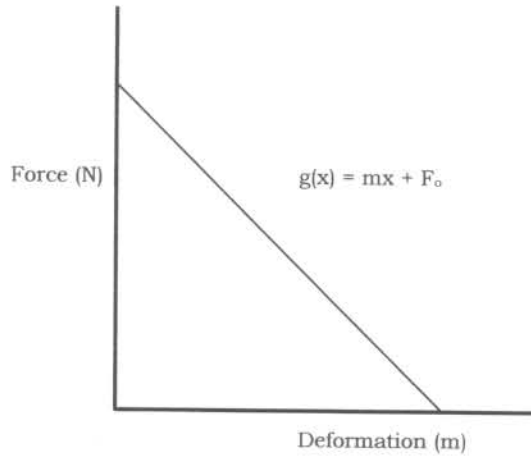


Figure 3.7: Graphical representation of a load line describing rockmass behaviour

(c) Combined model

The stope support and the rockmass models described in 3.2.1 (a) and in (b) are combined and compared during the third phase of the procedure and presented on a common force-deformation axis.

Stope support element performance is described by:

$$f_a(x) = f(x) \cdot Y \cdot H_f - \text{for timber and lightweight concrete packs; and}$$

$$f_a(x) = f(x) \cdot Y \cdot B_f - \text{for timber elongates.}$$

The rockmass behaviour is described by the rockmass load line as $g(x) = mx + F_0$ with all symbols as defined previously.

To evaluate the stability of the total attributed area that could be supported by a combination of different support types, the function of the support element(s) is multiplied by a factor n_n as:

$$F(x) = \sum n_n \cdot f_a(x) \quad (3.9)$$

where:

n_n = Number of support elements of say type n ,

= $A_a / (d \cdot s)$ for the specific support type;

A_a = Attributed area (m^2);

d = Dip spacing of support units (m); and

- s = Strike spacing of support units (m);
 $f_a(x)$ = Adjusted support performance function or the specific support type; and
 x = Deformation (mm)

This principle of superimposing the rockmass and support models is illustrated graphically in Figure 3.8.

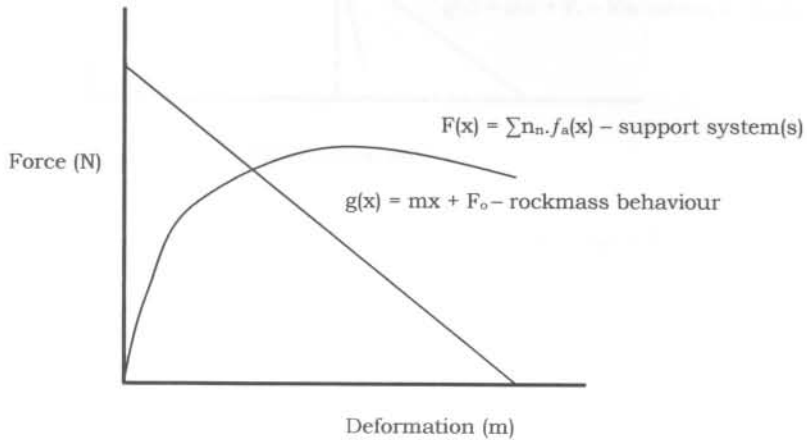


Figure 3.8: Graphical representations of the rockmass load line and stope support models on a common force-deformation axis

Unstable failure of the support will take place where the energy generated by the rockmass for a given interval of deformation exceeds the energy capacity that can be handled by the support system(s). The following criteria are used to test for stability/instability for a given mining geometry and support:

(i) Stiffness comparison analysis

The underground environment will potentially become unstable if the absolute value of the slope of the strata stiffness is less than that of the *post* failure stiffness of stope support system.

This is where:

$|m| < |\partial/\partial x[F(x)]|$ as illustrated in Figure 3.9 where the performance of both the stope support and the rockmass load line are superimposed on a common force-deformation axis.

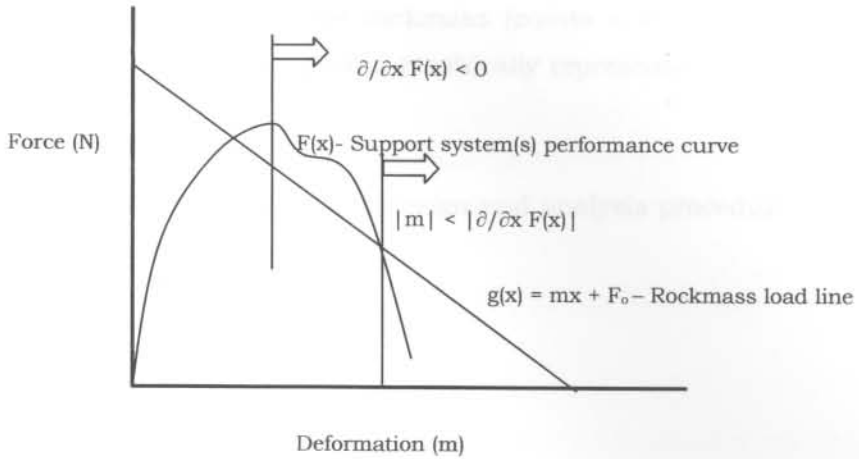


Figure 3.9: Combined models illustrating failure of the supports

(ii) Energy comparison analysis

The condition where the energy generated by the rockmass exceeds that which can be absorbed by the support system(s) may result in an unstable situation.

Mathematically where $\int_a^b g(x) \partial x > \int_a^b F(x) \partial x$ for a given deformation interval x , say a to b , will this result in unstable failure of the support system(s). This principle is illustrated in Figure 3.10.

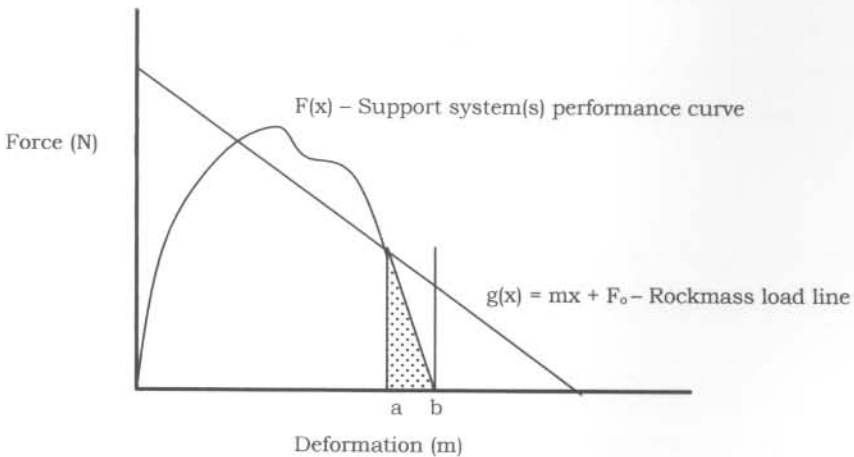


Figure 3.10: Graphical representation of unstable failure of a support system

The excessive energy generated by the rockmass (points a to b) that will result in unstable failure of the support system(s) is graphically represented by the shaded area in Figure 3.10.

Case studies where the application of this design and analysis procedure is illustrated are shown in Chapter 7.

REFERENCES

- Daehnke A., van Zyl M. & Roberts M.K.C. (2001). *Review and application of stope support design criteria*, Journal for the South African Institute of Mining and Metallurgy, Johannesburg, May/June 2001.
- Johansen K.W. (1962). *Yield-line theory*, Cement and Concrete Association, London, 1962.
- Mauracher M.J. (1998). *Determination of the behaviour of the hangingwall on Beatrix Mine with special regard to the local strata stiffness*, Master Thesis, Institut für Bergbau, Technische Universität Clausthal, Germany, 2 February 1998.
- Roberts M.K.C. & Brummer R.K. (1998). *Support requirements in rock burst conditions*, Journal of the South African Institute for Mining and Metallurgy, Johannesburg, March 1988.
- Roberts M.K.C. et al (1995). *Support Catalogue: SIMRAC Project report GAP 032*, Johannesburg, 1995.
- Roberts M.K.C. (2004). *Personal communication*.
- Ryder J.A. & Jager A.J. (2002). *Editors: A textbook on rock mechanics for tabular hard rock mines*, The Safety in Mines Research Advisory Committee (SIMRAC), Johannesburg, 2002.
- Salamon M.D.G. & Oravecz K.I. (1976). *Rock Mechanics in Coal Mining*, Coal Mining Research Controlling Council, Chamber of Mines of South Africa, Johannesburg, 1976.
- Scholtz J. (1997). *Sappi laboratory test press results*, Internal report: Sappi, Johannesburg.
- Smit J., Erasmus N. & Grobler R. (1998). *Report on Durapak® design methodology and findings of the rapid load tests conducted in Germany – March 1998*, Internal report: Grinaker-LTA, Johannesburg.

CHAPTER 4

STOPE SUPPORT MODEL

4.1 INTRODUCTION TO THE SUPPORT MODEL

The rock engineering practitioner has at his disposal laboratory test press results for a range of various stope support types. The majority of these tests are done in a laboratory at a much faster rate of deformation as compared to the underground environment. The laboratory test rate is typically of the order of tenths of millimetres per minute while the underground closure rate is normally quasi-static and generally in the order of millimetres per day. The rate of deformation can be rapid during rockburst conditions, and typically in the order of metres or fractions of metres per second.

There is no facility in South Africa where a full sized pack can be tested at a dynamic rate of say 1 to 3 metres per second. The information that is available to the South African mining industry arrives from work done by Taggart (1996) and by Smit, Erasmus and Grobler (1998) at the test facility at the Materialprüfungsamt Nordrhein-Westfalen in Dortmund, Germany.

The load or deformation rate as well as the height of the support element have an influence on the performance of a support element. The stope width at which the support unit is installed can vary quite significantly from the height of the unit that was tested. This phenomenon does not only have an impact on the support performance of packs but also on the potential for buckling failure in the case of timber elongates. For purposes of design and analysis of stope support it is important that these factors be taken into consideration when assessing a support element.

The stope support model that is described in the thesis is developed with the aim to be available as a design tool that rock engineering practitioners can use to quantify the in-situ performance of stope support. The engineer must be able to do this for very specific underground conditions and for different support types.

For the support model to reflect the in-situ response of stope support, all factors that can potentially have an influence on its performance must be taken into consideration. The laboratory test results must therefore be adjusted to compensate for these.

The model can only be used as a design tool if the effects of height and loading rate can be quantified in engineering and mathematical terms and incorporated into the model. The support model is not intended to make provision for so-called human errors such as poor support construction, erratic support spacing or stope support that is not installed at all.

Case studies have been used to describe the performance of stope support in an attempt to understand and quantify support reaction and behaviour. Here the capacity of the stope support is compared to the support demand imposed on it by the rockmass. These are described in Chapter 6 of this document with case studies illustrating the application in Chapter 7.

4.2 METHODOLOGY ADOPTED FOR DEVELOPMENT OF MODEL

Laboratory test curves of stope support units can be compared to a seismogram that is recorded by a seismic network. Even though this information is of some use to the trained and experienced seismologist, the seismogram will just remain another waveform. It is only when the seismogram is “translated” and presented in a mathematical format through a Fourier transformation that it is of more use to the seismologist as end-user. The character of a seismic event can be determined by studying its source parameters through the analysis of the seismogram. This approach represents a way in which the behaviour of the rockmass is described in some mathematical “language” that can be interpreted and understood by the seismologist.

This is also true for test curves of various stope support elements. Even though an experienced rock engineer can obtain some information from a load-deformation curve, more analysis is required to be able to quantify the characteristics of the support unit. It is therefore essential that the load-deformation curve be “translated” into some “language” that does not only give a true reflection of the laboratory test result, but also enables the end-user to quantify its performance characteristics. This is possible through the application of a mathematical process similar to that of a seismogram.

The ideal mathematical process must be able to quantify the capacity of a support unit. The capacity of the support units in this context refers to the in-situ performance of such an element for a certain underground environment. The factors that influence its performance are also presented in a mathematical format and taken into consideration. The final (or combined) model is in a format that can be manipulated by the end user to

describe the character of the support element. It enables him to quantify the effect that various influences have on the performance of such a support unit. The end user has the option to change some of these parameters and quantify the effect that it has on the capacity of the support unit.

4.2.1 Mathematical representation of laboratory test results

A polynomial of the n^{th} order was applied to best describe the laboratory test curves of support units mathematically. The order of the polynomial is a function of the accuracy with which the curve is reproduced. The majority of the support elements were found to be best described by a sixth order polynomial.

The mathematical equation representing a support unit is in the format:

$$y = f(x) = c_1x^6 + c_2x^5 + c_3x^4 + c_4x^3 + c_5x^2 + c_6x \quad (4.1)$$

where:

y = $f(x)$ = Load generated by element (kN);

x = Deformation (mm); and

c_n = Constants with $n = 1, 2, \dots, 6$.

Figure 4.1 shows a typical example of a laboratory test curve for a 75 cm x 75 cm Solid Hardgum Matpack, 1.8 m high that was tested at a rate of 14 mm/minute. The relatively good correlation that exists between the 6th order polynomial representing the curve and the laboratory test press result is illustrated. The 6th order polynomial that describes the mathematical fit shown in Figure 4.1 is:

$$y = 759.66x^6 - 1636.4x^5 + 1306.8x^4 - 440.47x^3 + 40.768x^2 + 13.918x.$$

This process was repeated for all the timber and concrete packs as well as timber elongates commonly used in the gold and platinum mining industry.

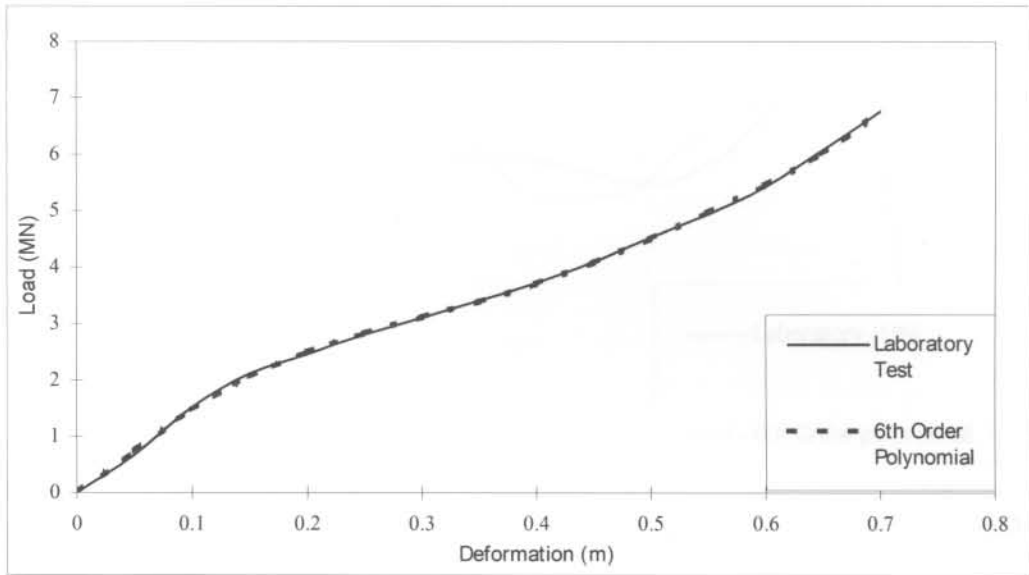


Figure 4.1: Laboratory test curve and the 6th order polynomial fit to the data for a 75 cm x 75 cm Solid Hard gum Matpack

Figure 4.2 shows the polynomial representation of a 200 mm diameter Wedge Prop, 2.0 m high and tested at a rate of 5 mm/minute. The polynomial equation was manipulated in cases where a perfect fit was not possible initially. The polynomial was altered so that the estimated energy over the total deformation range would be more or less the same as for the laboratory test curve.

A summary of all constants for the different support units that were analysed is given in Table 4.2 at the end of the chapter. The table shows all detail with respect to the type and dimensions of support as well as the rate of deformation during the laboratory test.

Graphs illustrating the polynomial fit to the laboratory data are included as Appendix 1.

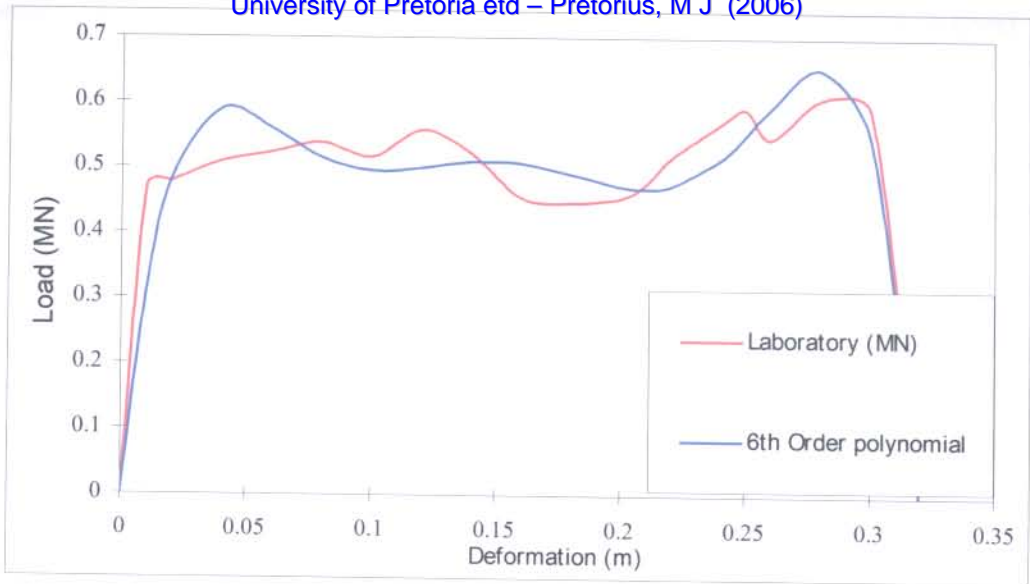


Figure 4.2: Laboratory test results and a 6th order polynomial fit to the data of a 200 mm diameter Wedge Prop, 2.0 m high and tested at a rate of 5 mm/minute

4.3 FACTORS THAT INFLUENCE SUPPORT PERFORMANCE

The following factors influence support performance and require adjustments to the support functions to be made:

4.3.1 Creep

According to Titherington (1970) creep refers to the slow but continuous deformation of a material under a constant stress. The effect of creep manifests in the difference between the support performances of a support element tested in a laboratory compared to the in-situ performance of the same unit. This comes as a result of the difference in rates of deformation.

Rate of deformation therefore has a major influence on support performance, and must be incorporated in the support function to fully describe and represent the performance of such an element.

The quasi-static underground rate of closure is much lower than the rate at which support units are normally tested. The in-situ performance of a support unit,

expressed in terms of the load generated under this slow rate of closure is lower than laboratory results for the same amount of deformation.

Rapid or dynamic loading has the opposite effect on both timber - and lightweight cementitious support units. In such cases the support unit generates an increased load of resistance when subjected to this higher rate of deformation.

The extent to which the laboratory support performance data must be up- or downgraded as a result of the effect of the rate of deformation, is a function of both material type and the differences between laboratory - and underground rates of deformation.

4.3.2 Height of pack

The taller a pack for the same pack type and base dimensions, the softer it is. This means that the taller pack will generate a lower load at the same amount of deformation than a squat pack with the same base dimensions. The latter is mainly because of an increase in voids, Kotzé (1987), and an increased probability for poor surface contacts between timber surfaces, Spearman and Pienaar (1987) as the slenderness ratio increases.

A method of predicting pack performance from the average contact area between adjacent mats in a pack was developed by Spearman (1983, 1987). The stress-strain relationships derived from pack tests were characterised by straight lines. In his analysis the moduli were correlated with the average percentage contact area of the mats in the packs. Spearman confirmed that the stiffness of the pack is directly related to the contact area.

Correction must be made for this aspect in the design process of support in order to represent the in-situ support reaction as accurately as possible.

4.3.3 Buckling failure of elongate support

Timber elongates tend to buckle and fail when exceeding a critical slenderness ratio. Valuable work has been done in this regard by Roberts, Jager and Riemann (1987) in order to quantify the buckling potential of timber elongate support. This aspect is also incorporated into the mathematical support model.

4.3.4 Pre-stress of support

Stope support is often pre-stressed during installation. This practice forms an integral part of stope support practices underground and influences the support performance at the very early stage during installation. It changes the support behaviour from passive to active as the unit exerts load onto the rockwalls before any deformation of the rockmass has taken place. The pre-stressing of a support element affects the support resistance generated by it on installation.

The support model must include this aspect in order to produce an accurate representation of support performance when quantifying the stope support capacity.

4.4 QUANTIFICATION OF INFLUENCING PARAMETERS

The factors affecting the behaviour and performance of support elements as discussed in 4.3 are expressed in mathematical and engineering terms as follows:

4.4.1 Loading rate factor

This factor describes the effect that the rate of deformation has on the performance of a support unit and compensates for the effect of creep as discussed in 4.3.1. The loading rate factor (Y) is determined for lightweight cementitious packs, timber packs and timber elongates. The effect of the loading rate is discussed under the headings that follow.

(a) Lightweight cementitious packs

A series of results was made available to the author by Smit (1998) of tests conducted by the manufacturer of the lightweight concrete Durapak.[®] Amongst these results were tests conducted under rapid loading, conventional laboratory tests as well as in-situ results from underground instrumentation.

The rapid loading tests were conducted at the test facility at the Materialprüfungsamt Nordrhein-Westfalen in Dortmund, Germany. The facility can handle up to 650 ton at a maximum loading rate of 400 mm/s. It also has the ability to induce rapid or impact loading at any stage during the test cycle.

University of Pretoria etd – Pretorius, M J (2006)

This test data is useful and makes it possible to develop a mathematical function that can be applied to the laboratory results in order to calculate the load generated by a support unit for the varying rates of deformation. The adjusted function is developed by applying the adjustment factor to laboratory results until it reproduced the performance curves that were recorded under either quasi-static or rapid deformation rates.

This was done repeatedly on a trial basis and the function continuously changed until the adjusted laboratory results produced a curve similar to the one recorded. The function is developed in a way that it up- or downgrades the performance function of the support unit for various rates of deformation.

Y denotes the load rate adjustment to be made to the support performance function:

$$Y = (1 + 10.4/100)^{-\log(V_0/v)} \quad (4.2)$$

where:

- Y = Loading rate effect adjustment to the support function;
- v = Underground rate of closure (mm/minute); and
- v₀ = Deformation rate of laboratory press test (mm/minute).

A graphical representation of the Y-factor is shown in Figures 4.3(a) and 4.3(b).

The support performance function $y = f(x)$ is multiplied by the Y-factor to compensate for the effect that the rate of deformation has on the performance of the unit. Where $Y > 1$, the load generated by the support unit is higher than that generated by the same unit under laboratory conditions. If $Y < 1$ the opposite is true and the load generated by the unit will be lower than that under laboratory conditions.

The value for the Y-factor of lightweight cementitious packs is closer to unity for both quasi-static and dynamic loading ranges as illustrated in Figures 4.3(a) and 4.3(b). It is concluded from this that the load rate has less influence on the performance of lightweight cementitious packs than on timber packs or timber elongates.

(b) Timber packs

The rate of loading has a major influence on the support performance of timber support as will be demonstrated and cannot be neglected during the support design process. The force-deformation behaviour of timber packs under rapid loading conditions has not been properly quantified in the past mainly because such a testing facility is not available in South Africa.

Roberts, Pienaar and Kruger (1987) first determined the relationship between the force-deformation behaviour of timber packs underground and the laboratory press. Through this relationship a percentage is calculated with which laboratory results should be reduced to account for the lower rate of deformation underground. This relationship was published as:

$$x = (H_{\text{perp}}/H) \cdot 7 \log(v_0/v) \quad (4.3)$$

where:

- x = Percentage reduction in load carried (%);
- H = Total height of pack (m);
- H_{perp} = Total height of the timber elements in the pack on which the load acts perpendicular to the grain of the timber (m);
- v₀ = Laboratory rate of deformation (mm/minute); and
- v = Underground closure rate (mm/minute).

These findings were extrapolated into an equation that yields the force-deformation behaviour of timber packs at loading rates that will be achieved during expected rockburst conditions of 0.3 m/s to 3.0 m/s. This equation was not verified by laboratory testing at the time because of a lack of a suitable testing facility.

To properly design stope support, it is essential that the support behaviour under rapid loading conditions be accurately quantified. More research has therefore been done in this regard by the CSIR Division of Mining Technology since the first series of tests. Tests were undertaken by the CSIR at the MPA-NRW test facility in Dortmund, Germany by Taggart (1996). The packs were tested at three different loading rates, namely 0.003 m/s, 0.03 m/s and 0.3 m/s. The results of the tests are described by Taggart (1996) who found a linear relationship between a change in deformation rate and the resulting change in pack force of approximately 16 per cent per order of

magnitude change in deformation rate. He also found that the variance is irrespective of the size and the composition of the packs. This relationship is given as:

$$F_{\text{fast}} = F_{\text{slow}} \cdot \{1 + (\% \text{inc} / 100)\}^{\log(v_0/v)} \quad (4.4)$$

where:

F_{fast} = Force at rapid rate of deformation (kN);

F_{slow} = Force at slow rate of deformation (kN);

%inc = Percentage increase in strength (%);

v_0 = Fast rate of deformation (m/s); and

v = Slow rate of deformation (m/s).

The previous equation was altered into a format with the ratio $F_{\text{fast}}/F_{\text{slow}}$ to be consistent to that of the lightweight cementitious packs. This ratio represents the relationship between the forces generated by the in-situ support unit to that of the laboratory unit and is a function of the respective deformation rates.

The Y-factor that describes this ratio is given as:

$$Y = (1 + (16/100))^{-\log(v_0/v)} \quad (4.5)$$

where:

v = Underground rate of closure (mm/minute); and

v_0 = Deformation rate of laboratory press test (mm/minute).

Figures 4.3(a) and 4.3(b) show the Y-factor value for timber-, lightweight cementitious packs and timber elongates for both quasi-static and dynamic loading conditions. A factor value 1 indicates a load-deformation performance that is equivalent to the test laboratory results. The analysis demonstrates that the load rate has more influence on the performance of timber packs than on that of timber elongates and lightweight cementitious packs.

The Y-factor varies most from unity in the case of timber packs where the Y-value can be as low as 0.5 for quasi-static conditions to a value of 1.75 under dynamic loading conditions. In practice the in-situ performance of a timber pack under quasi-static conditions can therefore be as low as 50% of the laboratory test results. For dynamic

University of Pretoria etd – Pretorius, M J (2006)

loading conditions of say 3 m/s this value can be as high as 1.75. This means that the pack will generate a load of 75% more than that of the laboratory test results.

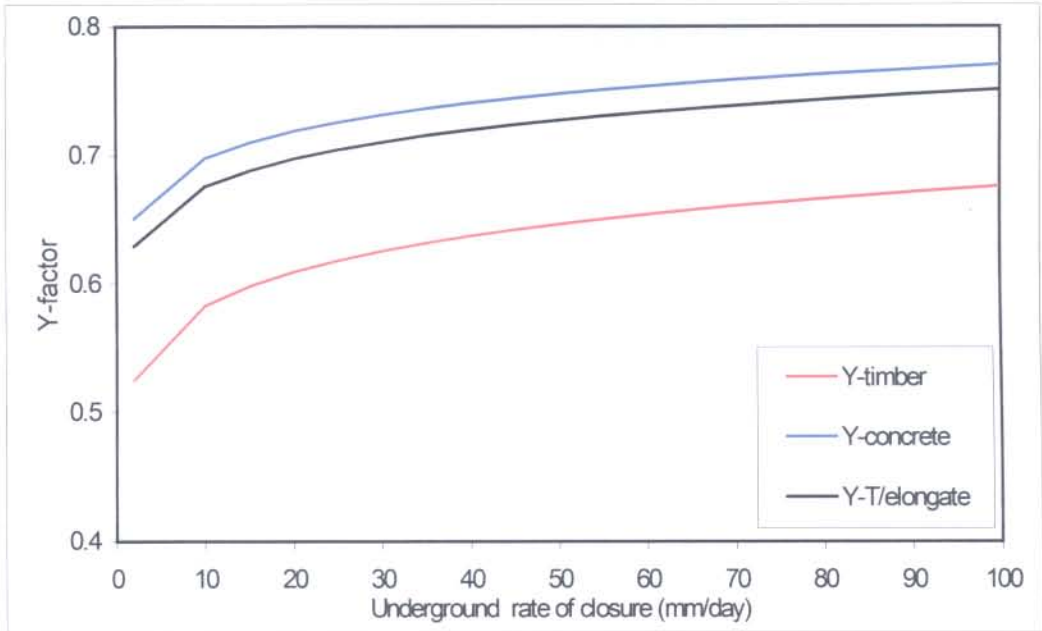


Figure 4.3(a): Y-factor values for timber-, lightweight concrete packs and timber elongates for quasi-static loading conditions

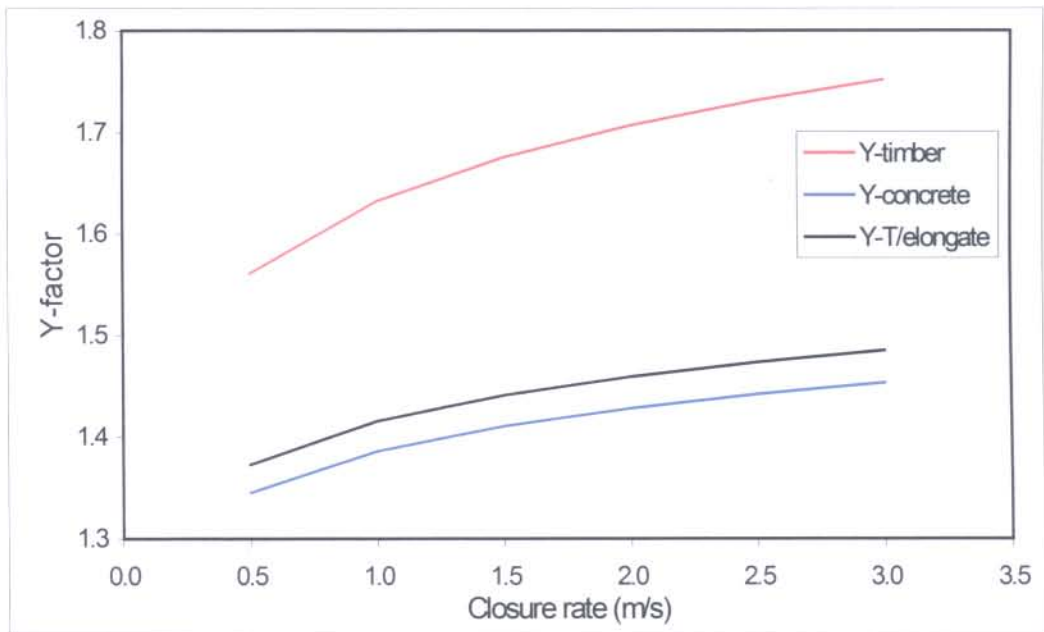


Figure 4.3(b): Y-factor values for timber-, lightweight concrete packs and timber elongates under rapid loading conditions

(c) Timber elongate support

The force-deformation curves can be adjusted up- or downward to account for different loading rates. This is done according to data published in this regard by Roberts (1987) as shown in Figure 4.4.

For example the logarithm of the two differing loading rates is taken and the force correction factor is read off the graph shown in Figure 4.4. If a force-deformation curve was determined in a laboratory test at 40 mm/minute and it is required to know the force-deformation behaviour of the unit under a stope closure of 10 mm/day, then:

$$\begin{aligned} \log(v_0/v) &= \log(40 \text{ mm/minute}/10 \text{ mm/day}) \\ &= \log(57600 \text{ mm/day}/10 \text{ mm/day}) \\ &= \underline{3,76} \end{aligned}$$

Reading the force correction from the graph indicates that the force should be multiplied by a factor of 0,76. This will result in a reduced force exerted by the unit of approximately 76% of that of the laboratory test.

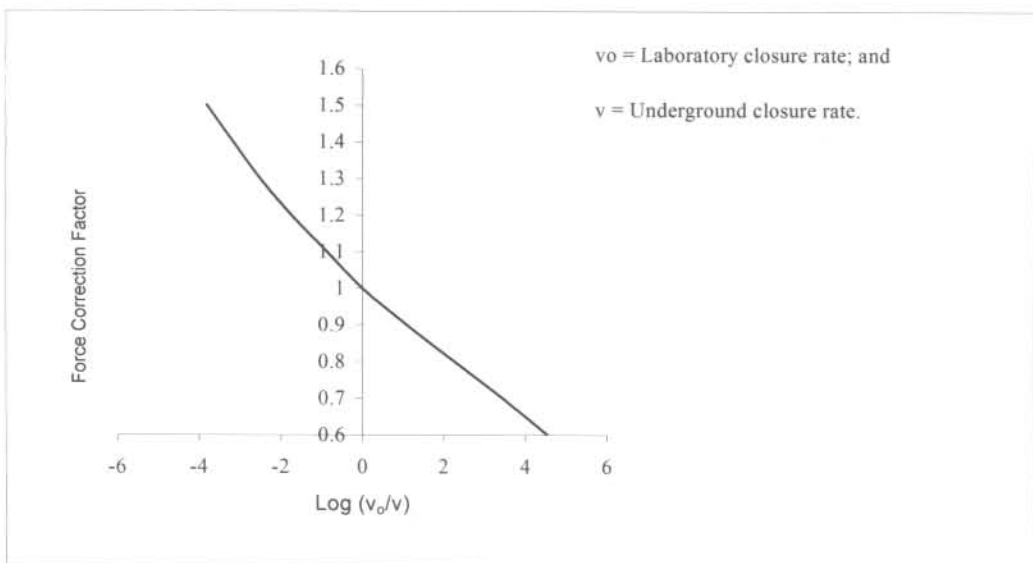


Figure 4.4: Force correction factor for timber elongates as developed by CSIR

This curve is represented mathematically in a format that allows it to be integrated with the support performance functions. Adjustments can be made from this to the support

performance function of timber elongated type of support. The equation that describes the force correction factor is given by:

$$Y = c_{e1} \cdot [\log (v_0/v)]^2 - c_{e2} \cdot [\log (v_0/v)] + 1 \quad (4.6)$$

where:

Y = Loading rate effect adjustment to the support function;

v = Underground rate of closure;

v_0 = Deformation rate of laboratory test;

c_{e1} = 5.3E-3; and

c_{e2} = 0.1084

Figure 4.5 illustrates how well the Y-factor quadratic equation describes the force correction curve that was developed by the CSIR.

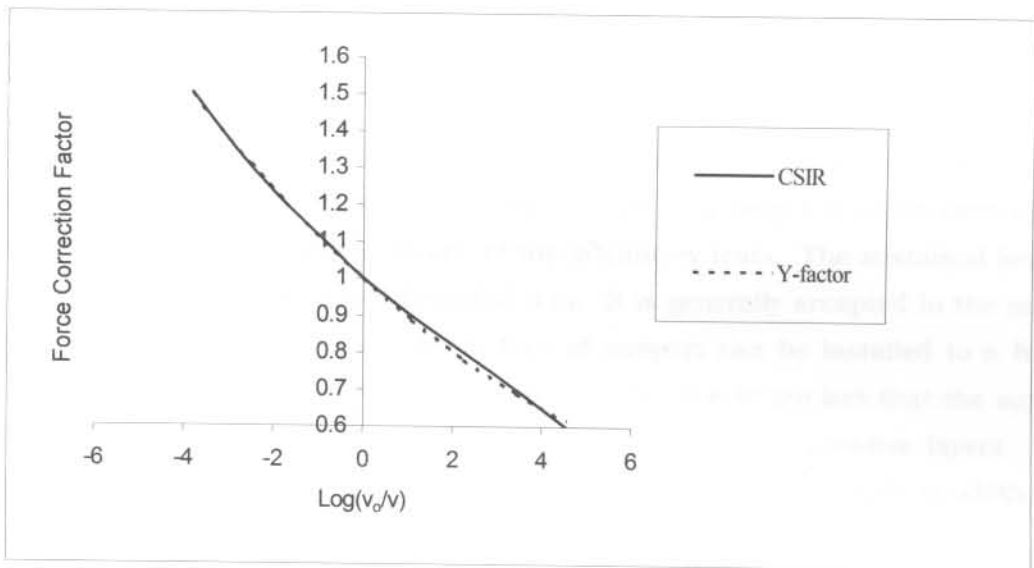


Figure 4.5: Correlation between quadratic Y-factor equation and curve developed by the CSIR

Figures 4.3(a) and 4.3(b) show the Y-factor value for timber-, lightweight cementitious packs and timber elongates for both quasi-static and dynamic loading conditions. The Y-factor for timber elongates varies less from the value of 1 than when compared to the results of a timber pack.

It shows that the Y-factor value can be as low as 0.62 for quasi-static loading conditions to a value of 1.45 under dynamic loading. This means that a conventional timber elongate unit will only be able to generate 62% of the laboratory test results under quasi-static loading conditions. It can however generate as much as 45% more load in-situ than in the laboratory during rapid deformation at a rate of say 3 m/s.

4.4.2 Support height factor

The influence that the height of a support unit has on the performance of both lightweight cementitious - and timber packs is described in 4.4.2(a) and (b).

(a) Lightweight cementitious packs

A number of laboratory test results that were done on different heights of packs were used for the purpose of this analysis. The sustained load of the different heights of packs are determined and plotted against the height of the pack. This relationship is described by fitting a mathematical function to the data.

The base dimension of the packs tested were 60 cm x 60 cm and the packs were constructed to a height of 180 cm. The latter relates to a height to width ratio of 3:1. No buckling failure was observed in any of the laboratory tests. The sustained load for taller packs was extrapolated to a height of 3 m. It is generally accepted in the mining industry that a lightweight cementitious type of support can be installed to a higher height to width ratio than conventional timber support due to the fact that the support matrix is homogeneous with firm and total contact between successive layers. It is expected that buckling failure will start taking place once a certain height to width ratio is exceeded, but no literature could be found that defines this upper limit.

It is established that the best way of predicting pack performance using the height factor (H_f) for lightweight cementitious packs was through the ratio of two fifth order polynomial functions. The height factor for a lightweight cementitious pack is given by the ratio of the functions of the pack installed underground to the one tested.

$$H_f = y_{sw}/y_{th} \quad (4.7)$$

where:

- H_f = Height factor adjustment to the support performance function;
 y_{sw} = 5th Order polynomial for the pack height (x_1) underground unit;
 $= c_1x_1^5 + c_2x_1^4 + c_3x_1^3 + c_4x_1^2 + c_5x_1 + c_6$
 x_1 = Stopping width or underground pack height (m);
 y_{th} = 5th Order polynomial for the pack height tested in the laboratory;
 $= c_1x_2^5 + c_2x_2^4 + c_3x_2^3 + c_4x_2^2 + c_5x_2 + c_6$
 x_2 = Height of pack tested in the laboratory (m)
 with:
 c_1 = -576.24
 c_2 = 5956.60
 c_3 = -24079.00
 c_4 = 47565.00
 c_5 = -45937.00
 c_6 = 17935.00

Figure 4.6 shows the sustained loads of lightweight cementitious packs for the different pack heights as well as the 5th order polynomial function that represents the data. The analysis indicated that a point is reached at a pack height of approximately 1.25 m where an increase in the height of the pack has hardly any influence on the sustained load of the pack.

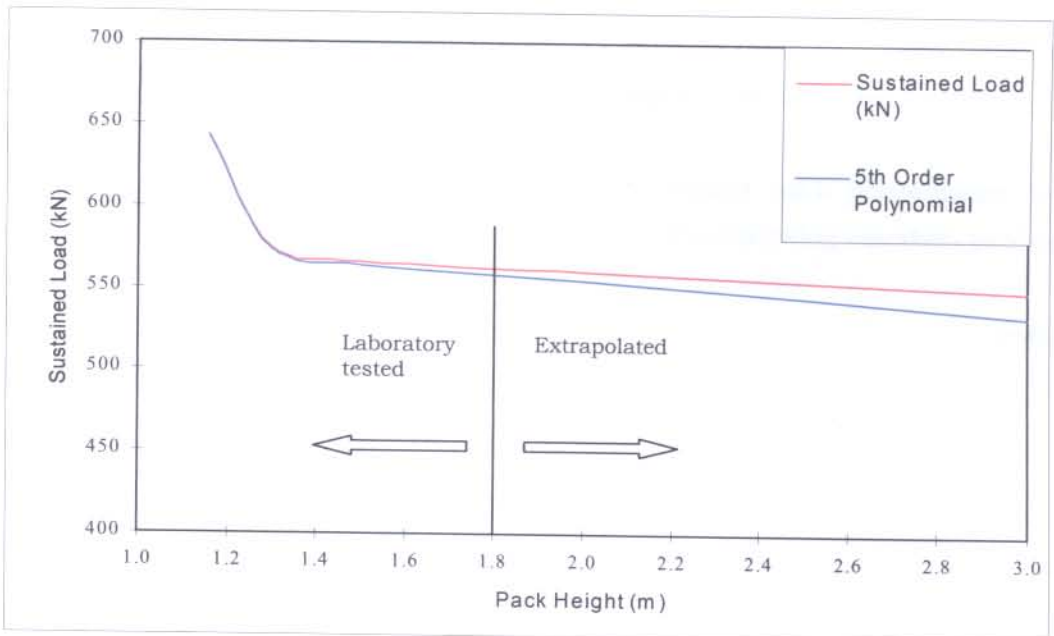


Figure 4.6: Sustained load and mathematical representation of the same data for different heights of lightweight cementitious packs

(b) Timber packs

It is known that the stability of packs decreases with increasing height according to Roberts et al (1995) and Ryder and Jager (2002). It is commonly assumed that timber packs with a height to width ratio exceeding 2:1 are unstable, particularly during dynamic closure. This is a qualitative assessment from underground experience and is assumed to be correct. According to Ryder and Jager (2002) the pack type does have an influence on its buckling potential, with the stiff end-grained types of packs having a higher buckling potential than conventional mat packs.

The pack height adjustment factor is used to adjust the pack performance curve and compensate for the influence that the height of the support unit may have on the performance of the support unit.

A series of tests was done on solid timber packs at different heights but with the same base dimensions. The objective is to develop a correction factor (H_f) to be applied to compensate for the difference in height. Such a function must ideally be able to account for the continuous change in width to height ratio of the support unit during the deformation process.

Tests were conducted on solid timber packs with base dimensions of 0,75 m x 0,75 m and heights of 0.9 m, 1.1 m, 1.3 m and 1.5 m. From these results a number of factors were developed to account for the differences in the support performance.

A number of different equations were developed to predict pack performance for a different pack height from an existing or known pack. The following equation produced the best fit to the pack performance curve it is intended to predict.

$$H_f = (T_h/S_w) \cdot (1 + [(D_{ef}/S_w) - (D_{ef}/T_h)]) \quad (4.8)$$

where:

T_h = Height of pack tested (m);

S_w = Stopping width (m); and

D_{ef} = Deformation (mm)

Figure 4.7 shows a typical application of this principle where the original test curve of a 1.1 m pack is plotted. It shows the prediction of a 1.1 m high pack curve extrapolated from data of the 1.5 m, 1.3 m and 0.9 m high packs respectively.

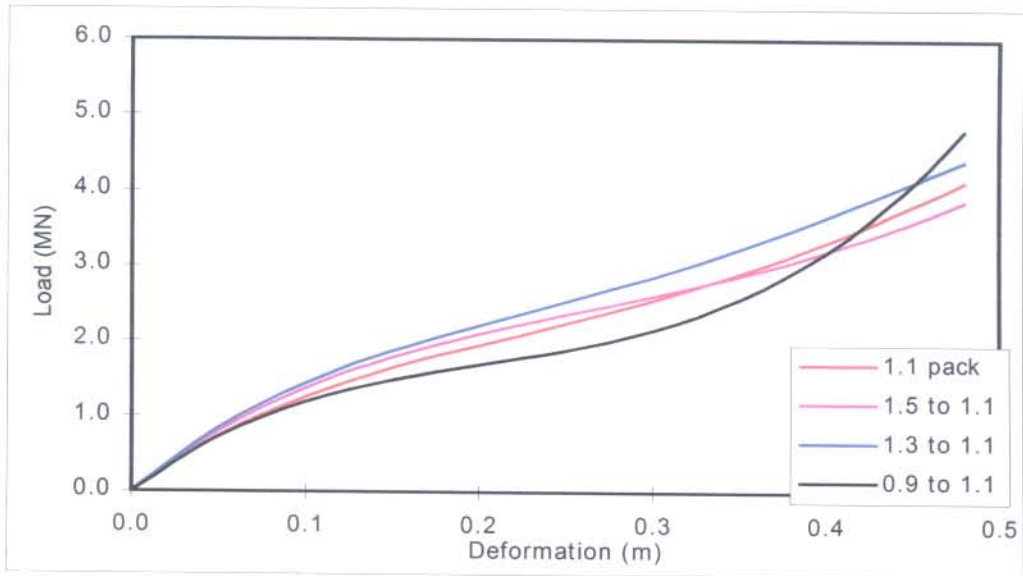


Figure 4.7: Prediction of a 1.1 m high solid matpack from data of 1.5 m, 1.3 m and 0.9 m high packs

It was accepted that this approach yields an adequately accurate representation of the load-deformation curve of a timber support unit that is predicted from the performance curve of a pack of the same type.

4.4.3 Buckling failure of timber elongate support

Buckling failure of an elongate has a major impact on the design of support since it influences the stability of the unit once a certain amount of deformation is exceeded. Buckling failure of elongate support does not only affect the ability to absorb energy but also the stiffness of the unit during deformation.

Props with an increased yield range have a higher energy absorption ability or capacity. According to Roberts (1991) high closure prior to the event reduces the ability of a yielding timber elongate to absorb energy during a rockburst.

The factor applied to account for buckling failure of elongate support is given below. Here the elongate support performance function is adjusted to represent the typical performance of an elongate under buckling failure conditions.

$$B_f = 1 - (S_w - 1) \cdot 10^{(10x-2)} \quad (4.9)$$

where:

- B_f = Buckling failure factor of elongate;
 S_w = Stopping width (m); and
 x = Deformation (m)

Note that:

for a stopping width $S_w < 1$ m, $B_f = 1$, and

for stopping width $S_w > 2.5$ m, $B_f = 0$

The effect that buckling failure has on the performance of a typical elongate is illustrated by Figure 4.8. The laboratory test result shows a 160 mm diameter Profile Prop, 1.0 m long that was tested at a rate of 10 mm/minute. The adjusted curve represents the effect of buckling of the same support element that is installed at a height of 1.8 m with an underground closure rate of 10 mm/day. This illustration shows that the buckling of the support unit does not only affect the peak load generated by the longer unit but also that it has shed all load at a deformation just over 200 mm as opposed to the 500 mm in the test press. The stiffness of the in-situ unit is also different to the laboratory test result.

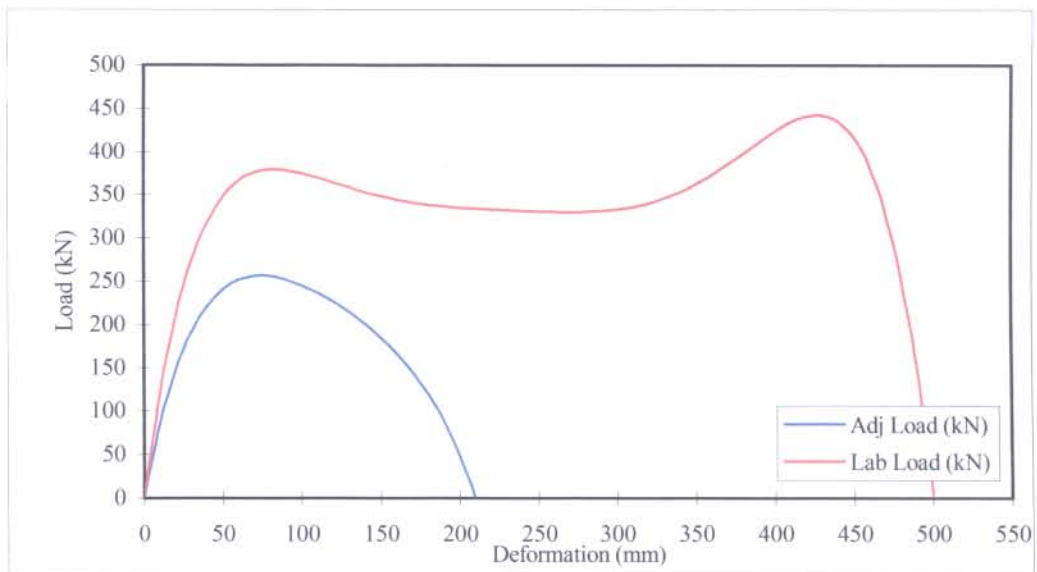


Figure 4.8: Effect of buckling on the performance of a 160 mm-diameter Profile Prop

4.5 ADJUSTED MODEL

All factors that influence the performance of a support unit are incorporated into a single mathematical equation to get an all-inclusive support performance model.

These factors are introduced and integrated in an adjusted support function. This function describes the in-situ performance of stope support elements. It represents its support performance for both quasi-static and dynamic loading conditions. It is given for the following support groups:

4.5.1 Pack support performance function

The adjusted function for pack support is described by the support performance function $f(x)$ that is adjusted to compensate for the rate of deformation (Y) and height influence (H_f). The adjusted support performance function $f_a(x)$ for pack support is given by:

$$f_a(x) = f(x) \cdot Y \cdot H_f \quad (4.10)$$

where:

- $f_a(x)$ = Adjusted support function for pack support;
- $f(x)$ = Function describing the support performance of a specific pack type (timber & lightweight cementitious material);
- Y = Loading rate factor as described in 4.4.1 (a) and (b); and
- H_f = Support height factor as described in 4.4.2 (a) and (b).

4.5.2 Timber elongate support performance function

The adjusted support performance function for elongated support is similar to that of the packs with the difference that a buckling factor B_f is introduced in the function. The adjusted support performance function is thus given as:

$$f_a(x) = f(x) \cdot Y \cdot B_f \quad (4.11)$$

where:

- $f_a(x)$ = Adjusted support function for timber elongates;
- $f(x)$ = Function describing support performance of a specific timber elongate; and
- Y = Loading rate factor as described in 4.4.1(c); and

B_f = Buckling failure factor for elongate as described in 4.4.3.

4.6 OUTPUT FROM THE ADJUSTED SUPPORT MODELS

The adjusted stope support performance function embodies information that is relevant to the design of stope support. Once the stope support performance function is presented in the format as shown in 4.5.1 and 4.5.2 the function can be applied mathematically to produce the following as output:

4.6.1 In-situ load

The in-situ load generated by a support unit is determined by substituting the deformation value of interest (x) into the adjusted function $f_a(x)$ for the specific support element. The load generated by the support element represents its actual or in-situ performance and takes into consideration all factors that influence its performance.

Figure 4.9 shows both the laboratory test press results as well as the in-situ load generated by a 75 cm x 75 cm Brick Composite pack. The pack is 1.5 m high and was tested at 30 mm/minute while an underground closure rate of 20 mm/day is simulated.

The effect that the slow deformation rate has on the support performance is illustrated.

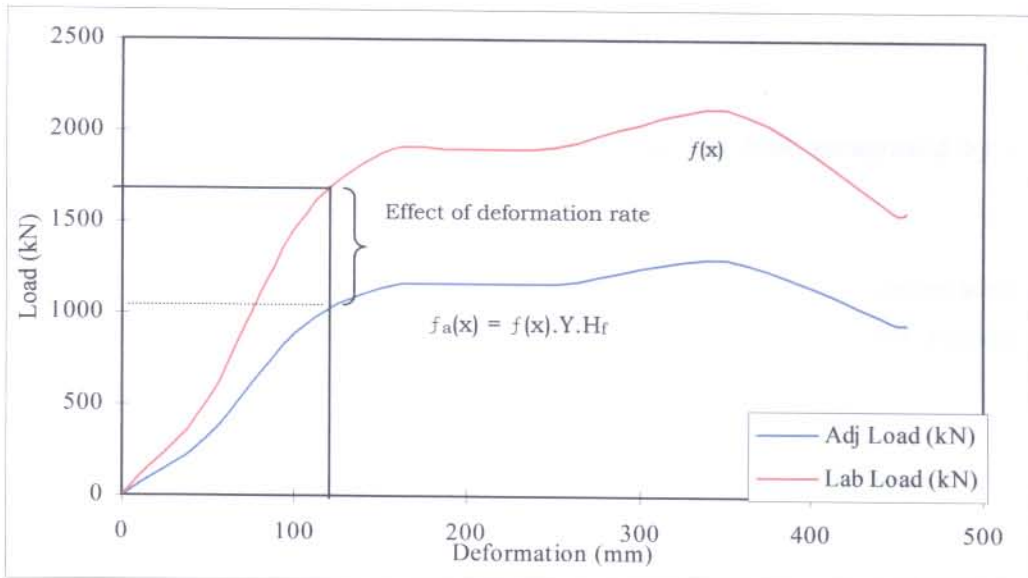


Figure 4.9: Laboratory and in-situ support performance of a 75 cm x 75 cm 9-Pointer Brick Composite pack

Figure 4.10 shows the effect that the buckling failure has on the support performance of a 160 mm diameter Profile Prop of 1.0 m high that was tested at 10 mm/minute. It illustrates the effect that buckling failure has on the load generated by the elongate. The underground unit that is simulated is 1.8 m in length with an underground closure rate taken at 20 mm/day.

The analysis demonstrates that total failure of the 1.8 m long Profile Prop has taken place after 210 mm of deformation. The laboratory test results of the 1.0 m long unit show that final failure starts to occur at approximately 450 mm deformation.

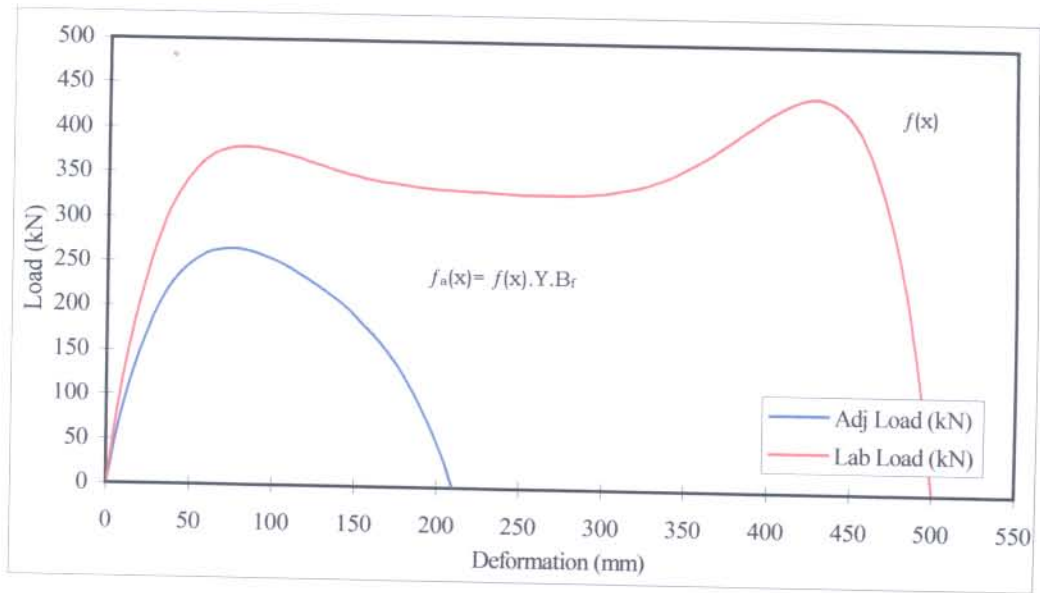


Figure 4.10: Effect of loading rate and buckling on the load generated by a 1.8 m long 160 mm diameter Profile Prop

Figure 4.10 illustrates that the in-situ load generated by the taller support unit for the same amount of deformation is less than that of the laboratory test results of the shorter one.

The analysis also demonstrates that the factors influencing its performance do not only have an impact on the stiffness of the support element but also on its energy absorption capacity as discussed in 4.6.3 and 4.6.4.

4.6.2 Support resistance

The support resistance (SR) of a unit is defined as the load generated per unit area for a given amount of deformation. It is assumed that a tributary area is allocated to a support unit. The tributary area is calculated as the product of dip - and strike spacing of the support. Support resistance is expressed in kilonewton per square meter, (kN/m^2).

The support resistance at the given point of deformation is calculated by dividing the load generated by the support unit by its tributary area. Support resistance is given as:

$$\text{SR} = f_a(x) / (D_s \cdot S_s) \quad (4.12)$$

where:

- SR = Support resistance (kN/m^2);
- D_s = Dip spacing of support elements (m); and
- S_s = Strike spacing of support elements (m).

4.6.3 Stiffness of support unit

The slope of the load-deformation curve represents the stiffness of the support element. Stiffness of a support unit is defined as the change in load generated per unit deformation and expressed in kN/mm . Stiffness also indicates strain hardening or softening of the support.

Stiffness of the support unit at any point of deformation is determined by differentiating the adjusted support performance function. It is calculated mathematically as $\partial/\partial x[f_a(x)]$ for any point (x) of deformation.

The stiffness of the support unit is given as $\partial/\partial x[f_a(x)]$ where $f_a(x) = f(x) \cdot Y \cdot H_f$ for packs and $f_a(x) = f(x) \cdot Y \cdot B_f$ for timber elongates. The combined function is differentiated as the product of two functions $f(x)$ and B_f (Buckling failure - elongates) or H_f (Height factor – packs) all functions of deformation x.

The adjustment functions are defined as given in 4.3 of this chapter namely the factors that influence support performance.

This concept is further illustrated in Figure 4.11 that shows the same load-deformation curve of the laboratory and in-situ Brick Composite packs presented in Figure 4.9.

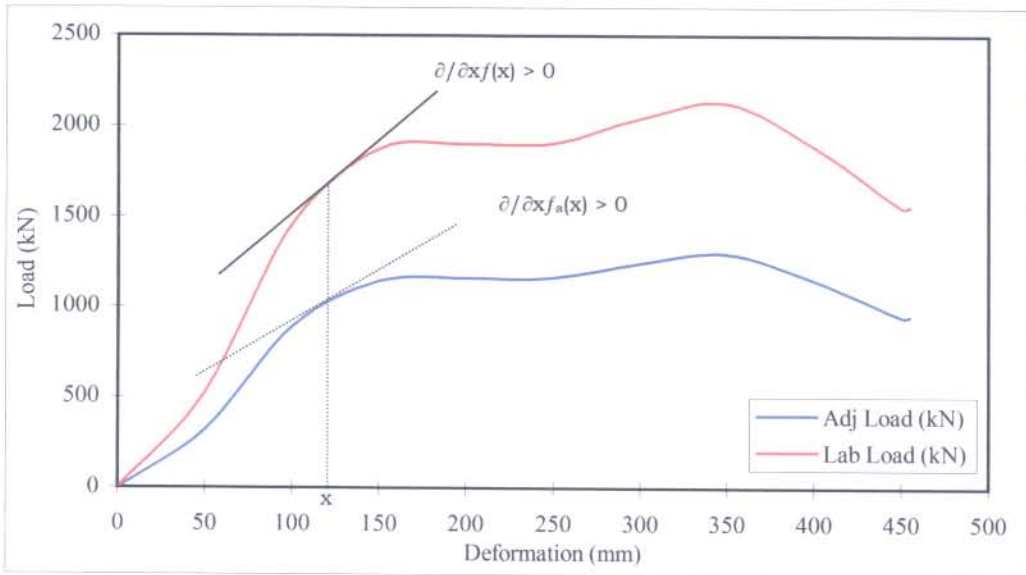


Figure 4.11: Difference in stiffness of the 75 cm x 75 cm Brick Composite pack for laboratory and in-situ performance functions

Figure 4.11 illustrates how the in-situ stiffness of an elongate can be different from the laboratory results for the same magnitude of deformation. The quasi-static underground rate of deformation is taken as 20 mm/day as opposed to a laboratory test rate of 10 mm/minute that is simulated.

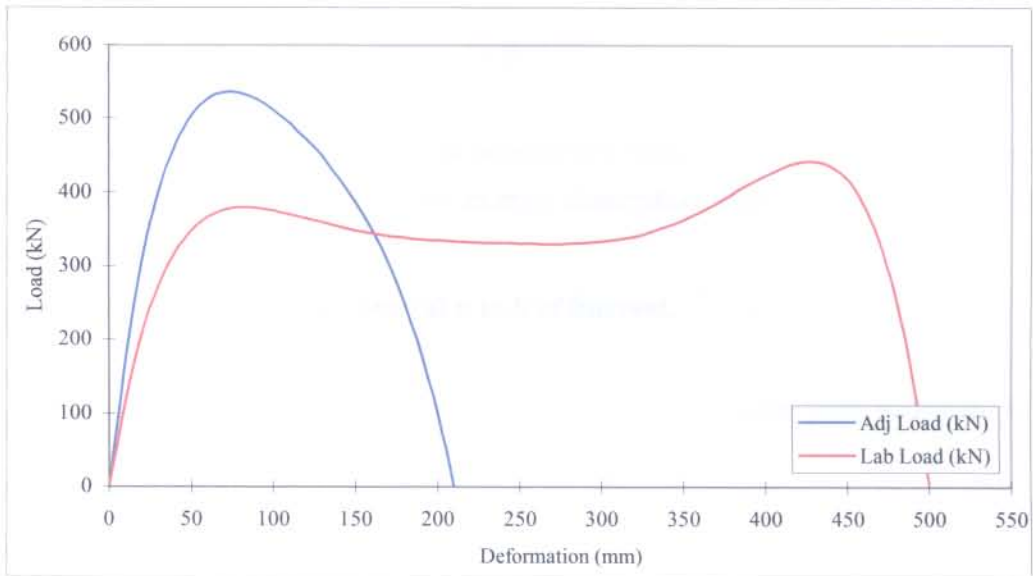


Figure 4.12: Effect of the rate of deformation and buckling of the elongate on the performance of a 160 mm diameter Profile Prop

Figure 4.12 illustrates that this is also true in the case of rapid deformation of the same unit. The curves that are produced show results of a Profile Prop 1.8 m in length, deformed at a deformation rate of 1 m/s as opposed to a laboratory test of the same unit of 1.0 m in length that was tested at 10 mm/minute. It illustrates how the rate of deformation can influence the stiffness of the support unit through the entire range of deformation.

The following data can be determined and quantified from the support stiffness analysis:

1. The magnitude of strain hardening and/or softening of a support unit at any given point of deformation as expressed in kN/mm, and
2. The point of where failure or strain softening starts occurring for any support type i.e. where $\partial/\partial x[f_a(x)] = 0$

4.6.4 Energy absorption capacity

As the rate of deformation influences the load generated by the support unit and likewise its stiffness, this will also have a direct influence on the energy absorption capacity of that particular support unit. The same is true for the underground height of

installation as opposed to the height of the unit tested. This also has an influence on the support performance of an element and therefore its capacity to absorb energy.

The energy absorbed by the support is determined mathematically by integration of the adjusted support function $f_a(x)$. The energy absorption capacity that is expressed in kilo-joule (kJ) is determined as:

$$\int_a^b f_a(x) \partial x \text{ for the deformation interval } a \text{ to } b \text{ of interest.}$$

This principle is illustrated for a 75 cm x 75 cm Brick Composite pack in Figure 4.13.

The following rule of partial integration applies when calculating the energy absorption capacity of a support unit:

$$\int_a^b f_a(x)g(x)\partial x = f(x) \cdot \int_a^b g(x)\partial x - \int_a^b [\int_a^b g(x)\partial x]f'(x)\partial x \text{ with the functions } f_a(x) \text{ and } g(x) \text{ as defined.}$$

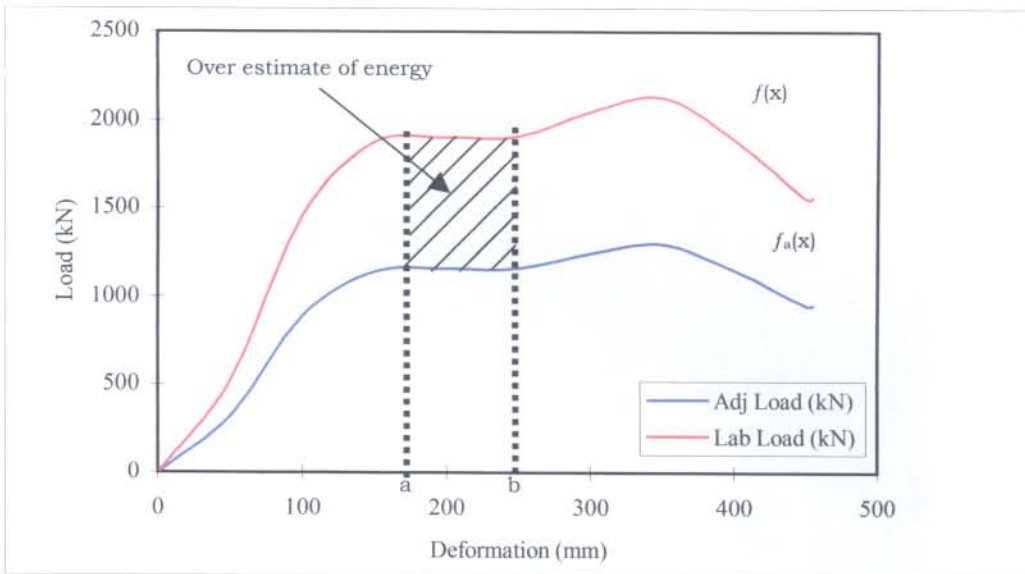


Figure 4.13: Effect of the rate of deformation and height of support on energy absorption capacity of a 75 cm x 75 cm Brick Composite Pack

4.6.5 Stress exerted onto hangingwall during quasi-static and dynamic loading

Current design of stope support during dynamic loading evaluates the stope support type based on the remaining energy absorption capacity of the support element. (Roberts (1995) - SIMRAC GAP032 Final Project Report.) The energy absorption capacity of a support element is calculated as the difference between the total energy capacity (prior to any deformation) and the amount of energy absorbed by the support element at the point of dynamic loading.

Damage often occurs to the stope hanging- or footwall during dynamic loading of the support in rockburst conditions or where the support spacing is too wide. Support may cause the excavation walls to fail around the support element if the load transferred to the walls exceeds its strength. In certain instances the support units suffer very little or no permanent damage at all.

A typical example of the previous statement is illustrated in Figure 4.14 where Hercules type of pack support was used. It shows stope hangingwall damage after a rockburst that measured 3.1 on the local magnitude scale at Unisel Shaft on Harmony Gold Mine in the Free State Gold Fields. The base dimensions of the packs are 75 cm x 75 cm with a stope width of approximately 150 cm prior to the rockburst.

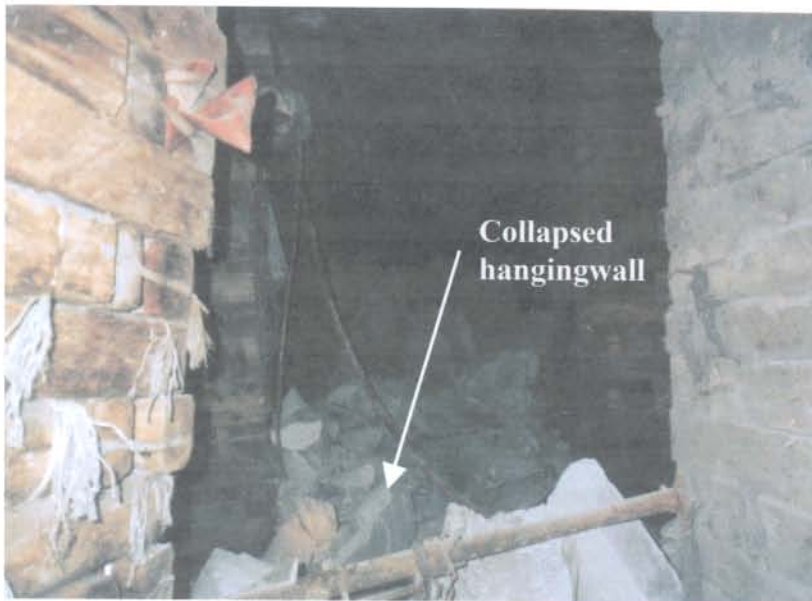


Figure 4.14: Damage to a stope hangingwall during a rockburst with a stiff type of permanent stope support

The stress generated by the support element and exerted onto the hangingwall during dynamic loading and deformation is important during the evaluation of a stope support system. This information can be used once the strength of a fractured stope hangingwall plate under dynamic conditions is fully understood and quantified.

The stress exerted onto the hanging- and footwall is calculated as:

$$\sigma_h = f_a(x)/A_p \quad (4.13)$$

where:

σ_h = Stress exerted onto excavation walls by the support element (MPa);

$f_a(x)$ = Adjusted support function; and

A_p = Support/excavation wall contact area (m²).

4.7 OTHER APPLICATIONS

During the development of the stope support model it became evident that it is possible that an estimate of the support resistance generated by a stope support system be determined. This is possible through the application of a pseudo three-dimensional elastic numerical model like Minsim W.

The Minsim W program has a feature where the user can define his/her own variable in the benchmark listing. The advantage of this or a similar model is that it makes it possible that a stope face configuration can be modelled, regional support incorporated, and support resistance calculated and contoured. One support type can be compared to another for the same underground layout and rate of closure through this approach. Areas with an insufficient support resistance as a result of say leads or lags can be identified and additional support introduced where required.

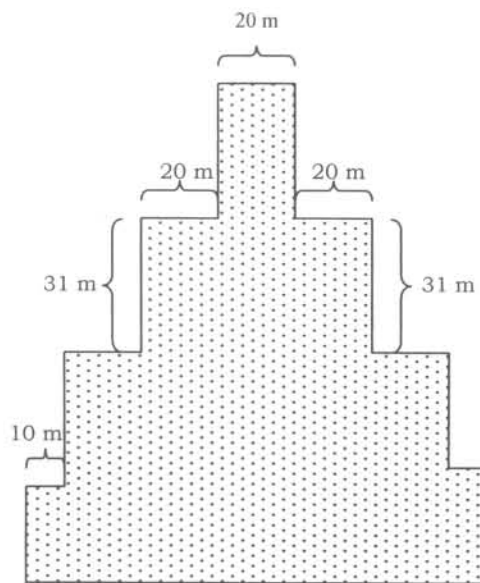
The Minsim W assumes the rockmass to be homogeneous, isotropic and elastic. To compensate for the inelastic deformation of the rockmass the Modulus of Elasticity is modified so that calculated elastic closure relates more closely to that observed underground. It must be noted that this only represents an estimate of the in-situ closure and must be interpreted as such.

To test the above, an area was modelled using Minsim W and the convergence at the centre of the panel calculated and compared to various underground closure rates in

mm/m face advance. This was done in mining steps in order to estimate values for the Young's modulus.

A constant face advance of 1 m per blast was assumed for the calculation for different underground rates of closure. The Young's modulus in the program was altered until the numerical analysis reproduces the same convergence at the centre of the panel as the inelastic or in-situ stope closure.

The layout modelled with leads, lags and limited spans is shown in Figure 4.15. Poisson's ratio was taken as 0.2 with horizontal virgin stress 50% of the vertical while a stope width of 1.5 m was modelled.



NOT TO SCALE

Figure 4.15: Schematic layout of area modelled for determining the modified Young's modulus

Table 4.1 gives a summary of the Young's Modulus that was obtained to reproduce the underground closure rates as shown.

Table 4.1: Modified Young's Modulus for different closure rates

| Closure rate (mm/m face advance) | Young's Modulus (MPa) |
|----------------------------------|-----------------------|
| 1 | 56193 |
| 10 | 5619 |
| 20 | 2810 |
| 30 | 1893 |

Any formulae can be introduced as a so-called OWN variable in Minsim W in order to calculate that what the user defines. The variable that was introduced in this case to calculate support resistance generated by a support system is given as:

$$\text{OWN} = f_a(s_z - s_n) / (D_s \cdot S_s) \quad (4.14)$$

where:

- OWN = Support resistance generated by the support system (kN/m²);
- $f_a(x)$ = Adjusted support functions compensating for the variables listed;
- s_z = Elastic convergence calculated by Minsim W (mm);
- s_n = Convergence that has taken place prior to the installation of the support at an installation distance n-meters from the stope face (mm);
- D_s = Dip spacing of support elements (m); and
- S_s = Strike spacing of support elements (m).

Figure 4.16 demonstrates the application of this methodology. It shows the support resistance contours generated by a 110 cm x 110 cm Hercules timber pack with an underground closure rate of 30 mm/m face advance. The packs are installed at a spacing of 3.0 m by 4.0 m at a stoping width of 1.5 m. The dip of the reef was modelled flat at 0°. The Young's modulus used in the numerical model in this case is 1893 MPa.

The other input parameters for the model are as follows:

- Vertical virgin stress gradient: 0.0270 MPa/m
- Horizontal virgin stress gradient: 0.0270 MPa/m
- Poisson's ratio (ν): 0.2
- k-ratio: 1.0
- Mining depth: 1000 m
- Grid size: 10 m

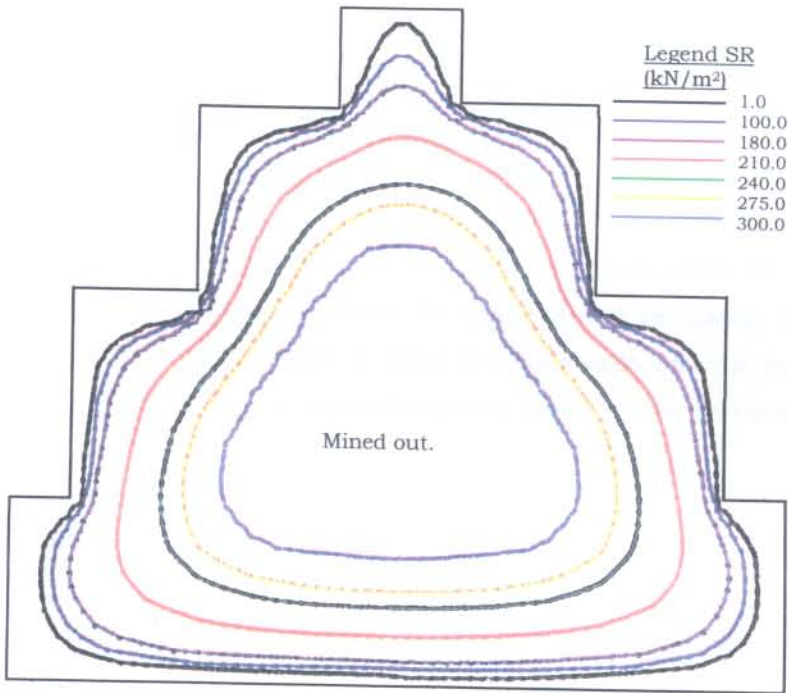


Figure 4.16: Support resistance contours of 110 cm x 110 cm Hercules type timber packs

It is possible that those areas can be identified where there is a lack of support resistance generated by the specific support type at the given support spacing. These areas developed as a result of leads and/or lags between panels for the layout that was modelled. Additional support in the form of temporary support can be introduced to compensate for this.

The stress exerted onto the hangingwall for any mining configuration can be determined in the same way. The area where the stress exerted or transferred onto the rockwalls exceeds the strength of the hanging- or footwall can be identified through this. The variable to calculate stress exerted onto the hanging- or footwall by the support system is given by:

$$\sigma_{rw} = f_a(s_z - s_n) / A_p \quad (4.15)$$

where:

- σ_{rw} = Stress exerted onto rockwalls by the support system (kN/m²);
- $f_a(x)$ = Adjusted support function compensating for all the variables defined;

- s_z = Elastic convergence calculated by Minsim W (mm);
 s_n = Convergence that has taken place prior to the installation of the support an installation distance n-meters from the stope face (mm); and
 A_p = Support/hangingwall contact area (m^2).

This methodology can be applied in practice by determining the in-situ closure rate first. An applicable Young's Modulus can be selected from Table 4.1 and the support resistance (kN/m^2) calculated as given by equations 4.14 using the underground support spacing. The stress exerted onto the rockwalls can be calculated by the equation given in 4.15 using the support contact area. It can be done for both quasi-static and dynamic conditions.

4.8 CONCLUSIONS

The study confirmed that it is possible to mathematically represent the laboratory load-deformation behaviour of both pack- and elongate types of support. This mathematical equation can be adjusted in order to compensate for factors affecting support performance such as:

1. Creep;
2. Height of support unit;
3. Buckling failure of elongate support; and
4. Pre-stress of support.

All these factors influencing support performance are also expressed in mathematical and engineering terms, and repeated for both timber and lightweight cementitious support types. The in-situ or adjusted performance function of the support unit captures all the parameters mentioned that influence the performance of the support unit.

This approach proves that it is possible to predict the in-situ behaviour of a support unit where the height of the laboratory test as opposed to the underground unit as well as the laboratory rate of testing and the underground rate of closure are known. The following output can be generated by the adjusted support function:

1. In-situ load generated by the unit;
2. Support resistance of the support;
3. Stiffness of the support unit;

4. Energy absorption of the support unit; and
5. Stress exerted onto the hangingwall.

It was concluded that the outcome of the study could also be used in another application such as calculating the support resistance of a support system through a pseudo three-dimensional elastic numerical model. The use of this approach has much potential where the support resistance for different mining geometries can be contoured and compared as illustrated in this chapter.

REFERENCES

- Kotzé T.J. (1987). *Views of the mining industry on timber supports* Proceedings: Mining Timber – From Stump to Stope, South African National Group on Rock Mechanics, June 1987, Pretoria
- Roberts M.K.C. (1991). *An evaluation of yielding timber props as a support system in rockburst conditions*, p1-7, Journal of the South African Institute of Mining and Metallurgy, Johannesburg, January 1991.
- Roberts M.K.C. (1995). Project Manager: *Final Project Report GAP032, Stope and gully support*, The Safety in Mines Research Advisory Committee (SIMRAC), Johannesburg, Web site www.simrac.co.za.
- Roberts M.K.C., Jager A.J. & Riemann K.P. (1987). *The performance characteristics of timber props*. Chamber of Mines Research Report Number35/1987, Johannesburg.
- Roberts M.K.C., Pienaar F.R.P. & Kruger F.C. (1987). *Properties of pack supports – comparison of the laboratory and underground performance* p122–135, Proceedings: From stump to stope seminar, South African National Group of Rock Mechanics, June 1987, Pretoria.
- Ryder J.A. & Jager A.J. (2002) Editors of: *A textbook on rock mechanics for tabular hard rock mines*, The safety in Mines Research Advisory Committee (SIMRAC), Johannesburg, 2002.
- Smit J., Erasmus N. & Grobler R. (1998). *Report on Durapak® design methodology and findings of the rapid load tests conducted in Germany – March 1998*, Internal Grinaker-LTA Report, Johannesburg.
- Spearman S.F. & Pienaar F.R.P. (1987). *Compression properties of timber and factors affecting them; performance prediction for packs*, p80–96, Proceedings: From stump to stope seminar, South African National Group of Rock Mechanics, Pretoria, June 1987.

Spearman S.F. (1983). *Improved timber mine supports: Predicting compression behaviour of most packs from contact area between mats*. Council for Scientific and Industrial Research Special Report HOUT 402, National Timber Research Institute, CSIR, Pretoria.

Spearman S.F. (1987). User notes for a computer-based program to predict the performance of mat pack mine supports, National Timber Research Institute, 1987, CSIR, Pretoria.

Taggart P.N. (1996). *Dynamic laboratory testing of pack based support elements. Part 1: The laboratory evaluation of timber and composite packs, single rise elements and pack and grout pre-stressing units*. Internal note: CSIR Division of Mining Technology, August 1994. Journal of the South African Institute for Mining and Metallurgy, Volume 92 No. 2, 1996.

Titherington D. & Rimmer J.G. (1970). *Applied Mechanics*, p144, McGraw Hill Publishing Company Limited, England.

Table 4.2: Constants of polynomials for pack and elongate types of support

| Pack Type | Base dimensions (cm x cm) | Height (m) | Lab. test rate (mm/min) | c₁ | c₂ | c₃ | C₄ | c₅ | c₆ |
|----------------------------|----------------------------------|-------------------|--------------------------------|----------------------|----------------------|----------------------|----------------------|----------------------|----------------------|
| Hercules 4-Pointer | 55 x 55 | 1.37 | 20 | 8126.1 | -10498 | 5074.9 | -1084.2 | 84.621 | 4.0203 |
| Solid Matpack | 55 x 55 | 1.1 | 5 | 2781.1 | -4572 | 2852.2 | -804.46 | 91.527 | 2.632 |
| Hardgum Matpack | 55 x 55 | 1.2 | 14 | -2854.8 | 4912.2 | -3301.7 | 1137.3 | -211.1 | 25.214 |
| Brick Composite 11R 4-Pt | 75 x 75 | 1.5 | 10 | -128.42 | 356.73 | -389.62 | 223.58 | -75.032 | 13.635 |
| Brick Composite 9-Pointer | 75 x 75 | 1.5 | 30 | 30968 | -44757 | 24333 | -6078.8 | 644.98 | -9.3052 |
| Hercules 16-Pointer | 75 x 75 | 1.87 | 20 | 2781.4 | -4995.1 | 3306.9 | -958.77 | 94.045 | 10.365 |
| Sandwich Pack | 75 x 75 | 1.4 | 10 | -5188.8 | 11435 | -9383.5 | 3503.6 | -587.17 | 44.556 |
| Solid Matpack | 75 x 75 | 1.5 | 15 | 626.05 | -2310.3 | 2347 | -989.28 | 178.35 | -3.8152 |
| Hardgum Matpack | 75 x 75 | 1.8 | 14 | 759.77 | -1636.4 | 1306.8 | -440.47 | 40.768 | 13.918 |
| Solid Timber | 75 x 75 | 1.4 | 10 | 427.86 | -225.73 | -292.15 | 311.73 | -106.37 | 18 |
| Timber Composite 9-Pointer | 75 x 75 | 1.5 | 10 | 1440 | -3144.7 | 2575.6 | -942.79 | 126.57 | 9.4529 |
| Brick Composite 11R 16-Pt | 110 x 110 | 1.58 | 16 | 15473 | -26035 | 16851 | -5120.8 | 675.86 | -9.7696 |
| Brick Composite 11R 9-Pt | 110 x 110 | 2.0 | 25 | 96.953 | -271.62 | 262.79 | -86.164 | -13.601 | 15.228 |
| Brick Composite 10R 9-Pt | 110 x 110 | 2.2 | 10 | -43.106 | 151.39 | -209.03 | 150.11 | -61.66 | 15.759 |
| Brick Composite 10R 16-Pt | 110 x 110 | 2.5 | 20 | -8.3346 | 36.128 | -60.162 | 57.564 | -39.383 | 17.552 |
| End-grain Pack 14R | 110 x 110 | 2.2 | 10 | 1126.8 | -2074.6 | 1238.1 | -201.18 | -53.074 | 24.204 |
| Hercules Pack | 110 x 110 | 1.7 | 15 | 31034 | -41715 | 20367 | -4099.6 | 180.59 | 45.113 |
| Sandwich Pack | 110 x 110 | 1.7 | 10 | 29810 | -42212 | 21796 | -4878.3 | 387.64 | 25.66 |
| Skeleton 16-Pointer | 110 x 110 | 2.1 | 10 | -10.627 | 49.947 | -86.411 | 78.193 | -37.171 | 11.668 |
| Solid Matpack | 110 x 110 | 1.8 | 10 | 307.11 | -971.74 | 915.69 | -294.17 | -2.5418 | 23.83 |

| Pack Type | Base dimensions (cm x cm) | Height (m) | Lab. test rate (mm/min) | C₁ | C₂ | C₃ | C₄ | C₅ | C₆ |
|-----------------------|----------------------------------|-------------------|--------------------------------|----------------------|----------------------|----------------------|----------------------|----------------------|----------------------|
| Hardgum Matpack | 110 x 110 | 2.5 | 14 | -6646.2 | 7935.4 | -2611.4 | -163.57 | 187.37 | -1.1599 |
| Solid Timber Pack | 110 x 110 | 1.7 | 10 | 21631 | -32122 | 18076 | -4646 | 481.49 | 11.69 |
| Solid Timber Pack | 110 x 110 | 2.0 | 10 | 1632.9 | -3584.7 | 2921 | -1044.4 | 133.33 | 13.304 |
| Timber Composite Pack | 110 x 110 | 2.0 | 10 | 60.777 | -195.52 | 214.86 | -77.338 | -13.334 | 15.123 |
| Solid Timber Pack | 140 x 140 | 1.98 | 14 | 15622 | -25959 | 16399 | -4775.6 | 575.91 | 4.1877 |
| Solid Timber Pack | 150 x 150 | 2.0 | 10 | 76751 | -93801 | 44431 | -9984.8 | 972.97 | 4.0109 |
| Durapak | 60 x 60 | 1.15 | 10 | -3054.4 | 5858.9 | -4328 | 1548.8 | -271.12 | 21.507 |
| Durapak | 90 x 90 | 1.2 | 10 | -3801.3 | 7774.1 | -6106.6 | 2311.2 | -435.93 | 39.096 |
| Durapak | 60 x 90 | 1.5 | 20 | -1973.7 | 3929.2 | -3081.7 | 1212.2 | -247.46 | 24.916 |
| Durapak | 120 x 120 | 1.2 | 10 | -4638.2 | 9409.7 | -7425.4 | 2859.4 | -549.74 | 48.522 |
| Durapak | 90 x 120 | 1.2 | 10 | -3777.6 | 7579 | -5890.8 | 2248.4 | -441.8 | 42.143 |
| RSS pack | 900mm Diameter | 1.2 | 10 | -4166.4 | 2487.8 | 1253.9 | -1070.5 | 153.76 | 9.5863 |
| Pambili Pack | 630mm Diameter | 1.5 | 15 | -132.98 | 260.79 | -180.94 | 61.823 | -21.535 | 7.3823 |
| Elongate Type | Diameter (mm) | Height (m) | Lab. test rate (mm/min) | C₁ | C₂ | C₃ | C₄ | C₅ | C₆ |
| Minepole | 116 | 1.8 | 5 | -416899 | 302132 | -82974 | 10578 | -618.23 | 14.312 |
| Minepole | 130 | 1.2 | 5 | 0 | 4E+07 | -9E+06 | 515888 | -11314 | 91.069 |
| Minepole | 130 | 1.5 | 5 | 0 | 0 | 0 | -47548 | 1275.3 | 0.3584 |
| Minepole | 132 | 2.25 | 5 | 0 | 90926 | -44174 | 7410.5 | -509.51 | 13.431 |
| Pencil prop | 150 | 1.8 | 10 | -7568.3 | 8991.8 | -4261.8 | 1019.7 | -131.64 | 9.5101 |
| Profile prop | 160 | 1.0 | 10 | -4838.9 | 7048 | -4069.2 | 1190.5 | -183.77 | 13.635 |
| Profile prop | 162 | 1.2 | 5 | -480518 | 274814 | -63834 | 7772.4 | -526.59 | 19.161 |

University of Pretoria etd – Pretorius, M J (2006)

| Elongate Type | Diameter (mm) | Height (m) | Lab. test rate (mm/min) | C1 | C2 | C3 | C4 | C5 | C6 |
|----------------------|----------------------|-------------------|--------------------------------|-----------|-----------|-----------|-----------|-----------|-----------|
| Profile prop | 170 | 1.5 | 5 | 0 | 0 | -7488.6 | 3062.5 | -405.69 | 20.074 |
| Profile prop | 180 | 1.8 | 10 | -35685 | 45552 | -21664 | 4692.5 | -454.58 | 17.104 |
| Wedge prop | 180 | 1.2 | 15 | -82110 | 79535 | -30070 | 5606.3 | -539.7 | 25.538 |
| Wedge prop | 200 | 2.0 | 5 | -172561 | 162641 | -59425 | 10628 | -959.25 | 39.485 |

CHAPTER 5 ROCKMASS MODEL

5.1 BACKGROUND TO THE STUDY – ROCKMASS STIFFNESS CONCEPT

The conventional classification of established mining methods is based on the type and degree of support provided in the mine structure created by ore extraction. Thomas (1973) recognised two fundamentally different types of mine structures:

- (a) naturally and artificially supported mine structures (generated by such methods as open stoping), and
- (b) caving structures (generated by block caving or sub level caving).

The mine stability objective is to ensure that unstable release of stored energy cannot occur. The distinction between various mining methods can be made on the basis of the displacements induced in the country rock and the energy redistribution that accompanies mining.

Whatever mining method(s) is applied in ore extraction, four general rock engineering objectives are to be satisfied in the design of the mine structure, these are to:

- (a) ensure the stability of the mining structure or opening as orebody extraction proceeds;
- (b) preserve unmined ore in a minable condition;
- (c) protect major service openings until they are no longer required; and
- (d) provide secure access to safe working places.

The stability of the mine opening ought to be considered as the prime design requirement. In a properly designed engineering structure, small changes in operating conditions and geometry should result in only small changes in the stability of the structure. According to Brady and Brown (1981) an unstable structure is one where small external disturbances produce large, sudden, and frequently catastrophic changes in the structure geometry. Avoiding such conditions in a mine opening should be a fundamental design requirement.

5.2 BACKGROUND TO THE FIRST APPROACHES

5.2.1 Instrumentation

Convergence is defined as the elastic rebound of the rockmass into the excavation due to the removal of stresses from the surface of the excavation, while closure is defined as convergence plus the inelastic rockmass movement due to bed separation. The closure component of deformation is utilised in the research as part of the process to determine the rockmass stiffness. The stope closure at a specific point quantifies the x-value of the load-deformation presentation of rockmass stiffness.

Stope panels were instrumented and stope closure at specific stations measured at regular time intervals for the purpose of determining the closure at a specific point at a given time. Measuring stations were initially installed approximately 6 m from the stope face and measured throughout the working life of the stope panel.

The measuring stations consist of survey pegs installed into the hanging- and footwall of the stope. The pegs were installed in such a way that closure was measured normal to the hanging- and footwall. Measurements were taken at monthly intervals except for panels where the stope closure rate was higher than the average of 2 mm/day. The reason for this was that any abnormality in the rate of closure could be identified in time and pro-active steps implemented prior to a potential stope collapse. This formed part of the mine's pro-active strategy to combat large falls of ground.

5.2.2 M-factor approach

It is vital that the magnitude of the force component be established to determine the rockmass stiffness, and this is perhaps the most complex value to determine for the purpose of this exercise. A number of different approaches were taken in an attempt to determine this value.

A methodology was developed that can be implemented without digitising and numerically model the area of interest at first. The objective was to enable the rock engineer to determine the force component for rockmass stiffness at a measuring station for any given mining geometry at the time. The aim is thus to relate the force component of the rockmass stiffness to the mining geometry. A number of different approaches were adopted and experimented with initially to determine the force

component for the rockmass stiffness. The very first one was to establish the force “required restoring the hangingwall” to its original or pre-mining position. The force determined this way was assumed at zero deformation, i.e. the deformation of the hangingwall prior to the mining operation. This value was used in fixing the one point on the force axis of the rockmass stiffness representation. The other fixed point, deformation, is taken as the measured deformation underground where the magnitude of the force exerted onto the hangingwall is assumed to be zero. The mathematical function connecting these points defines the rockmass stiffness.

It is not possible in reality to generate a load with sufficient magnitude that will restore the hangingwall to its original pre-mining position. An analytical method was employed for this in order to determine the magnitude of such a fictitious force. This was achieved through numerical modelling where the results of the analysis were related to the mine plan in a way that is to be described.

Deformation at any point in a mined out area relates to the mining span. Deformation at that point will increase as the mining span increases. When considering the rockmass stiffness concept, will the force component also increase as deformation increases. The force component is thus related to the mining span.

The fictitious force exerted onto the hangingwall that will result in zero deformation at that point for the given mining geometry was determined by numerical modelling. Minsim W was utilised for this purpose. This was accomplished by modelling a fictitious solid pillar at the position of the measuring station for the given mining geometry. Theoretically the deformation at that point is zero with the fictitious pillar in position. The stress on the pillar was converted into a force, taking into consideration the dimensions of the pillar.

The modelling was repeated for all the mining intervals at which measurements were taken underground. The objective of this part of the analysis was to establish the correlation between the mined area and the force that was calculated. Through this it was believed that the methodology would take into consideration the existing mining geometry and regional support.

The mined out area was determined by means of a planimeter and was repeated for all the mining steps. This was performed as a first attempt to determine the relationship between the force and the cumulative square meters mined up to the date that

underground closure measurements were taken. The calculated force was then compared to the cumulative square meters mined for that particular mining stage.

The objective with this approach was that it must be possible for the design engineer to determine the force exerted onto the hangingwall at any stage of mining from the cumulative area mined (m^2). It was foreseen that the force be calculated in practice through this potential relationship that might exist between the force and the cumulative area mined. A good correlation was found to exist between the calculated force and the cumulative square meters mined for any specific mining interval. This relationship was referred to as the so-called Mining factor or M-factor.

The M-factor was determined for the first analysis of the 15A47 Stope and yielded an average value of 0.2. The positions of the measuring stations and the consecutive mining steps are shown in Figure 7.2 of Chapter 7. The following table gives a summary of typical results for the different measuring stations that were obtained through the application of this methodology.

Table 5.1: M-factor for the 15A47 Stope

| Date (Mining Stage) | m ² mined | Cumulative m ² | Force @ Station 1(MN) | Force @ Station 1A (MN) | Force @ Station 1B (MN) | Force @ Station 2 (MN) | Force @ Station 2A (MN) | Force @ Station 3 (MN) | Force @ Station 3A (MN) |
|-------------------------------|----------------------|---------------------------|-----------------------|-------------------------|-------------------------|------------------------|-------------------------|------------------------|-------------------------|
| 5 July (A ₀) | 22300 | 22300 | - | - | - | - | - | - | - |
| 16 August (A ₁) | 3990 | 26290 | 5262 | 5605 | - | 5406 | - | 3184 | 3184 |
| 6 September (A ₂) | 2340 | 28630 | 5671 | 5940 | 4777 | 6025 | 4739 | 4353 | 4353 |
| 6 October (A ₃) | 3120 | 31750 | 6017 | 6225 | 5429 | 6452 | 5437 | 4853 | 4853 |
| 9 November (A ₄) | 2310 | 34060 | 6838 | 6920 | 6273 | 6941 | 6146 | 5406 | 5406 |
| 27 December (A ₅) | 4650 | 38710 | 7366 | 7385 | 6846 | - | - | 6270 | 6270 |
| Date (Mining Stage) | M-factor Station 1 | M-factor Station 1A | M-factor Station 1B | M-factor Station 2 | M-factor Station 2A | M-factor Station 3 | M-factor Station 3A | M-factor Station 5 | Estimate |
| 16 August (A ₁) | 0.20 | 0.21 | - | 0.21 | - | 0.12 | 0.12 | 0.22 | 0.18 |
| 6 September (A ₂) | 0.20 | 0.21 | 0.17 | 0.21 | 0.17 | 0.15 | 0.15 | 0.22 | 0.19 |
| 6 October (A ₃) | 0.19 | 0.20 | 0.17 | 0.20 | 0.17 | 0.15 | 0.15 | 0.21 | 0.18 |
| 9 November (A ₄) | 0.20 | 0.20 | 0.18 | 0.20 | 0.18 | 0.16 | 0.16 | 0.21 | 0.19 |
| 27 December (A ₅) | 0.19 | 0.19 | 0.18 | - | - | 0.16 | 0.16 | 0.20 | 0.18 |
| Averages | 0.20 | 0.20 | 0.18 | 0.21 | 0.17 | 0.15 | 0.15 | 0.21 | 0.18 |

Table 5.1 shows the M-factor calculated for the different mining stages at the measuring or observation stations as shown. Column 1 shows the date and stage of mining denoted as A_n , where n indicates the mining stage. Installation of the station is where $n=0$. The area mined during that stage is shown in the second column. The third column gives a summary of the cumulative square meters mined including that particular stage of mining. The rest of the columns show the forces that were determined for any given station in Mega-Newton (MN) as calculated numerically for the different mining stages.

The bottom row of Table 5.1 shows the M-factors that were calculated at the measuring stations for the different stages of mining. The analysis produced an average value of 0.18 for the M-factor.

The aim in using this approach was to apply the M-factor in the analysis of an area where the cumulative square meters mined is determined from the mine plan and the force calculated from it. It is possible that the force exerted onto the hangingwall at a measuring station be calculated without the use of any numerical analysis this way. The force is calculated as the product of the M-factor and the cumulative m^2 mined.

This methodology was repeated for other working places for a number of mining stages. It also yielded a constant but different magnitude for the M-factor.

(a) Shortcomings of the M-factor approach

It is important that the M-factor should be constant, correct and reliable since it has a major impact on the magnitude of the force that is calculated from it.

This methodology was discontinued even though different underground sites yielded a constant value for the M-factor. Every analysis that was performed yielded a different value for the M-factor. The reason for this is that the initial cumulative area mined (A_0) is not fixed and cannot be established for a stope layout in order to yield the same and constant value for the M-factor.

5.2.3 Elliptical approach

The objective remains that the methodology that is developed should be simple to use by the design engineer.

The mining areas of interest were modelled using Minsim W numerical analysis to calculate the force required to restore the hangingwall to its pre-mining position at the particular measuring station as for the M-factor approach. This exercise was repeated at all the stations where underground measurements were taken for the different mining stages.

The deflection of a simple single beam clamped on both ends is a function of the span, beam thickness and material properties of the beam. The total deflection of combined orthogonal beams is also a function of the orthogonal spans, material properties and beam thickness of the two independent beams.

The second approach in the analysis was to evaluate the combined deflection of two orthogonal beams with the centre at the measuring station in the stope. This was achieved by fitting two orthogonal beams at the point of interest to the closest solid abutments or to regional pillars as illustrated in Figure 5.1.

This principle was put to use in determining the relationship that existed between the force calculated as mentioned and some parameter that can be related to the two orthogonal beams of an ellipse fitted with its the centre at the point of interest.

The forces calculated using numerical modelling at these points were compared to different variables of the ellipse described by the short and long axes of the two orthogonal beams. This approach gave a very good correlation between the force calculated numerically and what is defined as the effective side of the ellipse.

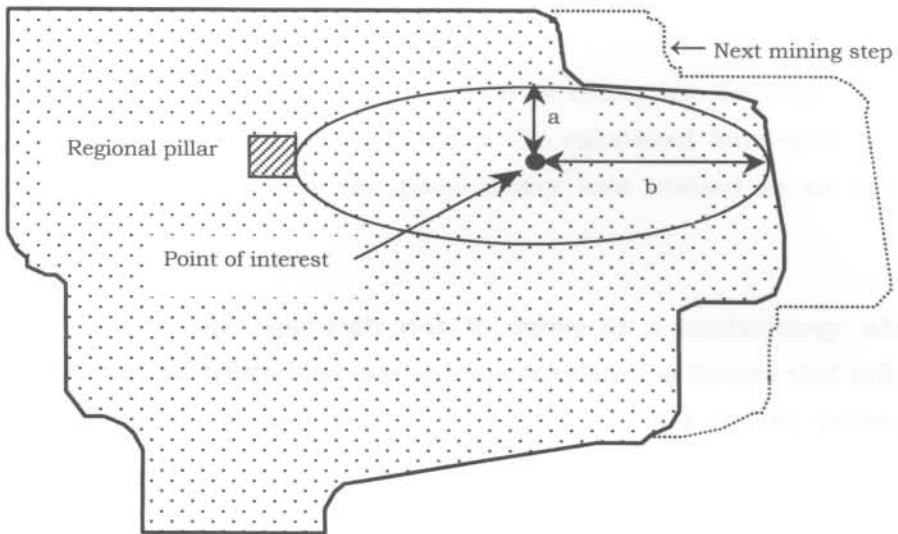


Figure 5.1: Illustration of the elliptical fit at a point of interest to a specific mining geometry.

The effective side (E_s) is defined as the square root of the area of the ellipse:

$$E_s = (\pi ab)^{1/2} \quad (5.1)$$

where:

- E_s = Effective side of the ellipse (m);
- a = Short axis of the ellipse (m); and
- b = Long axis of the ellipse (m).

The limitation of this approach is that mining can take place outside the influence area covered by the ellipse but still close enough in proximity to the measuring station to have an influence on the force. This analysis is not able to record this and calculations done under such circumstances may be inaccurate.

5.3 APPLYING THE YIELD LINE THEORY AND CONCEPTS

The previous analysis suggested that the solution to determine the magnitude of the force lies in the correlation that exists between the calculated force and the mining geometry. For the next approach the plate theory was utilised in an attempt to represent rockmass behaviour.

The aim of reverting to this approach was to derive at a methodology where the rockmass stiffness can be determined taking into consideration factors that influence it such as mining geometry, proximity to an abutment, as well as the presence and position of regional support.

At failure, plastic deformations occur along yield lines where the reinforcement has yielded, while the parts into which the slab is divided by the yield lines are only deformed elastically. Since the elastic deformations can be ignored in comparison with the plastic ones, can the individual parts of the slab be regarded as a plane, and their intersections, that is the yield lines, as straight lines with a good degree of approximation. It is thus assumed that deformation occurs only in the yield lines, consisting of relative rotation of the two adjoining parts of the slab about axes whose location depends upon the supports. Each part may be regarded as plane, and will be treated as that. With the aid of this yield lines were constructed for the same underground geometry shown in Figure 5.1 and is as illustrated in Figure 5.2.

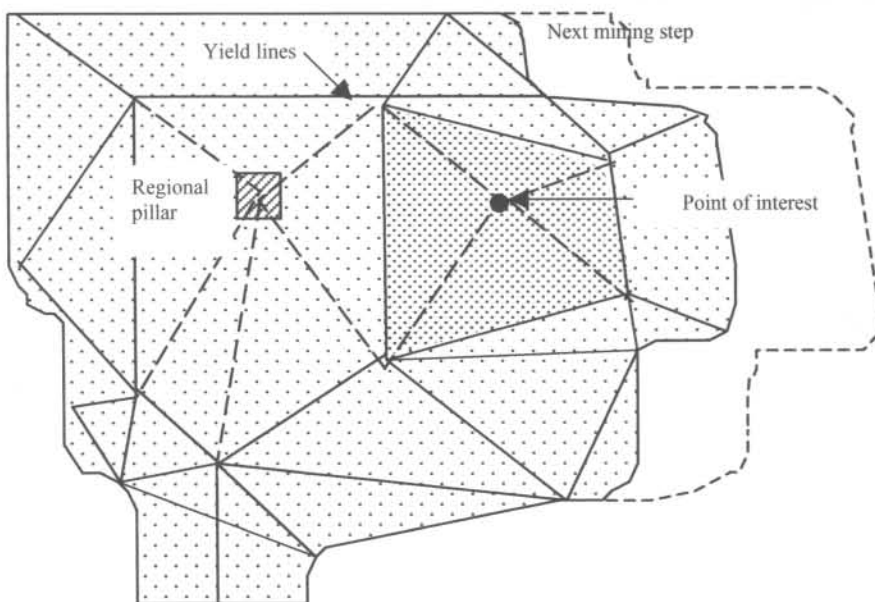


Figure 5.2: Yield Lines for the same underground geometry as shown in Figure 5.1

The area surrounding the measuring station where the stress convention of the skin of the hangingwall is compressive is delineated as the shaded area shown in Figure 5.2. This shaded area was compared to the numerical value of the force determined at that point for the given mining geometry. This yielded a constant Force (MN) to Yield Line Area (m^2) ratio between 2.4 to 2.8.

The force can therefore be calculated with reasonable accuracy when compared to the numerical analysis, once the yield line area is determined. An average value of 2.6 is applied as a constant.

The force is calculated as:

$$\text{Force (MN)} = \text{Yield line area (m}^2\text{)} \times \text{Constant of 2.6.}$$

A good correlation was repeatedly found to exist between the calculated force using the yield line area and the magnitude of the force calculated numerically as described earlier.

The major advantages of this methodology as identified at the time were that this methodology other than the other approaches is able to compensate for a changing mining geometry and the presence of regional support. Mining in close enough proximity to the measuring station can be taken into consideration as the position and orientation of yield lines are determined by the mining geometry. Cognisance is also taken of the presence and position of regional support.

5.4 DEVELOPMENT OF THE ATTRIBUTED AREA ANALYSIS

5.4.1 Introduction

The stiffness representation of rockmass behaviour is the focus of this stope support assessment methodology.

The Yield Line Methodology showed much potential but was a time consuming process and open to interpretation errors when constructing the yield lines and keeping in mind the rules that have to be applied. With the objective that the methodology must be simple and user friendly for the rock engineering practitioner to use, slight modifications were made to the methodology in order to simplify it.

Another phenomenon that was identified during the previous processes were the orders of magnitude difference between the force that was calculated in “restoring” the hangingwall to its original position (as determined by numerical analysis) and the force generated by support units currently being used in the mining industry. In order for the rockmass stiffness concept to be applicable and of use, must the force component of rockmass stiffness and that of the support units be of the same order of magnitude.

5.4.2 Attributed area

A so-called attributed area was created for every measuring station in a similar way than the Yield Line Areas. The previous process was simplified in the way that an area gets attributed to a measuring station, taking into consideration the mining geometry and the presence and position of regional pillars.

The following basic rules are applied during this process:

1. Abutments are assumed to be support points; and
2. A single point at the centre of the pillar represents the regional pillar. This is illustrated in Figure 5.3(a).

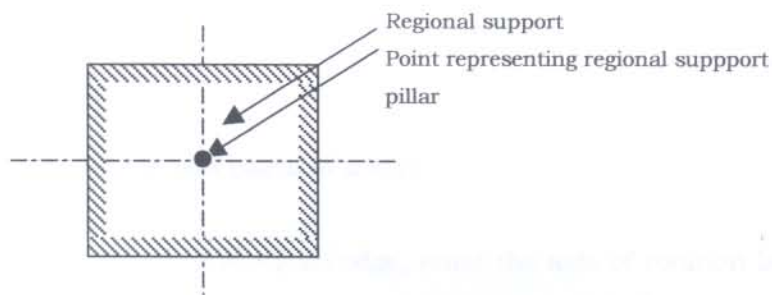


Figure 5.3(a): Regional support represented by a single point

3. Lines demarcating the attributed area are constructed in a similar fashion than the yield lines while the following applies:
 - Lines demarcating the attributed area are drawn midway between the point of interest and the solid abutment in a direction perpendicular to the shortest line connecting the two. This is illustrated in Figure 5.3 (b).

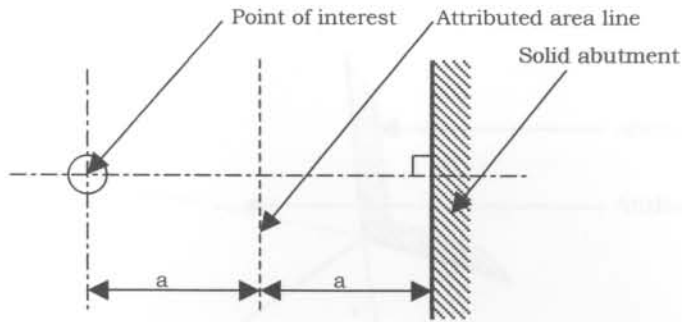


Figure 5.3(b): Line demarcating the attributed area between point of interest and solid abutment

- Attributed area lines between two parts of a slab must pass through the point of intersection of their axes of rotation.

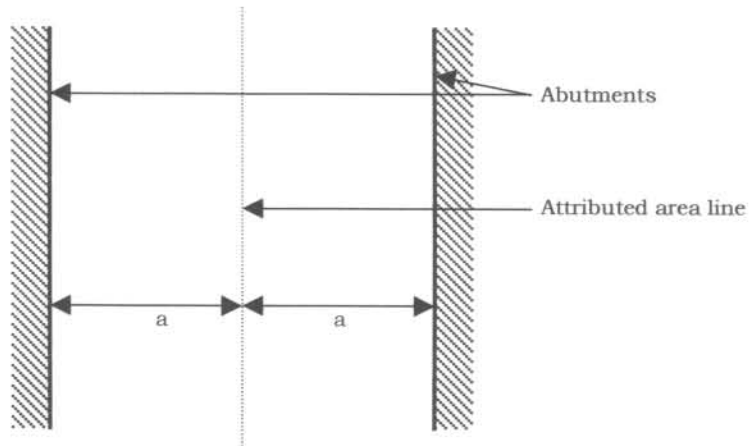


Figure 5.3(c): Attributed line for two parts of a slab

- For a part of a slab supported along its edge, must the axis of rotation lie along the edge, and for a part supported on a column will the axis pass over the column. This is of significance and relevant in the case of regional support in the form of pillars.

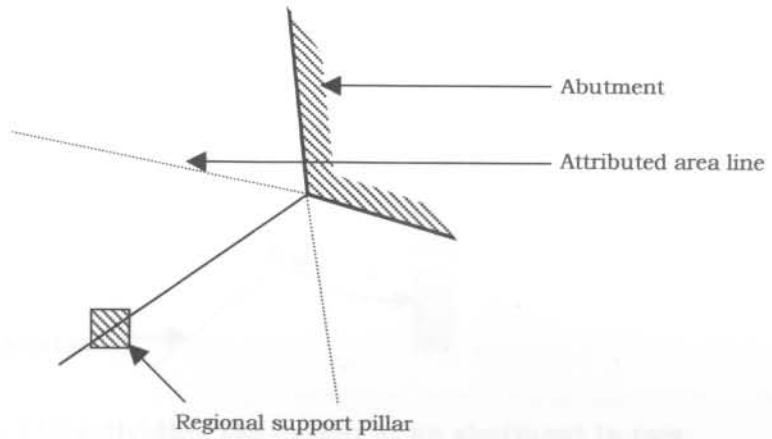


Figure 5.3(d): Attributed area line shown for a slab supported on the edge of an abutment with regional support in the area

- The attributed area line passes midway between two support points and is perpendicular to a line connecting these two points. A point of interest at a measuring station is treated as a support point for purposes of the analysis.

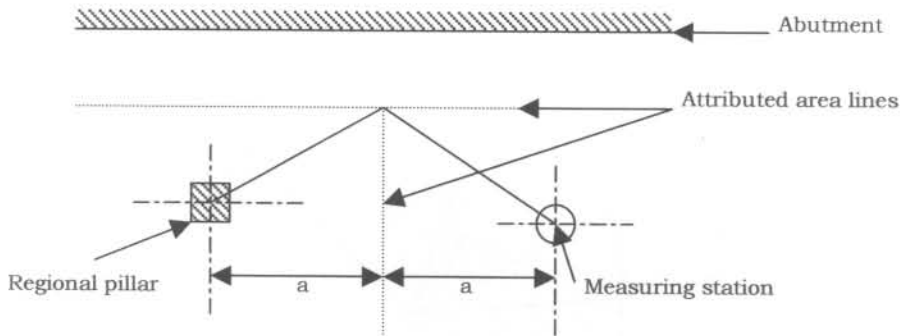


Figure 5.3(e): Attributed lines for a solid abutment, regional pillar and measuring station

- An attributed area line out of a mined corner divides the corner into two equal parts.

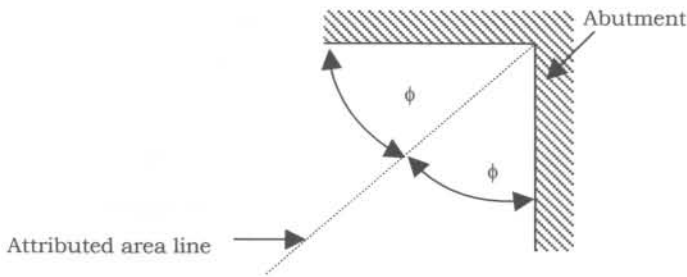


Figure 5.3(f): Attributed line dividing the corner at an abutment in two

With the aid of this, the attributed area was constructed for the same underground geometry as shown in Figure 5.1 and is as illustrated in Figure 5.4. The attributed area is thus a function of the mining geometry and will vary as the mining geometry changes.

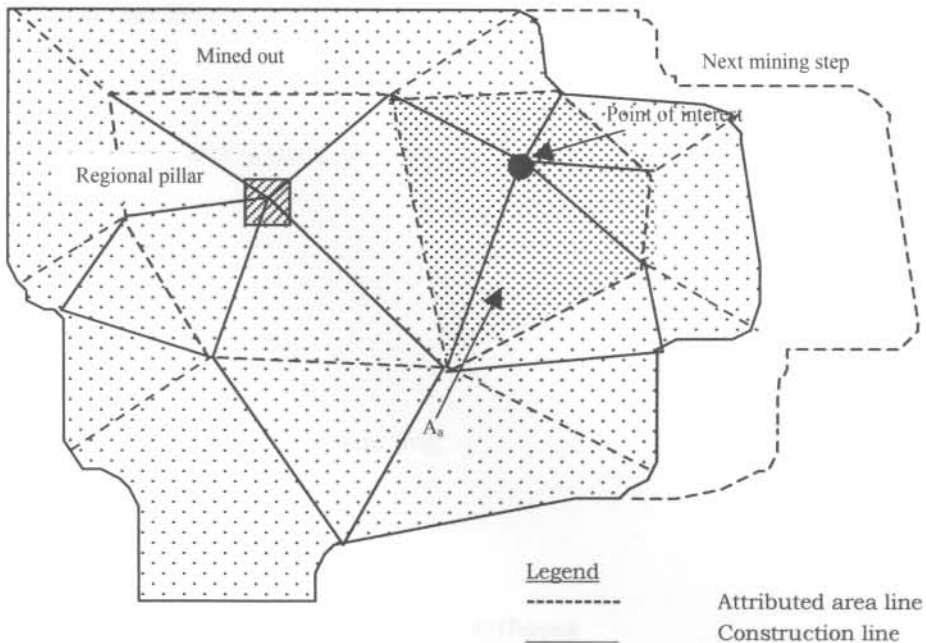


Figure 5.4: Mining geometry showing the Load Attributed Area A_a for the given point of interest

5.4.3 Magnitude of the force component for rockmass stiffness representation

The area represented by the attributed lines around a measuring station is referred to as the Attributed Area (A_a). This area can be determined by using a planimeter or by adding the triangular areas demarcated by the attributed area lines.

The force component (F_o) for rockmass stiffness is determined by assigning a hangingwall plate or beam thickness to the attributed area. The beam thickness is determined using the Voussoir beam for a given span as determined for Beatrix Mine by Kotzé (1991). The beam thickness will therefore change as the mining span increases with consecutive mining steps, and will be specific for a particular reef. The force is calculated by taking the weight of the rockmass plate of the attributed area for a given plate thickness.

The local rockmass stiffness for that particular point in the underground environment is determined using the force component from the attributed area and the closure component as is measured underground. The force component for representation of the rockmass stiffness can be determined for different mining geometries at various stages of mining.

The attributed area force (F_o) is thus given by:

$$F_o = \rho \cdot h_t \cdot A_a \cdot g \quad (\text{N}) \quad (5.2)$$

where:

- F_o = Attributed area force (N);
- ρ = Rockmass density (kg/m^3);
- h_t = Thickness of hangingwall beam (m);
- A_a = Attributed area (m^2); and
- g = Gravitational acceleration (m/s^2).

5.4.4 Deformation component of rockmass stiffness

To represent rockmass stiffness is it essential that both the force and deformation components be quantified. The force components for the different stages of mining are determined as discussed in 5.4.3

The deformation component for the rockmass stiffness for the different stages of mining at a measuring station is measured underground as discussed in 5.2.1.

5.4.5 Rockmass stiffness representation

The force and deformation for a given mining interval is calculated as discussed in 5.4.3 and 5.2.1 and presented on a force-deformation axis. The slope of the line represents the rockmass stiffness for that particular mining interval.

The yield line representing rockmass stiffness is described by the following equation:

$$g(x) = mx + F_0 \quad (5.3)$$

where:

- m = $\tan \lambda$ = Rockmass stiffness (N/m);
- x = Deformation of the stope at the measuring station (m); and
- F_0 = Attributed area force (N) where deformation $x = 0$.

Note: It is assumed that the system behaviour is linear. This approach may be criticised but further work is required to determine it accurately.

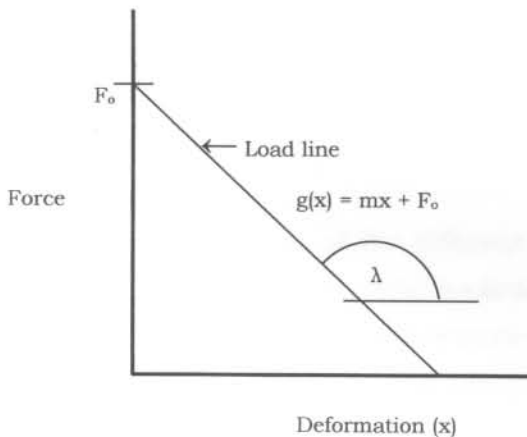


Figure 5.5: Load line representing rockmass behaviour

5.5. FACTORS INFLUENCING THE ROCKMASS STIFFNESS MODEL

The following factors influence the force component of the rockmass stiffness:

1. The mining geometry;
2. The position and dimensions of regional support;
3. The thickness of the hangingwall beam;
4. The density of the rockmass; and
5. The position of the point of interest relative to the mining abutments and regional support.

The deformation component of the rockmass stiffness is represented by stope closure as is measured underground at the point of interest for the given stage of mining.

The following factors influence stope closure at a given point in the stope:

1. The position of the point of interest relative to the mining abutment;
2. The mining geometry;
3. Presence and position of regional support;
4. Rockmass properties;
5. Depth of mining; and
6. Virgin stress condition.

5.6 CONCLUSIONS

This chapter describes the evolution of the different approaches that were developed and tested to represent the behaviour of the rockmass by quantifying the rockmass stiffness. The different approaches that were examined and tested are the so-called M-factor and Elliptical approaches. The shortcomings of each of these are described.

The application of the yield line theory and concepts led to the development of the so-called Attributed Area analysis. The basic rules that are applied in order to derive the attributed area for the point of interest in the stope are described in this chapter. This is done for any given mining geometry. The magnitude of the force component for the representation of rockmass behaviour for the particular mining stage can be calculated applying the attributed area. The deformation component for the rockmass stiffness for

the different stages of mining at the point of interest, is as measured at the different time intervals.

The factors that influence the rockmass stiffness are also listed.

This model makes it possible that the rockmass behaviour and stope support performance can be represented and compared on common force-deformation axis.

REFERENCES

- Brady B.G.H. & Brown E.T. (1981). *Energy changes and stability in underground mining: design applications of boundary element methods*. Paper published in Trans. Institution of Mining and Metallurgy. (Sect A: Min. industry), April 1981.
- Kotzé T.J. (1991). *Internal rock engineering report for Beatrix Gold Mine*, Gengold, South Africa.
- Salamon M.D.G. & Oravecz K.I. (1976). *Rock Mechanics in Coal Mining*. Coal Mining Research Controlling Council, Chamber of Mines of South Africa, Johannesburg, 1976.
- Thomas L.J. (1973). *An introduction to mining*, p436, Sydney: Hicks Smith and Sons, 1973.

CHAPTER 6

COMBINED MODELS

6.1 PRINCIPLE OF SUPERIMPOSING DATA

The objective of this method of analysis and design is to represent both the rockmass demand and stope support capacity on a common two-dimensional graph. Both the stope support and the rockmass models described in Chapters 4 and 5 are combined and compared during the third stage of the study.

The effect that changes in some of the variables might have on the stability of the excavation is presented on the graph and its effect determined from a stability analysis of the rockmass/support interaction. This is achieved through the analysis that is described in this chapter.

Stope support element performance, or the capacity of stope support elements for timber and lightweight cementitious and timber elongates respectively are described by the combined mathematical functions given in Chapter 4 while the rockmass demand is described in terms of rockmass stiffness in Chapter 5.

The function of the support element(s) is multiplied by a factor n to compensate for the total attributed area supported by what can be a combination of different support types:

$$F(x) = \sum_{i=1}^n n_i \cdot f_a(x) \quad (6.1)$$

where:

- n_i = Number of support elements of say type i ;
= $A_a / (d_i \cdot s_i)$ for the specific support type i ;
- A_a = Attributed area (m^2);
- d_i = Dip spacing of support element type i , (m); and
- s_i = Strike spacing of support element type i , (m).

This principle of superimposed data is graphically illustrated in Figure 6.1.

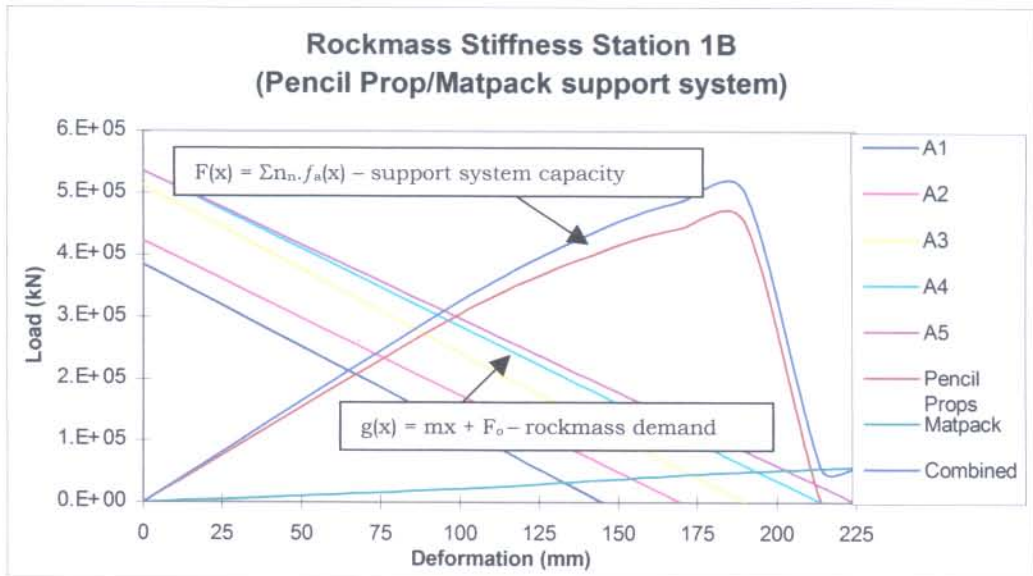


Figure 6.1: Example of graphical representation of both the rockmass and stope support models on a common force-deformation axis for 5 consecutive mining steps

Figure 6.1 shows the combined load generated by the Pencil Props and Matpacks for the given attributed area A_a . The “Combined” curve represents the sum of the forces generated by the support system as given by equation 6.1.

The load lines for the rockmass are also shown for the five consecutive mining steps A1 to A5.

6.2 STABILITY TEST

Potential instability or unstable failure will occur where the energy released by the rockmass for a given interval of deformation is more than the energy that can be absorbed or tolerated by the support system.

The following criterion is used to test for stability for any given mining geometry and/or support type:

6.2.1 Stiffness comparison

Failure of the supports occurs when the load on the support exceeds its strength. This failure may occur in a stable or unstable manner. The slopes of the lines are relevant to the post failure of the support in defining the mode of failure of the supports. Unstable failure of the support will take place when the slope of the rockmass stiffness is less than that of the post failure stiffness of that of the stope support element. Mathematically this is where:

$|m| < |F'(x)|$ as illustrated in Figure 6.2 that is where $|\tan\gamma| > |\tan\lambda|$ with angles γ and λ as shown.

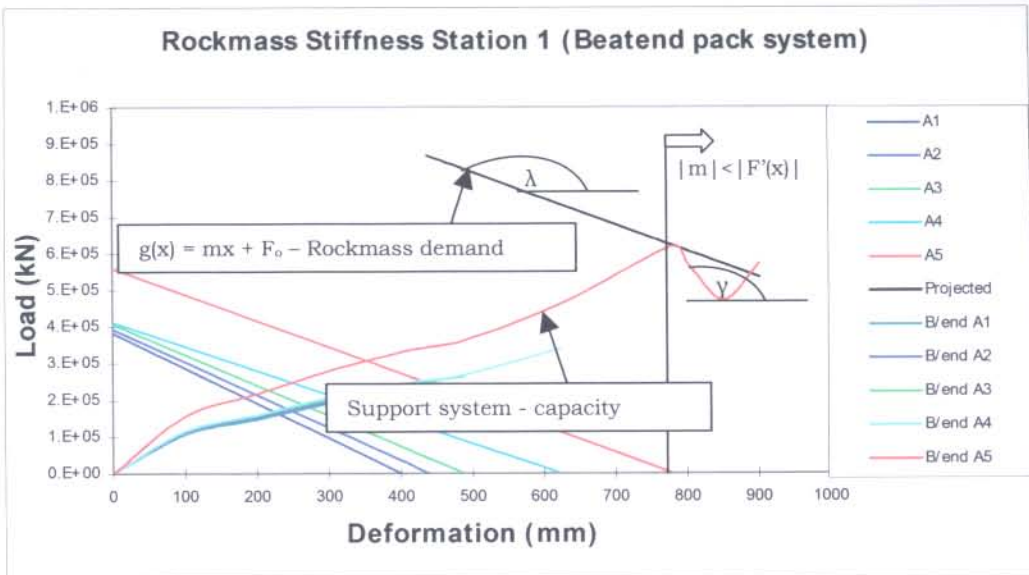


Figure 6.2: Combined models demonstrating the unstable failure of the stope support starting at 790 mm deformation during the mining stage A5

6.2.2 Energy comparison

The condition where the energy released by the rockmass for further deformation exceeds that which can be absorbed by the support will result in a potentially stable or unstable failure of the supports. The terms stable and unstable failure are defined in Chapter 9 – Glossary of terms.

Mathematically this is the true where:

$\int_a^b g(x) \partial x > \int_a^b F(x) \partial x$ for a given deformation interval. This condition will result in the unstable failure of the supports. The energy released by the rockmass and that absorbed by the stope support for the deformation interval from 780 mm to 885 mm for the last mining step A5 given in Figure 6.2 is illustrated in Figure 6.3.

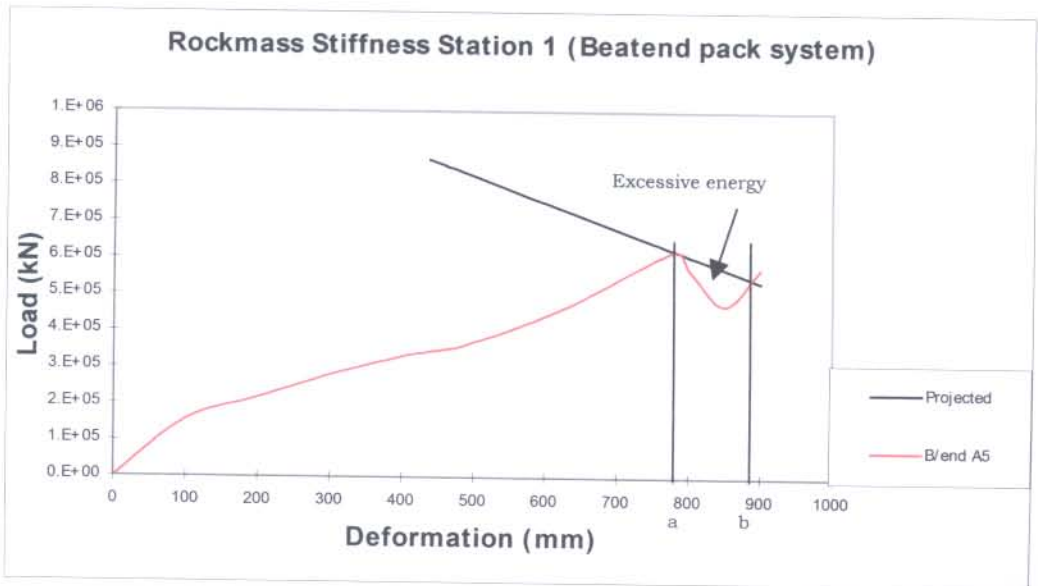


Figure 6.3: The excessive energy released by the rockmass for the given deformation interval shown by the shaded area

6.3 INPUTS AND ITS INFLUENCE ON THE COMBINED MODEL

The design process is executed on a comparative basis where different stope support and mine layout options can be compared to one another and inputs varied to examine for stability. A number of parameters have an influence on the excavation stability. The influence of each of these parameters must be evaluated in order to assess the underground layout and support combination for the purpose of a stability analysis. Each of these parameters for the rockmass and stope support system is discussed under the headings 6.3.1(a) to (g) and 6.3.2 (a) to (f). This is achieved by changing the relevant input variables and by examining the impact that it has on stability. It is through this analysis that the effect of each of those can be compared to other options and/or density of support.

6.3.1 Demand - Rockmass model

(a) Layout and configuration of underground mining environment

The rockmass stiffness is directly related to the attributed area constructed in and for the given underground excavation layout. The attributed area is constructed according to the Guidelines described in Chapter 5.

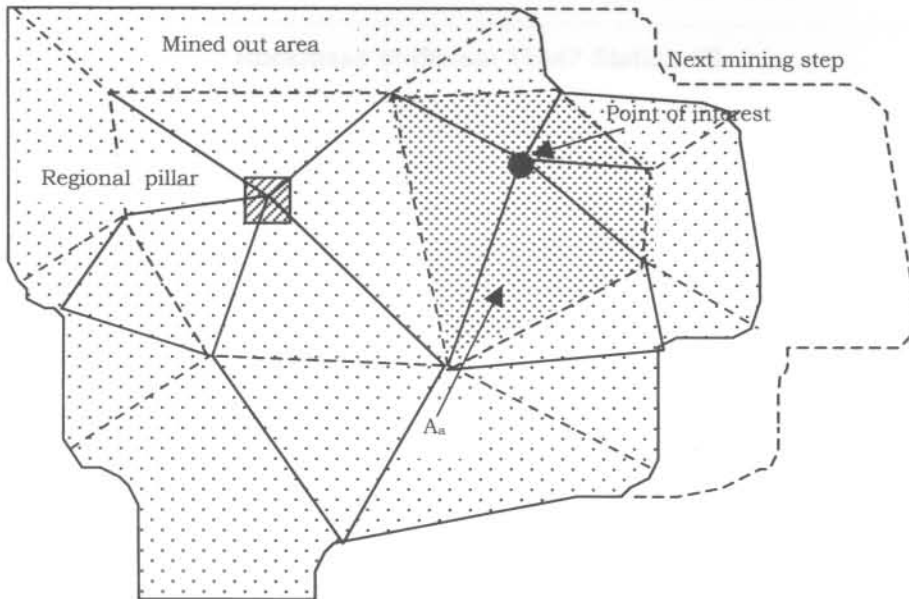


Figure 6.4: Attributed area (A_a) at the point of interest for a given mining geometry

The attributed area is influenced by the mining span and presence and position of regional support and changes in time with consecutive mining steps as illustrated in Figure 6.4. The attributed area in turn influences rockmass stiffness. The rockmass stiffness is described mathematically by the function $g(x) = mx + F_0$, with the symbols as defined previously.

The magnitude of the force F_0 is a function of the attributed area, the thickness of the hangingwall beam, rockmass density and gravitational acceleration.

The rockmass stiffness is associated with the amount of closure at the point of interest. The closure at a given point in the stope is again directly related to the mining span and its proximity to the abutment and/or regional support. The mining span and presence and position of regional support therefore have a direct influence on the rockmass

stiffness. The larger the amounts of deformation at any given point for the same magnitude attributed area force F_0 , the softer the rockmass, that is an increase in the magnitude of the angle λ as defined before.

The decrease of rockmass stiffness for consecutive mining steps (A2 to A5) and hence an increased mining span for one of the measuring stations of the 15A47 Stope is shown in Figure 6.5.

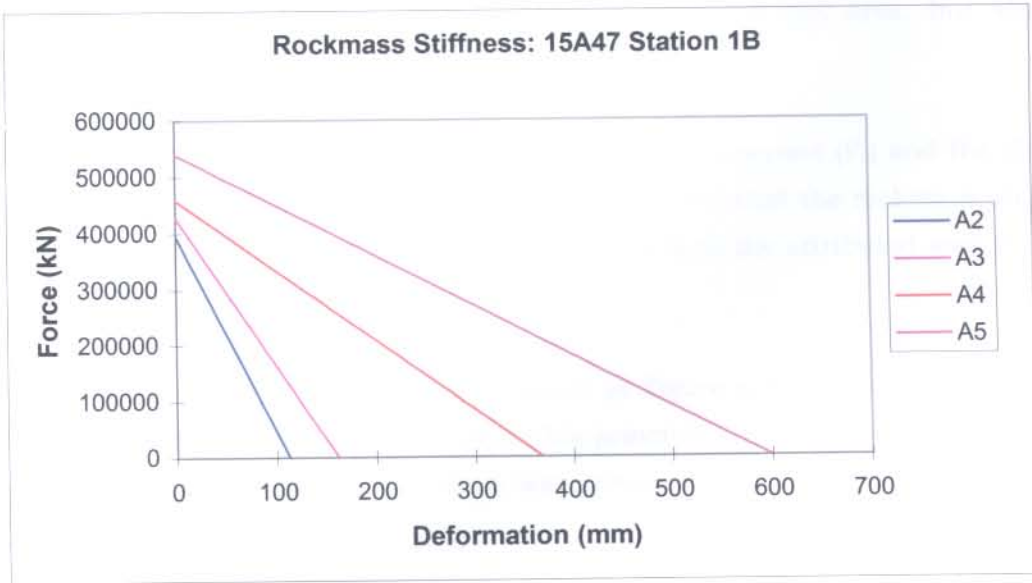


Figure 6.5: Decrease in rockmass stiffness (softening) for four consecutive mining steps

(b) Stope face position for successive mining intervals

The mining span increases as the position of the stope face is advanced. The position of the stope face relative to the point of interest (station) thus dictates the attributed area A_a as demonstrated in Figure 6.4. The further the face is away from a measuring station, the larger the mining span and hence the softer the rockmass.

(c) Position and presence of regional support

The presence and relative position of regional support influences the attributed area A_a , as demonstrated in Figure 6.4. Regional support breaks the mining span provided that the pillars remain intact. The mining span on the other hand is directly related to the

attributed area A_a . The presence and position of regional support therefore has a direct influence on the rockmass stiffness since the latter is related to the mining span.

(d) Physical position of the point of interest in the stope

The attributed area is calculated for a point of interest with that point as the focal point of the attributed area calculation as demonstrated earlier. As the position of the point of interest is moved, the distances to the abutments will also change. These distances not only have a direct bearing on the shape of the attributed area, but also its attributed area (A_a).

The rockmass stiffness is determined by both the force component (F_o) and the closure measured at the particular point. From this it is apparent that the rockmass stiffness will vary from one position in the stope to the next as both the attributed area (A_a) and stope closure (deformation component) will vary.

A simple two-dimensional mining slot presented in Figure 6.6 shows that the closure varies from one point to the next illustrates this principle. The principle applies to the three dimensional models where closure was measured during the instrumentation program.

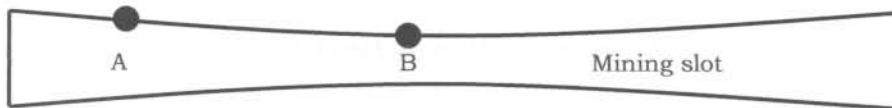


Figure 6.6: Two-dimensional mining slot showing different closure at different positions

(e) Closure at the point of interest for the different mining intervals

The rockmass stiffness is calculated from the force component (F_o) and the closure at the point of interest for a particular mining geometry. For the same magnitude force but with different closure components will the rockmass stiffness changes accordingly. The larger the stope closure (deformation) component for the same force component (F_o) the softer the rockmass i.e. the larger the angle λ , and vice versa. The closure at a given point will change with every consecutive mining interval, and hence influence rockmass stiffness.

The rockmass stiffness is therefore constantly changing at different points in the stope as mining continues. This is illustrated in Figure 6.7 where the bold printed line shows the rockmass stiffness history for measuring Station 1B during the 4 stages of mining.

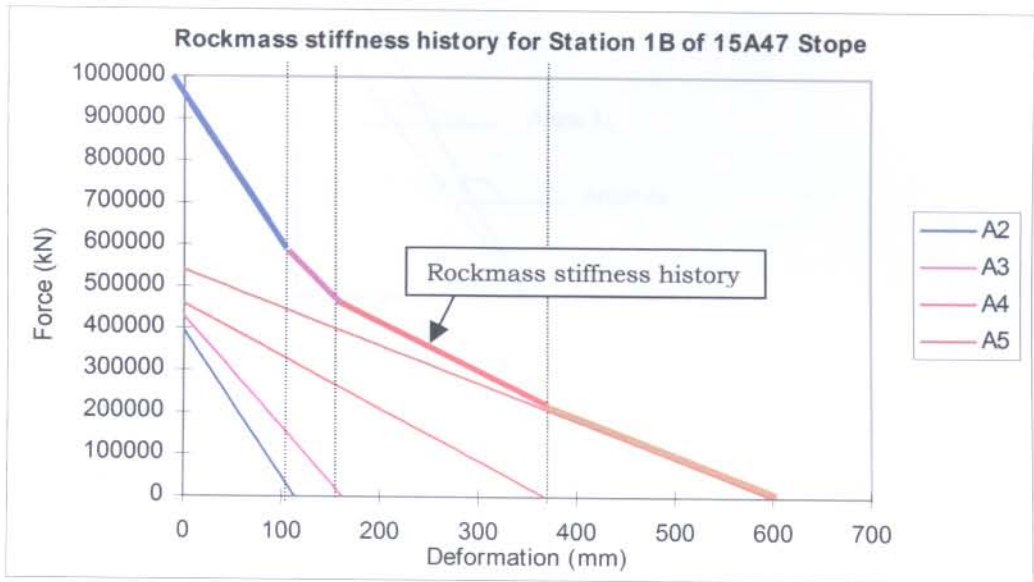


Figure 6.7: Rockmass stiffness history for a measuring station during 4 mining stages

(f) Hangingwall beam thickness

The attributed area force is (F_o) a function of the hangingwall beam thickness (m). The higher the beam thickness for the same attributed area A_a , the higher the attributed force (shown as $F_o(2)$ in Figure 6.8) will be. For the same amount of stope closure the rockmass will therefore be stiffer with an increased beam thickness. In the latter case the angle λ_2 will be smaller.

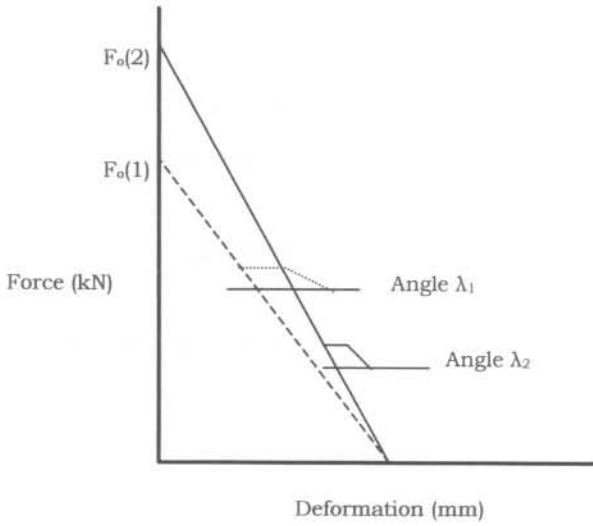


Figure 6.8(a): Effect of increased beam thickness on the rockmass stiffness with same deflection on rockmass stiffness

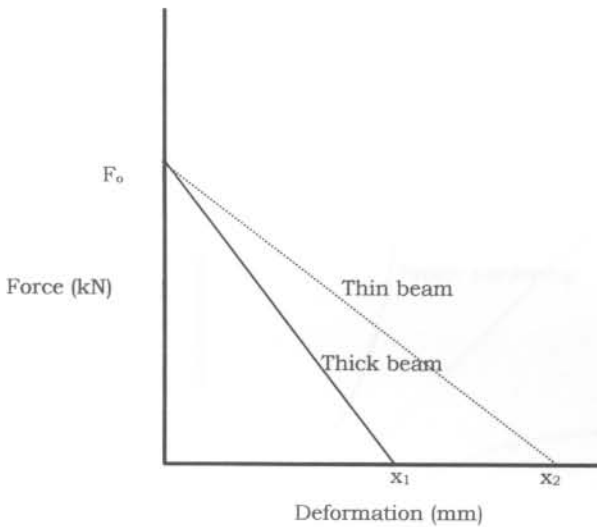


Figure 6.8(b): Effect of increased beam thickness on the rockmass stiffness with same attributed area force Fo

This principle is confirmed by the beam theory where the deflection of a beam is given as:

$$\eta \propto \gamma L^4 / Et^2 \tag{6.2}$$

with:

η = Deflection of beam (m);

- γ = Weight per unit length ($=\rho g$) (N/m);
 L = Beam span (m);
 E = Young's modulus of the beam material (GPa);
 T = Beam thickness (m), and

where a number of thin beams will deflect more than fewer thicker ones.

6.3.2 Capacity - Stope support model

Different types of support have different performance characteristics. The support performance represents the capacity of a unit to generate load during increased deformation of the element.

The performance characteristic of a support unit is described in Chapter 4 and demonstrates the unique capacity of each of the different supports. Strain hardening refers to the situation where the load that is generated as deformation takes place increases at a non-linear rate. Strain softening refers to the condition where the load decreases non-linearly as deformation takes place.

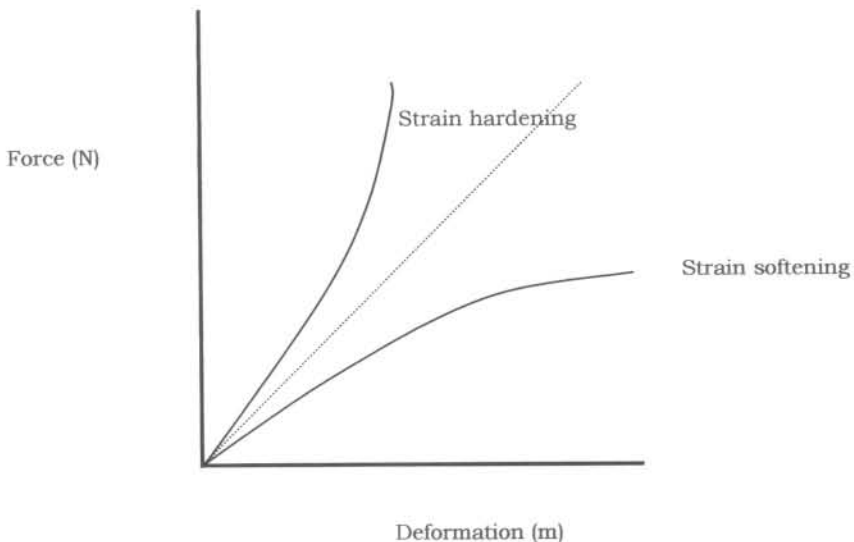


Figure 6.9 Illustration of strain hardening and strain softening of supports

Not only is the load bearing characteristics different for the various support types as deformation increases, but other factors such as loading rate and the slenderness ratio

will influence its behaviour in different ways. The following aspects all form part of input to the models.

(a) Rate of deformation

The extent to which the laboratory support performance data must be up- or downgraded as a result of the effect of the rate of deformation, is a function of material type and the differences between laboratory - and underground rates of deformation and is described in detail in Chapter 4

(b) Height of pack tested versus installed

The stope width is often different to the height of the support unit that was tested. To quantify the support performance of any type of pack it is important that this is quantified and the effect that it has on the performance of such a unit taken into consideration during the design process.

(c) Buckling failure of timber elongate support

Buckling failure of an elongate has a major impact on the design of support since it dictates the stability of the unit once a certain amount of deformation is exceeded. It does not only affect the ability to absorb energy but also its stiffness. Props with an increased yield range have a higher energy absorption capacity.

Buckling failure reduces the effective yield life of an elongate and will therefore affect its capacity to absorb energy. According to Roberts (1991) high closure prior to the event reduces the ability of a yielding timber elongate to absorb energy during a rockburst.

(d) Installation spacing of support

The function of the supports is multiplied by a factor n to compensate for the number of support elements of different types that are installed to support the attributed area. This total force is calculated as:

$$F(x) = \sum n_n \cdot f_a(x) \quad (6.3)$$

where:

n_n = Number of support elements of type n ;

= $A_a/(d.s)$ for the specific support type;

A_a = Attributed area (m^2);

d = Dip spacing of support elements (m); and

s = Strike spacing of support elements (m).

This principle is graphically illustrated by Figure 6.10 where the number of support elements for the given attributed area A_a is determined for a given dip and strike spacing of the specific support type.

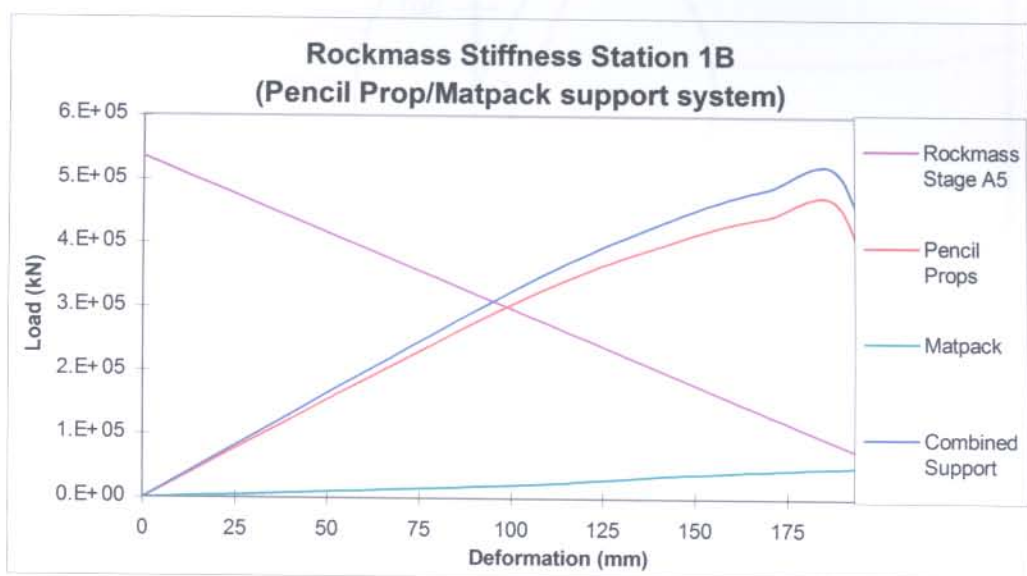


Figure 6.10: Graphical representation of rockmass and stope support models for mining stage A5

(e) Support pre-stressing

The pre-stressing of support during installation has become a routine practice in the South African mining industry. The benefit of pre stressing is the fact that the support is not blasted out that easily, and that it alters the support characteristic from passive to active. (See definition in Chapter 9: Glossary of Terms.) Both packs and elongate types of support can be pre-stressed.

Not only does the pre-stressing of a support element increase the load generated by the element upon installation but also the energy generated during the early stages of deformation since the latter relates to the area underneath the force-deformation curve.

The influence that pre-stressing of support has on its performance is illustrated in Figure 6.11 showing a 160 mm diameter Profile Prop, 1.0 m high that is pre-stressed with effective pre-stress of 100 kN. It shows the loss in pre-stress load from 100 kN to an effective 68 kN due to the creep of timber.

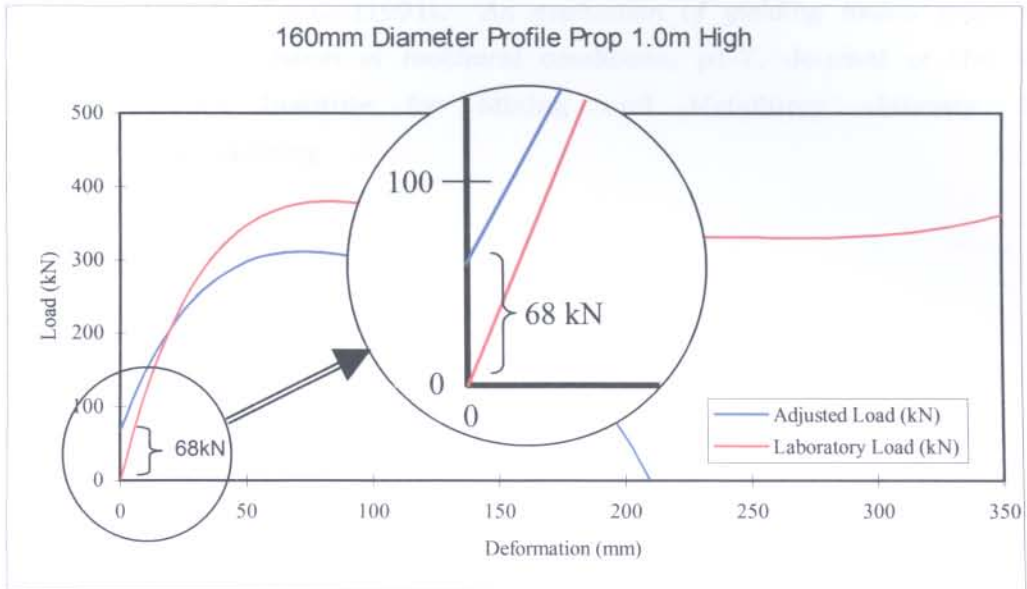


Figure 6.11: Effect of timber creep on the performance of a 160mm diameter Profile Prop

6.4 CONCLUSION

It has been demonstrated in this chapter how both the rockmass demand as well as the support capacity can be represented on a common two-dimensional force-deformation graph. Once this is achieved can a stability analysis be done where both the stiffness and the energy of the two components can be compared for a given deformation and for a given deformation interval respectively.

The inputs and its influence on to the combined model are described, and is repeated for both the rockmass as well as the stope support models.

REFERENCES

Kotze T.J. (1991). Internal rock engineering report for Beatrix Gold Mine, Gengold, South Africa.

Roberts M.K.C. (1991). *An evaluation of yielding timber props as a support system in rockburst conditions*, p1-7, Journal of the South African Institute for Mining and Metallurgy, January 1991, Johannesburg.

CHAPTER 7 CASE STUDIES

7.1 INTRODUCTION

The following two case studies demonstrate attempts to confirm the models that were developed for purposes of evaluating stope support, and examples whereby the principles given in this research are tested. The study demonstrates the stable- and unstable failure of stope support.

Both the case studies were carried out at Beatrix Gold Mine. The mine is situated on the southern brim of the Free State Gold Field and is considered to be a shallow to intermediate depth mining operation.

The Beatrix Reef that is mined is the major gold bearing horizon and occurs as the basal conglomerate of a channel deposit at or near the base of the Turffontein Sub Group in the area. This channel deposit is correlated with the Aandenk Channel of the formation as developed on St Helena and Unisel Mines. The reef channel width varies from 20 cm to as much as 7 m and consists of a multi-cycle upwards fining sequence of poorly sorted conglomerates and quartzite. The overall gold mineralisation is generally very high in the wide channels and lower grades are encountered in the narrower channels. The reef sub-outcrops at approximately 800 m below surface. Mining depth varied at the time of the study from 800 m to approximately 950 m below surface. The general strike direction of the reef is north-south while the reef dip varies from near vertical in the vicinity of the western basin edge over-fold to an estimated 5 degrees in the east.

The hangingwall of the Beatrix Reef is a competent quartzite and can be described as massive with well-defined parting planes. The uniaxial compressive strength of the hangingwall ranges from 190 – 220 MPa. The footwall may be considered as weak with a uniaxial compressive strength of approximately 160 MPa. In-situ measurements confirmed a horizontal to vertical virgin stress ratio of 1.

In the first case study namely the 15A47 Stope unstable failure of the supports occurred whereas stable failure of the supports occurred in the second case study namely the 23A79 Stope.

A number of stope panel collapses occurred on the mine in the early 1980's. After these collapses it became a common strategy on the mine to instrument stope

panels with the objective to identify abnormally high closure rate panels on the mine. This formed part of the mine's policy to timeously identify these potentially unstable panels. The majority of the stopes were therefore instrumented at the time of the study as part of this pro-active safety policy on the mine.

7.2 CASE STUDY 1: 15A47 STOPE – UNSTABLE SUPPORT FAILURE

7.2.1 Support capacity

The 15A47 was one of the stopes that was instrumented and where a major collapse of the stope occurred. Nobody was injured during this incident as the systematic stope closure measurements indicated accelerated stope closure prior to the collapse and all workers were prohibited from entering the working place. This incident became an ideal case study to apply and confirm the rockmass stiffness principles that were developed.

The 15A47 Stope was supported by means of an end-grained type of timber pack that will be called the Beatrix End-grain pack in this document. The term end-grain is defined in Chapter 9 of this document. The pack shows a steady increase in the load generated by it as deformation takes place. It was only after the stope collapsed and the support units were tested to destruction that the strain softening behaviour of the pack was identified for the first time. The mathematical representation of the load deformation performance curve for the Beatrix End-Grain pack is shown in Figure 7.1. The constants of the polynomial that quantifies its capacity are listed in Table 4.2 in Chapter 4.

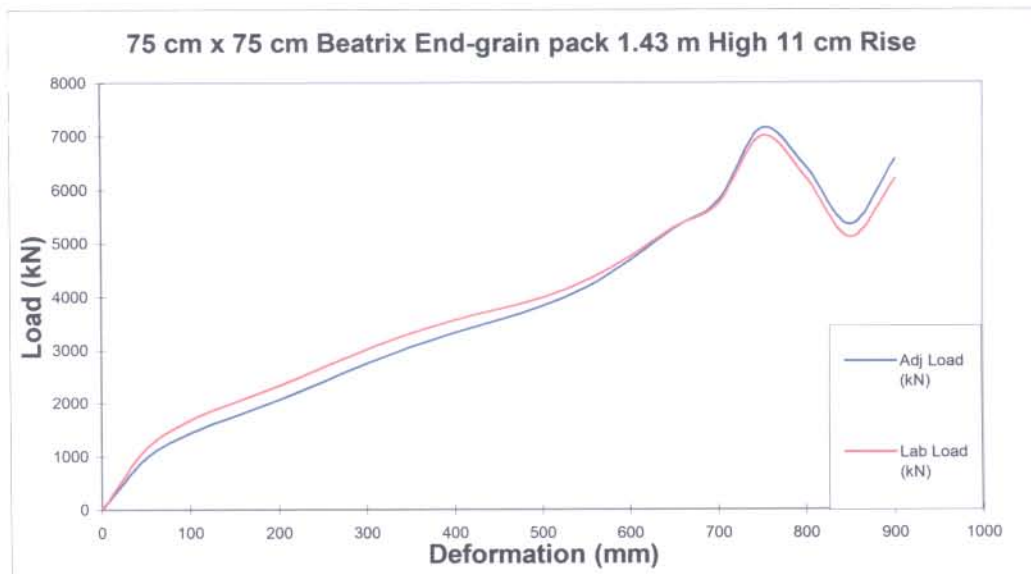


Figure 7.1: Load-deformation curve of Beatrix end-grained pack used in the 15A47 Stope

7.2.2 Rockmass demand

The different stages of mining of the 15A47 Stope as well as the positions of the measuring stations are shown on the plan in Figure 7.2. It also shows the pillar towards the centre of the stope that was left and that acted as regional support. The numbers and the positions of the measuring stations are also shown. The dip of the reef in this area is approximately 12° with the dip direction shown.

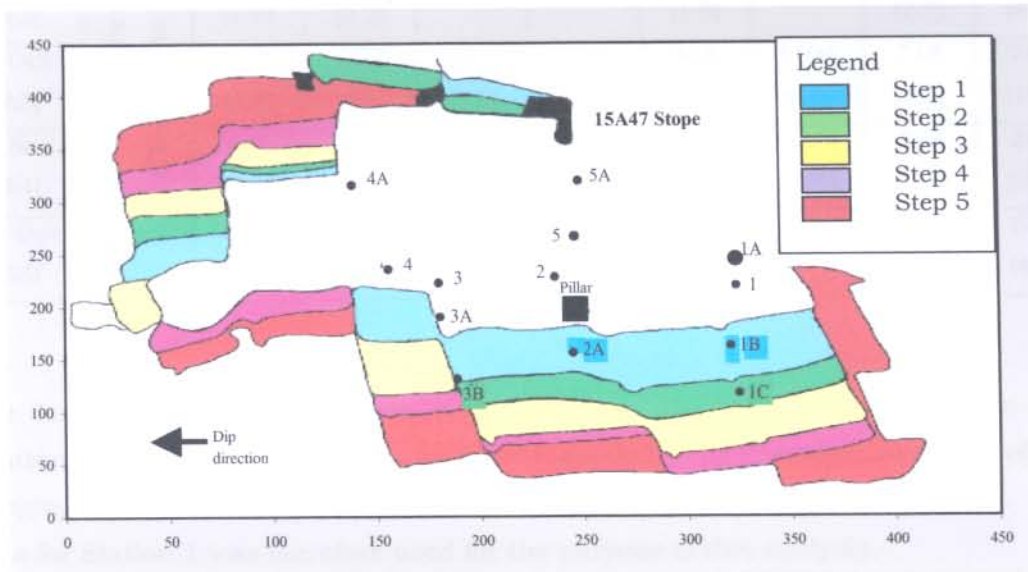


Figure 7.2: Layout and mining steps of the 15A47 Stope

Table 7.1 gives a summary of the stope closure measurements and stope closure rates of reliable stations for the last 5 mining stages (A1 to A5) before the stope collapsed. Reliable stations refer to stations where it was considered that the data obtained was not influenced by human error or where the pegs were replaced at some later stage due to damage or loss of the pegs as a result of the blasting or cleaning operations.

Where no values are given in the tables below it is due to the fact that the station was either:

* not installed at that stage of mining, or

** where the measuring station was lost.

Table 7.1: Summary of closure and closure rates for 15A47 Stope

| Date (Mining Stage) | Measuring Station | | | | | | | | |
|---------------------------|---|--------------|-------------|--------------|--------------|--------------|---------------|---------------|--------------|
| | | 1 | 1A | 1B | 1C | 2 | 2A | 3A | 5 |
| 16 Aug (A1) | Closure (mm) (Closure rate (mm/day)) | 400 | 90 | * | * | 345 | * | 588 | 165 |
| 6 Sept (A2) | | 439 (1.9) | 95 (0.2) | 113 | * | 384 (1.9) | 1184 | 644 (2.7) | 205 (4.8) |
| 6 Oct (A3) | | 488 (1.6) | 100 (0) | 162 (1.6) | 302 | 446 (2.1) | 1194 (0.4) | 718 (2.5) | 240 (1.2) |
| 9 Nov (A4) | | 623 (4.0) | 100 (0) | 368 (6.1) | 502 (5.9) | 593 (4.3) | 1274 (2.4) | 893 (5.1) | 349 (3.2) |
| 26 Dec (A5) | | 779 (3.3) | 100 (0) | 600 (4.9) | 800 (6.3) | ** | ** | 1140 (5.3) | 555 (4.4) |

The last closure measurements were taken on the 26th December when the continued acceleration in closure rate was identified. The first signs of failure of the hangingwall beam started to occur in the area of measuring Station Number 1. The data for Station 1 was therefore used for the purpose of this analysis.

The Attributed area (A_a) was determined for each of the measuring stations for all the mining steps according to the methodology described in Chapter 5. The Attributed areas for each of the measuring stations at the different mining intervals are given in Table 7.2.



Figure 7.3: Stope closure at the measuring stations – 15A47 Stope

The stope closure of the measuring stations for the 5 stages of mining of the 15A47 Stope is shown in Figure 7.3. The accelerated closure prior to the collapse of the stope is demonstrated where this was common to all the measuring stations except Station 1A. The hangingwall beam sheared in close proximity to station 1A and the measuring station never registered any closure for this reason.

Table 7.2: Attributed areas for measuring stations – 15A47 Stope

| Date (Mining Stage) | Measuring Station | | | | | | | |
|------------------------|-------------------|------|------|------|------|------|------|------|
| | 1 | 1A | 1B | 1C | 2 | 2A | 3A | 5 |
| 16 Aug (A1) | 1771 | 1815 | * | * | 1973 | * | 1060 | 2156 |
| 6 Sept (A2) | 1822 | 1885 | 1830 | * | 1978 | 1194 | 1301 | 2200 |
| 6 Oct (A3) | 1884 | 1986 | 1985 | 1585 | 2212 | 1595 | 1568 | 2257 |
| 9 Nov (A4) | 1910 | 2087 | 2124 | 1819 | 2400 | 1652 | 1883 | 2315 |
| 26 Dec (A5) | 2596 | 2555 | 2500 | 2176 | ** | ** | 2618 | 2693 |

A Voussoir Beam study was done by Kotzé (1991) for Beatrix Mine to determine stable spans for varying beam thicknesses. The design procedure is based on the voussoir beam model for a roof bed and is illustrated in Figure 7.4(a) while the forces operating in the system are defined in Figure 7.4(b).

In the equilibrium condition, the lateral thrust is not transmitted either uniformly or axially through the beam cross section. The section of the beam transmitting lateral load is approximated by the parabolic arch traced on the beam span. The outcome of this study is summarised in Figure 7.5 where the beam thickness for a stable span is plotted.

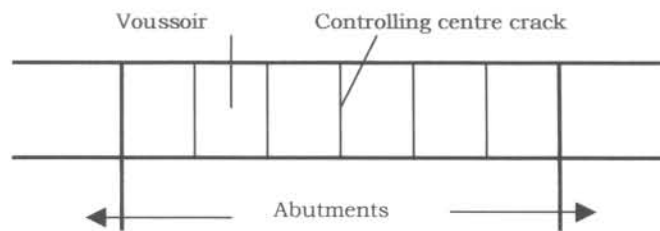


Figure 7.4(a): Voussoir beam model for a roof bed after Kotzé (1991)

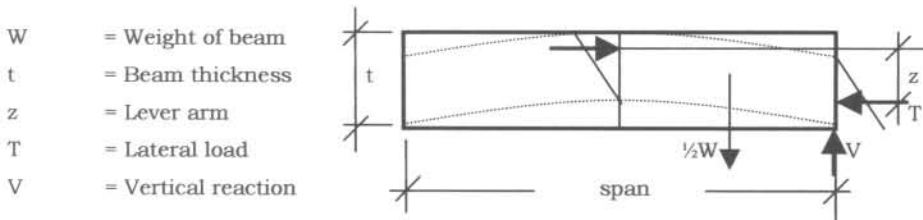


Figure 7.4(b): Forces operating in Voussoir beam system

The mining span between regional supports was 65 m at the time that failure started to occur. This relates to a beam thickness of 8 m. A beam thickness of 8 m was thus accepted for the purpose of this study.

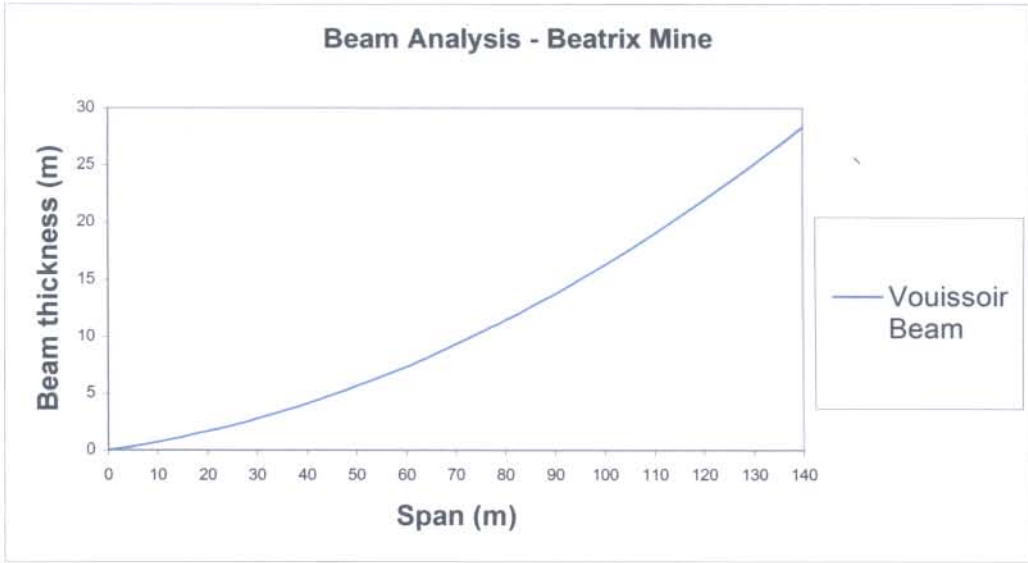


Figure 7.5: Voussoir beam analysis for Beatrix Mine after Kotzé (1991)

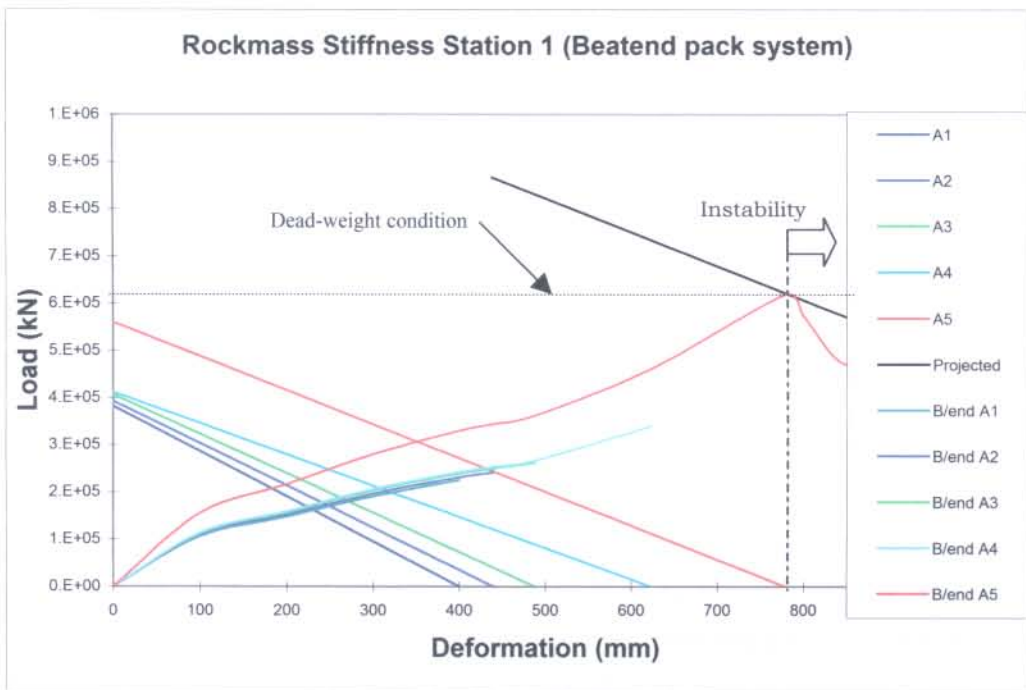


Figure 7.6: Rockmass-support interaction for the 15A47 Stope

Figure 7.6 shows the rockmass/support interaction for the 15A47 stope during five stages of mining denoted by A1 to A5. The analysis illustrates how the stiffness of the rockmass changes as the mining span increases with the consecutive mining steps. The slope of the line representing rockmass stiffness decreases and the rockmass thus reacts in a softer fashion as shown in Table 7.3. This study confirms

the statement made by Ozbay and Roberts (1988) that the rockmass stiffness is related to the mining span.

The force generated by the support system, comprising Beatrix end-grained packs is shown in Figure 7.6. This force that is calculated for the consecutive mining steps takes into account all the factors that influence the support performance as described in Chapter 4. For the purpose of the analysis the actual closure rate for the different stages of mining with support spacing of 3 m (on dip) by 4 m (on strike) were used, with no pre-stressing of the supports.

The area totally collapsed after the fifth stage of mining and closure measurements were therefore only taken up to the fifth stage of mining, i.e. up to 779 mm of stope closure. The excavation was stable during these five stages of mining.

The support system started failing after the fifth stage of mining where the energy released by the rockmass exceeds that generated by the support system as given in Table 7.3. The last stage of mining (denoted by “projected”) is a prediction of strata stiffness assuming that total closure has taken place. The projected line representing the rockmass stiffness as post stage 5 of mining is assumed to be parallel to that of mining stage A5. A more conservative approach to this would have been to represent rockmass stiffness with a horizontal line where this option would have represented a dead-weight condition of the hangingwall rockmass.

(a) Stability analysis

The rockmass stiffness and the energy generated and absorbed by the rockmass and supports respectively for the 5 mining steps of measuring Station 1 is summarised in Table 7.3. It shows the stiffness and energy for both the rockmass and the supports for the different intervals of deformation during the mining stages. For purposes of the analysis the calculations were extrapolated for a “Post A5” stage where entry into the working place was not possible.

Examples of the stability analysis calculations are shown as Appendix 1 at the end of the chapter.

Table 7.3: Stability analysis summary for Station 1

| Mining Stage | Deform. interval (mm) | Stiffness (kN/mm) | | Energy (kJ) for mining stage | | Comment |
|----------------|-----------------------|-------------------|----------|------------------------------|--------------------------|------------------------------|
| | | Rockmass | Supports | Released by the Rockmass | Absorbed by the Supports | |
| A1 | 0-400 | -956 | + 516 | 70443 | 71806 | Stable |
| A2 | 400-439 | -896 | + 318 | 681 | 11057 | Stable |
| A3 | 439-488 | -833 | + 335 | 1005 | 14911 | Stable |
| A4 | 488-623 | -662 | + 680 | 6029 | 50723 | Stable |
| A5 | 623-779 | -719 | + 6149 | 8751 | 108594 | Stable |
| Post A5 | 779-900 | -719 | -1209 | 85038 | 62617 | Unstable failure of supports |

The analysis shows that the energy released by the rockmass for the different intervals of deformation at Station 1 prior to failure (Mining Stages A1 to A5) is less than the energy absorbed by the supports. Once the deformation value of 779 mm is exceeded (Post A5 Mining Stage), the energy released by the rockmass exceeds the capacity of the supports, and unstable failure of the supports occurs. The energy released by the rockmass in mining stage post A5 is 85038 kJ as opposed to the 62617 kJ absorbed by the supports during the deformation interval 779 - 900 mm.

The rockmass stiffness has negative slope for the first 5 mining stages while that of the supports are positive for the same five stages of mining. For the mining stage post A5 the slope of the rockmass is less than the supports and indicates unstable support failure. The stiffness of the rockmass for this deformation interval is -719 kN/mm as opposed to the -1209 kN/mm of the support.

This approach validates the evaluation methodology from both stiffness and energy comparison points of view. The study confirms that the instability could have originated in the vicinity of Station 1 as was observed underground.

7.3 CASE STUDY 2: 23A79 STOPE – STABLE SUPPORT FAILURE

After the stope collapse of the 15A47 Stope, a decision was taken by management on the mine to introduce a systematic pillar layout as regional support. The objective of this strategy was to limit the mining span and through this limit stope closure. The effect of this strategy was that it would in turn affect the stiffness of the rockmass. After some experimental stopes it was decided to use Pencil Props as permanent stope panel support with Matpacks as gully support.

The mining depth of the 23A79 Stope is approximately 800 m below surface. Regional support in the form of 6 m x 3 m pillars were introduced in this area as part of the mine's strategy. In practice the pillars were cut slightly larger than was required after the 4th stage of mining as shown in Figure 7.8.

7.3.1 Support capacity

The mathematical representation of load-deformation performance curves for a Profile Prop and a Matpack that were used in the 23A79 Stope is shown in Figures 7.7 and 7.8. The graphs represent the in-situ performance of the support units installed in the 23A79 Stope where the laboratory test results were adjusted to compensate for the factors influencing its performance. The rate of deformation for each of the mining steps was taken as determined from the in-situ measurements shown in Table 7.4. The support units were not pre-stressed during installation.

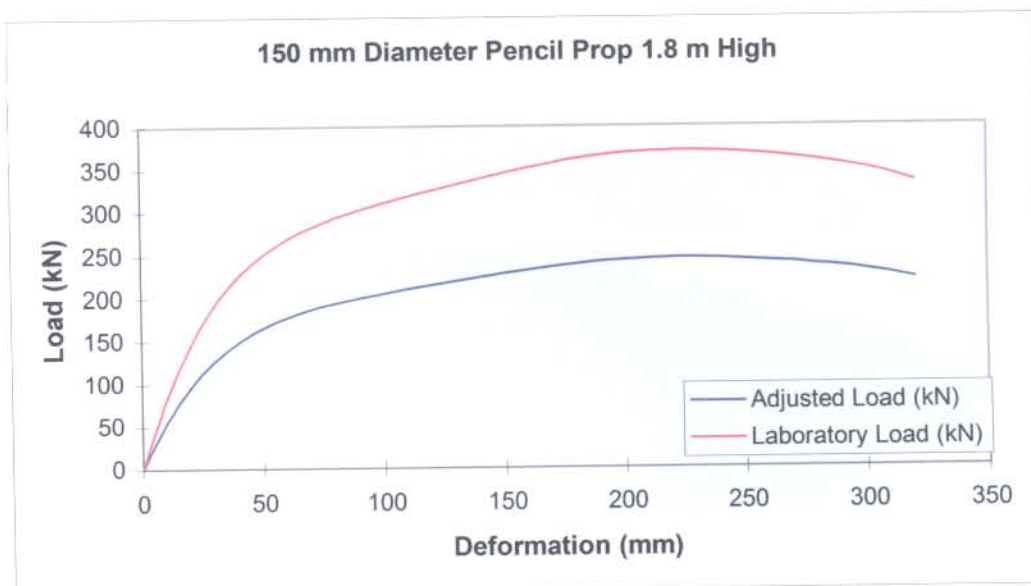


Figure 7.7: Load–deformation curve for a 150 mm Diameter Pencil Prop used in the 23A79 Stope

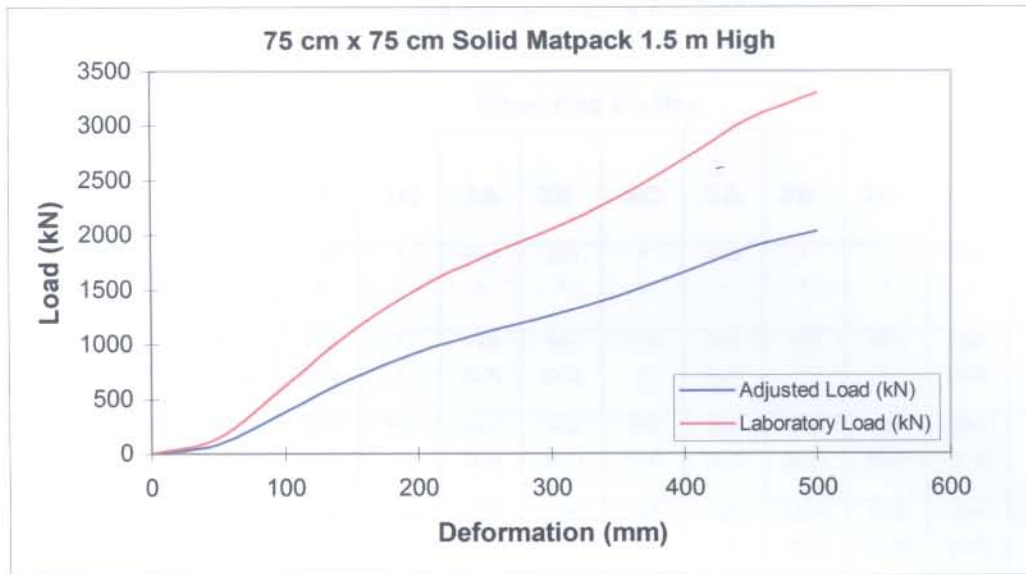


Figure 7.8: Load–deformation curve for a 75 cm x 75 cm Matpack used in the 23A79 Stope

7.3.2 Rockmass demand

The mining steps during the five stages of mining of this working place is shown in Figure 7.9. The dip-oriented pillars can be seen where these were introduced after the 4th mining stage. The effect that the pillars have on the measurements in this stope is illustrated in Tables 7.4 and 7.5 and will be discussed later.

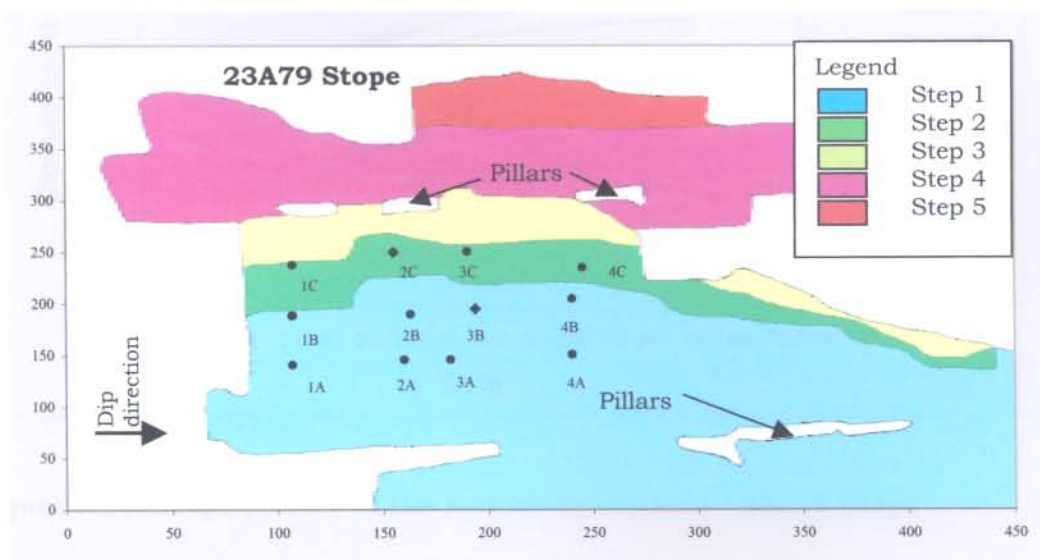


Figure 7.9: Layout and mining steps of the 23A79 Stope

Table 7.4: Summary of closure and closure rates for 23A79 Stope

| Date (Mining Stage) | Measuring Station | | | | | | | | | | |
|------------------------|-------------------|--------------|--------------|--------------|--------------|---------------|--------------|---------------|--------------|--------------|--------------|
| | 1A | 1B | 1C | 2A | 2B | 2C | 3A | 3B | 3C | 4A | 4B |
| 2 Oct (A1) | 625 * | 145 * | * * | 695 * | 310 * | * * | 490 * | * * | * * | 520 * | * * |
| 2 Nov (A2) | 675 (1.7) | 170 (0.8) | * * | 775 (2.7) | 406 (3.2) | 710 * | 587 (3.2) | 750 * | 387 * | 680 (5.3) | 426 * |
| 5 Dec (A3) | 702 (0.8) | 190 (0.6) | 371 * | 887 (3.4) | 562 (4.7) | 897 (5.7) | 708 (3.7) | 932 (5.5) | 595 (6.3) | 823 (4.3) | 640 (6.5) |
| 4 Jan (A4) | 713 (0.4) | 214 (0.8) | 399 (0.9) | 935 (1.6) | 628 (2.2) | 975 (2.6) | 755 (1.6) | 1000 (2.3) | 675 (2.7) | 874 (1.7) | 732 (3.1) |
| 2 Feb (A5) | 722 (0.3) | 225 (0.4) | 410 (0.4) | 961 (0.9) | 665 (1.3) | 1022 (1.6) | 778 (0.8) | 1034 (1.2) | 716 (1.4) | 897 (0.8) | 777 (1.6) |

Where no values are given in the tables below it is due to the fact that the station was either:

- * not installed at that stage of mining, or
- ** was lost.

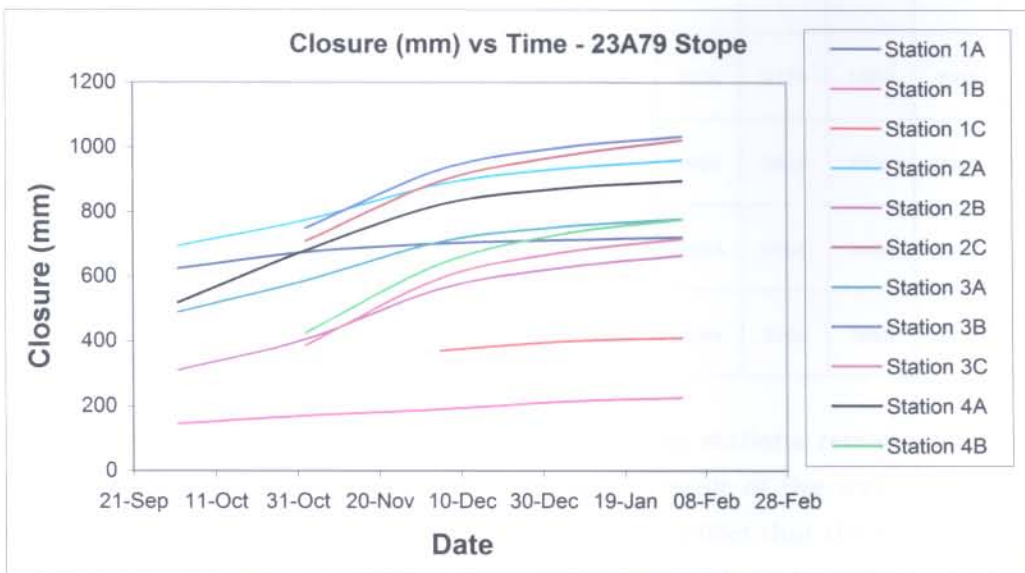


Figure 7.10: Stope closure at the measuring stations – 23A79 Stope

The stope closures at the different measuring stations for the 23A79 Stope are shown in Figure 7.10. The effect that the regional support has in restricting the magnitude of the closure is illustrated by the fact that the closure rates at the

measuring stations decreases with time. The limiting effect that the regional support has on the stope closure at the measuring stations is evident since the closure tends to asymptotically reach a plateau.

The interaction of the rockmass and the supports used in the 23A79 Stope is illustrated in Figure 7.11. The closure rates given in Table 7.5 were used for the different mining stages, while the number of supports that were used in the analysis was determined from the attributed areas as shown in Table 7.5 and the support standards on the mine. Pencil Props were installed on a grid pattern of 1.5 m on strike by 1.0 m on dip, while the matpacks were installed at 3.0 m centre to centre on all dip and strike gullies. The beam thickness was taken as varying from 7.0 m to 14 m with the increasing mining span and is determined from the Voussoir beam study after Kotzé (1991) as shown in Figure 7.5.

Table 7.5: Attributed areas for measuring stations – 23A79 Stope

| Date (Mining Stage) | Measuring Station | | | | | | | | | | |
|---------------------------|-------------------|------|------|------|------|------|------|------|------|------|------|
| | 1A | 1B | 1C | 2A | 2B | 2C | 3A | 3B | 3C | 4A | 4B |
| 2 Oct (A1) | 1814 | 2040 | * | 1803 | 1893 | * | 1830 | * | * | 1560 | * |
| 2 Nov (A2) | 2147 | 2239 | * | 2277 | 2193 | 2288 | 2330 | 2174 | 1869 | 2279 | 1925 |
| 5 Dec (A3) | 2729 | 2710 | 2679 | 2944 | 2507 | 2785 | 2837 | 2810 | 2558 | 2480 | 2393 |
| 4 Jan (A4) | 2913 | 2836 | 2899 | 2968 | 2969 | 2864 | 2944 | 2968 | 2869 | 2730 | 2802 |
| 2 Feb (A5) | 2913 | 2836 | 2899 | 2968 | 2969 | 2864 | 2944 | 2968 | 2869 | 2730 | 2802 |

The Attributed Areas calculated for all the measuring stations remained the same for the last two mining stages. This comes as a result of the way in which the Attributed Areas are calculated and demonstrates the effect that the presence of the regional support has on the rockmass stiffness that will be calculated from it. The rate of closure at all the measuring stations decreased from the 4th to the 5th stages of mining. It confirms what one would have intuitively expected that the rockmass stiffness should remain almost constant once the regional support starts having a restricting effect of the closure of the area between them.

Figure 7.11 shows the rockmass/support analysis for the 23A79 Stope during the five mining stages (A1 to A5) of mining. This area remained stable even though some of the Pencil Props started to fail some 39 m back from the stope face. No sign of rockmass or stope hangingwall failure was observed during the total extraction of the area. This condition may therefore be described as a stable failure of the stope supports.

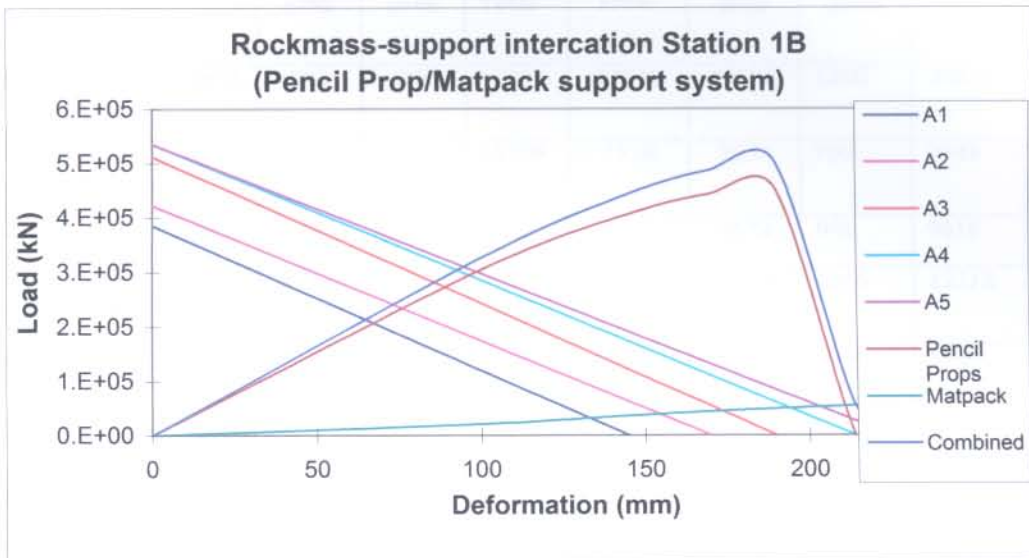


Figure 711: Rockmass and stope support interaction at Station 1B of the 23A79 Stope

(a) Stability analysis summary for station 1B

The rockmass-support interaction is graphically represented in Figure 7.11 while Table 7.6 summarises the stiffness and energy for both the rockmass and supports during the five stages of mining for measuring station 1B.

Table 7.6: Stability analysis summary for Station 1B

| Mining Stage | Def. interval (mm) | Stiffness (kN/mm) | | | | Energy (kJ) for mining stage | | | | Comments |
|--------------|--------------------|-------------------|-------------|----------|--------|------------------------------|--------------------------|----------|-------|---------------------|
| | | Rock-mass | Supports | | | Released by rock-mass | Absorbed by the Supports | | | |
| | | | Pencil prop | Mat-pack | Total | | Pencil prop | Mat-pack | Total | |
| A1 | 0 - 145 | -2657 | +2801 | +202 | +3003 | 27930 | 34000 | 1210 | 35210 | *See comments below |
| A2 | 145 - 170 | -2487 | +1483 | +226 | +1709 | 1110 | 8657 | 766 | 9423 | |
| A3 | 170 - 190 | -2693 | +533 | +256 | +789 | 1077 | 8672 | 946 | 9618 | |
| A4 | 190 - 214 | -2503 | -18915 | +223 | -18691 | 1442 | 10966 | 1246 | 12212 | |
| A5 | 214 - 250 | -2380 | 0 | +198 | +198 | 288 | 0 | 614 | 614 | |

*Comments:

- Pencil Props start failing 39 m from the stope face that is during mining stage A4.
- Less energy generated by rockmass per mining stage after stage A4 when regional support is established.
- The effect that the regional support has on the energy generated by the rockmass during the 5th mining stage is shown in Table 7.6.
- Pencil Props at this station 1B failing in stage 4 and have failed completely by mining stage A5.
- Matpacks remain stable during all stages of mining.

The stiffness of the rockmass remains negative for all five stages of mining and softens slightly towards the 5th mining stage. The stiffness of the Pencil Props are positive during the first three stages of mining but drastically changed to a strain softening (negative) value during the 4th mining stage. The absolute value of the Pencil Props stiffness is higher than that of the rockmass. This implies that failure of the Pencil Props will take place during the 4th stage of mining. The failure of the Pencil Props explains the increased closure rate during the 3rd mining stage where some of this failure of some of the units could have already started to take place, and the soft matpacks not being able to arrest the closure. The matpacks maintained a positive stiffness during all five stages of mining.

The energy capacity of the supports exceeds that of the rockmass during all five stages of mining even though some of the Pencil Props have failed. This is mainly due to the increased load generated by the matpacks during increased deformation. This condition can therefore be described as stable failure of the supports and explains the fact that the stope remained stable. It also explains the fact that large collapses are arrested by packs that have the capacity to increase their load bearing capacity with increased deformation.

The rockmass behaviour at the particular measuring stations for the two stopes is summarised in Figure 7.12. It shows the five stages of mining and demonstrates that the rockmass stiffness for the 15A47 Stope is much softer than that of the 23A79 Stope for the five stages of mining. It is evident that the pillars in the 23A79 Stope restricted the inelastic deformation of the stope and therefore stiffens the rockmass behaviour as shown in Figure 7.12 below. The influence of the systematic stope pillars on stope closure is clear when comparing the underground closure trends during the five mining stages of the two case studies, i.e. Figures 7.3 and 7.10.

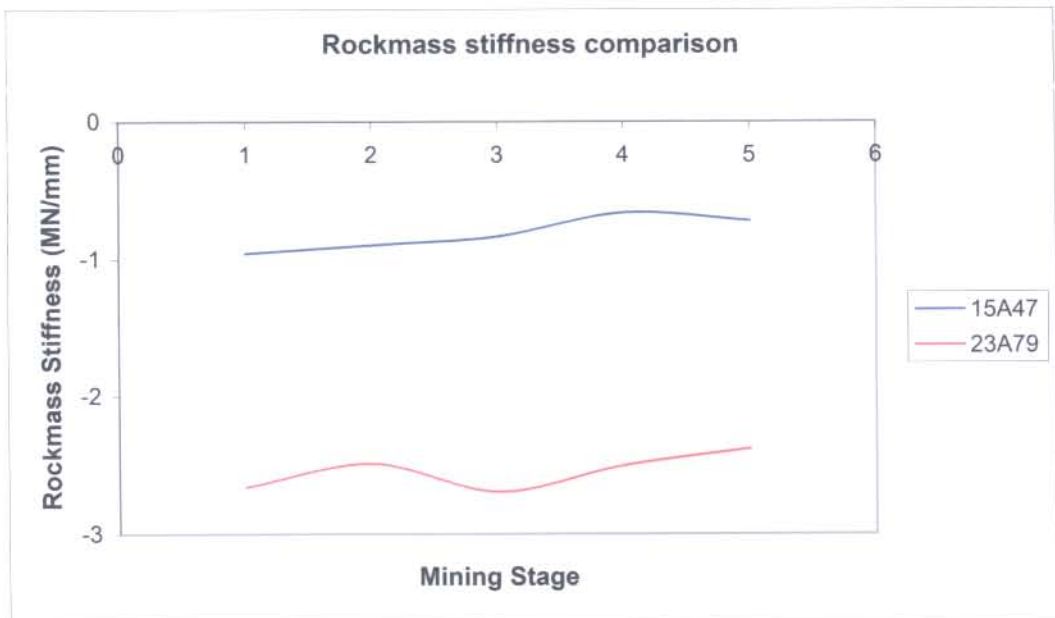


Figure 7.12 Comparison of the rockmass stiffness (MN/mm) for the five mining stages of the two case studies

7.4 CONCLUSION

The applications of the methodology as described in the previous chapters were applied to two case studies at Beatrix Gold Mine. In the first case study unstable failure of the supports occur, while the support in the second case study failed in a stable manner. The in-situ stope support capacity was calculated for the supports of the two case studies, taking into consideration the factors that affect its behaviour.

The rockmass stiffness was also calculated for the different mining stages of the two areas taking into consideration the factors that influence its behaviour such as mining span and geometry, regional support and deformation for the different stages of mining.

The stability analyses that followed from the above where the energy generated and absorbed by the rockmass and support respectively were compared for both case studies. The stiffness of the rockmass and the stope supports were similarly compared as part of the stability analysis. The stable- and unstable failure of the supports that were observed underground is confirmed by this study.

The study shows that the introduction of systematic pillars stiffens the rockmass behaviour by reducing the deformation. This will also reduce the probability for unstable failure of stope support.

REFERENCES

Kotze T.J. (1991). Internal rock engineering report for Beatrix Gold Mine, Gengold, South Africa.

Ozbay M.U. & Roberts M.K.C. (1988). *Yield pillars in stope support* – Proceedings of the first Regional Conference in Africa, South African National Group on Rock Mechanics, Swaziland.

APPENDIX 1**Calculations demonstrating the stability analyses****Working place: 15A47 Stope****(a) Rockmass**

| | |
|-----------------------------------|--|
| Measuring station: | Station 1 |
| Attributed area: | 1884 m ² (Mining stage A ₃) |
| Mining span: | 60 m |
| Beam thickness (h _t): | 8.0 m (from Voussoir beam analysis, Figure 7.5) |
| Rockmass density (ρ): | 2750 kg/m ³ |
| Gravitational acceleration (g): | 9.81 m/s ² |

The attributed area force (F_o) is given by:

$F_o = \rho \cdot h_t \cdot A_a \cdot g$ (N) where:

- F_o = Attributed area force (N);
- ρ = Rockmass density (kg/m³);
- h_t = Thickness of hangingwall beam (m);
- A_a = Attributed area (m²); and
- g = Gravitational acceleration (m/s²).

| | |
|--|--|
| Attributed area force (F _o): | 406 605 kN |
| Deformation interval (mm): | 439 – 488 (Mining: stage A ₃) |
| Rockmass stiffness (m): | -833 kN/mm |
| Rockmass force is described by: | $g(x) = F_o + mx$ $g(x) = 406\,605 - 833x$ (kN) |

Rockmass energy demand (kJ):

$$\text{Energy demand} = \int_a^b g(x) dx = \int_{439}^{488} g(x) dx = 1005 \text{ kJ}$$

(b) Stope support system

Type of support: Beatrix Endgrain pack

Support dip spacing (m): 3.0

Support strike spacing (m): 4.0

Stoping width (cm): 145

Support performance function:

$x < 700$ mm: $f(x)_1 = -1683.7x^6 + 3720.9x^5 - 3140.5x^4 + 1282.3x^3 - 266.85x^2 + 33.445x$

$x > 700$ mm: $f(x)_2 = 1956.1x^5 - 2678.8x^4 - 1127.9x^3 + 2899.7x^2 - 1019.8x$

Underground closure rate (mm/day): 1.6

Pack test height (cm): 143

Rate of laboratory test (mm/minute): 30

Load rate factor (Y_f): 0.52

Pack height factor (H_f): 0.98

Pre-stress load (kN): nil

Pack stiffness (kN/mm) at 464 mm deformation:

$\partial/\partial x[f_a(x)] = +2.14$ kN/mm

Support system stiffness (kN/m²): +335.4

Support energy capacity for the deformation interval $439 \leq x \leq 488$ mm

$\int_{439}^{488} f_a(x) \partial x = 95.0$ kJ

Support system energy capacity (kJ): 14911

(c) Comparisons

| Stability item | Rockmass | Support system | Comment |
|---------------------|-----------------------|--------------------------|--|
| Stiffness (kN/mm) | - 833 | + 335 | Stable support failure: Support stiffness positive, rockmass stiffness negative. |
| Energy balance (kJ) | 1 005 (Energy demand) | 14 911 (Energy capacity) | Stable support failure: Support energy capacity > rockmass demand. |

CHAPTER 8 CONCLUSION FROM THE STUDY

8.1. INTRODUCTION

The objective of the study described in the thesis is to evaluate stope support by means of a rockmass stiffness approach. In a similar fashion as where the supply of a product is compared to the demand in business economics, the capacity of stope support is compared to the demand placed on it by the rockmass. It is achieved by quantifying the capacity of stope support and then to compare this to the rockmass demand.

Three models were developed for the purpose of the study. The first model describes and quantifies the support capacity while the second one describes rockmass behaviour though the rockmass stiffness approach. These two models were successfully combined and the capacity compared to the demand in the third part of the study when applied to two case studies. The case studies represent both an unstable failure as well as a stable failure of the stope support.

In the past different researchers referred to the concept of rockmass or strata stiffness, but no magnitudes were attached to the rockmass stiffness. The statement made by Ozbay and Roberts (1988) that the rockmass stiffness will decrease, that is that the rockmass will react softer as the mining span increases is confirmed by this study.

8.2 STOPE SUPPORT CAPACITY

Stope support behaviour is expressed in the thesis by a polynomial function and is a novel approach that has never been done for these particular applications. The constants for the polynomial functions are given for the support described in the thesis as well as other popular support types used in the mining industry at the time of the study.

The mathematical representation of support performance made it possible that the equations can be manipulated and adjusted to compensate for the aspects that influence support performance. It proves to be an effective way to quantify the capacity of stope support as the in-situ performance of a particular support can be calculated and compared to the laboratory test result of the same unit. All the relevant aspects that influence the support performance were successfully described

into a mathematical format and integrated into a single equation that represents the capacity of a support element.

This exercise was successfully repeated for timber packs, lightweight cementitious packs as well as the timber elongates used in the mining industry at the time of the study. The aspects that influence support behaviour and that are successfully incorporated into an ‘all inclusive’ mathematical representation of support capacity is the following:

- Type of support;
- Rate of deformation from quasi-static (mm/day) to dynamic loading of support (m/s);
- Height of unit installed as opposed to the height of the unit tested (m);
- Pre-stressing of the unit during installation (kN); and
- Support spacing of support (m).

From the above the in-situ performance of supports was determined and the buckling failure calculated in the case of timber elongates. The following is calculated as output from the mathematical representation of the support capacity model:

- Load generated by the support element (kN);
- Height factor (H_f) that quantifies the influence that the difference in the height of the support installed versus the test height;
- The buckling failure factor (B_f) that is applicable to timber elongates;
- The stiffness (both positive and negative) of the support element (kN/mm);
- Energy generated by a support element for a given deformation interval (kJ);
- Support resistance generated by the support taking into consideration the dip and strike spacing of supports (kN/m²);

The approach makes it possible that various conditions and influences on the support behaviour cannot only be quantified, but also described for the different deformation intervals to coincide with the mining during that particular mining interval.

8.3 ROCKMASS DEMAND

The rockmass demand is described during the second phase of the study. The objective with the study was to develop a way in which the support capacity and the rockmass demand can be represented on a common graph. The rockmass demand and the support capacity can be compared directly this way.

The rockmass demand is represented by the rockmass stiffness and is represented on a common force-deformation graph with that of the supports. This methodology is a novel one and has proven to a successful way to evaluate stope support.

Both the force and deformation components are required to establish the rockmass stiffness. The attributed area technique where an area gets allocated to a measuring station for successive mining steps was developed during the study. This novel approach has also proven to be successful and makes it possible that the mining layout and the presence of regional support be incorporated in the study.

All aspects that influence rockmass stiffness are taken into consideration and are the following:

- Mine layout that is related to the mining span;
- Presence and location of regional support;
- Beam thickness of the immediate hangingwall;
- Rockmass density; and
- The position of the point investigated relative to the solid abutments and regional support.

The study confirms the statements made by Ozbay and Roberts (1988) that the rockmass stiffness is related to the mining span. This is best illustrated when the rockmass stiffness is plotted for consecutive mining steps where the slope of the line representing the rockmass behaviour flattens with every mining step, or as the mining span increases.

The influence of regional support is also illustrated in the study where the rockmass stiffness decreases to a certain magnitude as mining progresses. With the stope closure that is limited by the regional support at that point will the rockmass reach a certain stiffness after which it remains unchanged as mining progresses.

8.4 COMBINED MODELS

This methodology gives the design engineer the opportunity to evaluate a combination of different support types that support the area attributed to a measuring station for any given mining stage. Here the capacity of a support system as a whole can be compared to the demand of the rockmass. It gives the engineer the opportunity to take into consideration the various aspects that influence rockmass behaviour and the characteristics that are unique to a specific support type(s).

Two illustrative case studies are described in Chapter 7. These case studies illustrate the applicability of the models that are proposed in the thesis, and confirm that it can be applied to assess permanent stope support.

The methodology also proves that it is possible to evaluate stope support even when a combination of different supports is used as permanent stope support. The latter is achieved by adding the capacities of the stope support as deformation takes place and compare that to the rockmass stiffness for the same mining steps.

In the first case study a total collapse of the excavation took place. This condition is simulated and reproduced by the study and shows that unstable failure of the support has taken place after the fourth stage of mining. The underground observations were confirmed by the outcome of the evaluation of support and rockmass interaction. The energy released by the rockmass, that is rockmass demand, exceeded the capacity of the stope support after the fourth stage of mining. The absolute value of the rockmass stiffness was also less than the absolute value of the load-deformation curve of the stope support for the same mining interval.

Underground observations were again confirmed during the second case study. Here the Pencil Props failed some distance of approximately 39 m from the stope face. In this case the absolute value of the rockmass stiffness was less than the magnitude of the negative load-deformation curve of the Pencil Props, while the Matpacks have a positive load-deformation behaviour throughout the deformation process. In the latter case the total energy generated by the rockmass never exceeded the capacity of the permanent stope support. This is referred to as stable failure of the stope support where part of the permanent support failed whilst the excavation remained open and stable.

The principle of comparing rockmass demand to the capacity of stope support can be done by comparing both stiffness and the energy released by the rockmass to that absorbed by the stope support for a given deformation interval or mining stage.

The author believes that research done and presented in this thesis can reproduce and quantify some aspects of the behaviour of stope support observed and measured underground, and that is a useful tool for stope support evaluation and analysis. It is believed that this work will contribute towards a better understanding, analysis and design of stope support in the discipline of rock engineering.

There is a concentration of the underground workforce in a stope. The stope represents a relatively small area where the workforce spends at least five hours per shift. An understanding and quantification of the rockmass-support interaction in turn has the potential to contribute towards a more stable and safe stoping environment in the mining industry.

8.5 FUTURE WORK

The study confirms the publication by Salamon and Oravecz (1976) that the surrounding strata behave as a progressively softer loading machine as the width of the mining panel is increased. The statement made by Ozbay and Roberts (1988) that the rockmass stiffness decreases as the mining span increases is also confirmed.

It was assumed in this study that the rockmass stiffness is linear for every mining interval as shown in Chapters 5 and 6. The system stiffness may in fact react in a non-linear fashion when considering the history of a particular point in an excavation through different stages of mining as demonstrated in Figure 6.7 of Chapter 6. It is suggested that further research be done in determining the linearity of the rockmass stiffness.

It is important that the rockmass stiffness approach be tested and expanded to intermediate and deep-level mines. It is likely that a fractured and blocky hangingwall will react in a *softer* fashion and may reach a condition of zero rockmass stiffness with dead-weight fall-outs. More research is required to confirm this statement. The study should therefore be repeated for a stratified and fractured rockmass such as the Carbon Leader-, Leader- and Vaal reefs where these stopes have a large inelastic component of closure. The large inelastic component of

closure is due to local mechanisms in the immediate hangingwall such as sliding bedding planes that are induced by face fracturing. With the large magnitude of deformation and the potential narrower hangingwall beam may this well result in a softer rockmass behaviour that needs to be quantified.

It is recommended that the potential for buckling failure of all the new generation elongate type of support be quantified. This will also address one of the concerns expressed by Daehnke et al. (2001).

Further research is also needed to determine the upper height to width ratio limit to which cementitious packs can be installed underground. It is generally accepted in industry that this type of support is less likely to fail by buckling due to its homogeneous composition and proper contact between consecutive layers, and support is therefore often installed to a height to width ratio that is not necessarily confirmed by research.

REFERENCES

Daehnke A. & Roberts M.K.C. (2001). *Review and application of stope support design criteria*, The Journal of the South African Institute of Mining and Metallurgy, Johannesburg, May/June 2001.

Kotzé T.J. (1991). Internal rock engineering report for Beatrix Gold Mine, Gengold, South Africa.

Ozbay M.U. & Roberts M.K.C. (1988). *Yield pillars in stope support – Proceedings of the first Regional Conference in Africa*, South African National Group on Rock Mechanics, Swaziland, 1988.

CHAPTER 9 GLOSSARY OF TERMS AND CONCEPTS

9.1 DESIGN AREAS FOR STOPE SUPPORT

The condition of the rock around stopes depends largely on the type of rock in which the gold bearing reef occurs, the geological structures and the depth at which mining takes place. In South African gold mines most stoping takes place in rock strata comprising strong brittle quartzite, separated by thin layers of poorly argillaceous material. Other common rock types that may form the country rock enclosing gold-bearing reefs are well-bedded shales and massive lavas.

The underground production environment includes all working places in areas where the workforce is involved with some activity related to the production of ore. These excavations all have different active working life spans depending on the functions of the excavations. This as well as the dimensions and orientation of the excavation relative to strata will impact on the support design in terms of the type and density of the support units.

The content of this research is restricted to the higher risk area namely the stope as the majority of the workforce is concentrated in this confined area.

9.1.1 Face area

The face area is defined as the area on the stope face for a distance of approximately six meters back towards the mined out area. This is the area where pre-entry examination, installation of temporary support, marking-off of drill holes as well as drilling and cleaning operations take place.

Temporary support along the stope face in this area normally consists of an elongate type of support. Permanent support is installed as follow-on support behind the temporary support and consists of elongates, packs, backfill and/or a combination of these. Tendon or internal hangingwall support often complements temporary and permanent support.

9.1.2 Working area

The working area is defined as the face area to a distance of about twelve meters back to the so-called sweeping line. It includes all access- and travelling ways as well as dip- and strike gullies.

Gully support normally consists of tendon or internal support with packs on the gully ledges.

9.1.3 Back area

The back area of a stope is described as the area behind the sweeping line to a distance varying from approximately twenty to thirty meters towards the mined out area. No work that is related to the production of ore is normally performed in this area.

9.1.4 Remote back area

The remote back area can be classed as the area from the back area towards the original central raise of the stope.

9.2 SUPPORT TYPES AND AREAS IN WHICH USED

9.2.1 General

Temporary support is support that will be removed. Temporary support is installed on the stope face during pre-entry examination of the stope face. It normally consists of an elongated type of support that can be manufactured from either timber or steel. In some instances these units are pre-stressed during installation to actively exert a force onto the hangingwall. The pre-stressing of temporary support can be done hydraulically, pneumatically or mechanically. Temporary support is mostly released remotely before the blasting operation if it is not a blast-on type.

Permanent support is support that once installed is not removed. Permanent support is installed on the stope face as follow-on support behind the temporary support. It is normally installed on fixed dip and strike spacing. As suggested by its classification this support is installed for its permanency and may only be removed in accordance with legally prescribed procedures. Permanent support consists mostly of packs,

elongates or a combination thereof. It can be pre-stressed in a similar way as the temporary support.

Stiff support can be classed as support with a high initial stiffness where little deformation is required for the support to generate a high resisting force. A stick is a typical example of a stiff support type.

Soft support on the other hand has a relatively low modulus and more deformation is required for the support element to generate a high resisting force. A matpack is a typical example of such an element.

Active support exerts a load onto the excavation walls during installation. This is achieved by a loading mechanism of some kind. The support does not require any deformation of the excavation to take place for it to generate a resisting force. Even in those early days of mining on the Witwatersrand, the miners were aware of the need for the pre-stressing of stope support. One of the developments to achieve this need in those days was the so-called "Q-block." The Q-block consisted of two pieces of round timber, 15-20 cm in diameter and 30 cm in length, which were drawn together by a bolt with washers and nuts. By tightening the nuts, head or footblocks placed above and below can be wedged tightly against the rock surfaces. According to Jeppe (1946) Q-blocks could be installed easily and quickly and proved to be very successful in narrow stopes. A typical example of a modern day active type of support is a hydraulic prop.

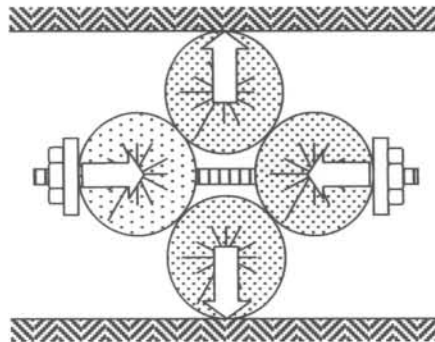


Figure 9.1 – Mechanism of the Q-block described by Jeppe (1946)

Passive support does not exert a load onto the excavation walls during installation and requires deformation of the excavation to take place for it to generate a resisting force.

A typical example of such a type of support is a minepole that is not pre-loaded during installation.

Face support relates to the support installed on the stope face and may consist of elongates, pack support or a combination thereof.

Regional support refers to the support required to stabilise the working area and excludes packs and elongate types of support. Regional support can be rock left in-situ during the mining process or backfill to support local hangingwall. The aim of regional support is to stabilise the macro-working environment.

Tendon support or internal support refers to support installed into the walls of the underground excavation with the objective of reinforcing the rockmass skin surrounding the excavation. Tendon type of support can be used in conjunction with elongate and pack types of support, meshing and lacing.

Stable failure of support refers to the condition where the stope supports fail, while the mine opening remains open and stable. This type of failure of the supports does not have any detrimental effect on the production cycle.

Unstable failure of the supports refers to a condition where the supports fail in such a way that the excavation collapses and that the production cycle cannot continue. Extreme measures are normally required to open the excavation or alternative measures are implemented to re-establish the excavation.

9.2.2 Elongates

Elongate support can be defined as support where the diameter of the unit is small in relation to the height or length of the element. Props and sticks fall in this category. Elongate support is normally a stiff type of support and has varying yieldability depending on the type and design of the support unit. Elongates are used as temporary and/or permanent stope support and is mainly manufactured from timber or steel.

Props refer to an elongated type of stope support. Limitations of ordinary timber sticks were realised early on in the history of the South African mining industry. According to Jeppe (1946), the timber support elements used in those early years were varied. The most common element was the timber prop that was used for local support.

The development of the Pipe-stick in the early 70's heralded a revolution in permanent elongate support practices. This was followed by a wide variety of columnar timber support units that were devised to give improved post-failure yielding properties. These props are generally machined timber poles with either one or both ends modified by tapering or grooving to allow it to yield in a controlled fashion.

A number of different types of elongates have been developed over the last decade and a half with the objective of producing a type of prop with the maximum yielding while maintaining a constant yield load. Several types of materials are used in this process of which steel and timber form the main components. Props are used as a permanent type of stope support.

A stick in the context of stope support refers to timber poles installed as support. It has a low yieldability and is a stiff type of support. According to Jeppe an attempt to overcome the lack of yieldability in a stick was achieved by sharpening one end of the stick to induce yield at a lower load. Jeppe also reported favourably on a compressible pipe support filled with sand.

Minepoles with no engineered yield performance are used in stopes either as permanent support in shallow and/or wide reef stopes where stope closure is limited or as temporary stope face support.

9.2.3 Timber packs

The use of timber as a medium for stope support dates back to 1886, and it is remarkable to reflect that a century later, timber still constitutes the major component of stope support in the gold and platinum mining industry. According to Jeppe (1946) Hildick Smith on Nourse Mines first introduced matpacks in April 1928. The matpack is still used on quite a number of South African gold and platinum mines today.

The use of timber for back area support is a common practice in the South African mining industry although the types of pack in use vary considerably depending on the mining depth, stope width and hangingwall condition. Timber packs are normally a soft support but can be designed and constructed into a stiff type of support by changing the orientation of the timber fibres within the composition of the pack. The incorporation of stiffer elements such as concrete bricks can influence the load-bearing

characteristic of a timber pack quite significantly when compared to the conventional matpack.

End-grain type of support refers to a pack where components of the pack are constructed with the timber fibres oriented in the direction of the applied force, i.e. with the fibres oriented vertically in the pack. The end-grain component of the pack produces a stiffer behaviour of the pack.

9.2.4 Cementitious packs

Cementitious packs have been introduced in the mining industry as a substitute for timber packs. Lightweight concrete packs have mainly been developed over the last decade and a half when requirements for support performance have been specified more accurately.

Cementitious packs consist of either pre-cast blocks or can be constructed underground on-site by grout pumped into a pack construction or containment of some kind. These packs can either be square or circular, stiff or soft, depending on the design and construction of the pack matrix. Concrete packs are used as permanent stope support and are often used for specialised applications such as shaft pillar extraction and as gully support.

9.2.5 Reef pillars

Reef pillars can be described as ore left in-situ during the mining process with the aim to support the local hangingwall, or to provide stability to the mine or portion thereof²⁸. In shallow mines where convergence rates are low and where the hangingwall stratigraphy is such that bed separation to a height of several metres can occur, may conventional support be unable to prevent stope collapse. This is due to the mass of the hangingwall exceeding the strength of the support elements. To overcome this problem, support systems comprising systematically spaced reef pillars, together with intervening rows of yielding stope support such as timber elongates are used.

The reef pillars are designed so that they are able to crush or yield in a controlled manner in order to ensure the stability of the excavation.

Over the past 30 years strike- and dip stabilising pillars have been used on a number of deep level gold mines as a means of regional support. To date the implementation of stabilising pillars has been based on the understanding that through limiting elastic convergence, will this reduce the elastic deformation in the stope and therefore influence the seismicity in the working area.

REFERENCES

Jeppe C.B. (1946). *Gold mining on the Witwatersrand* pp. 815-829, Transvaal Chamber of Mines.